

ปฏิบัติการไฮโดรจีนชั้นแบบเลือกเกิดของอะเซทิลีนบนตัวเร่งปฏิบัติการแพลเลเดียม
บนตัวรองรับไททานเนียมไดออกไซด์ที่มีอัตราส่วนรูโพลและอนาเทส ต่างๆ



นางสาว กัลยาลักษณ์ คนธภักดี

วิทยานิพนธ์นี้เป็นส่วนหนึ่งของการศึกษาตามหลักสูตรปริญญาวิศวกรรมศาสตรมหาบัณฑิต

สาขาวิชาวิศวกรรมเคมี ภาควิชาวิศวกรรมเคมี
คณะวิศวกรรมศาสตร์ จุฬาลงกรณ์มหาวิทยาลัย

ปีการศึกษา 2548

ISBN 974-17-5740-9

ลิขสิทธิ์ของจุฬาลงกรณ์มหาวิทยาลัย

SELECTIVE HYDROGENATION OF ACETYLENE ON
PALLADIUM CATALYSTS SUPPORTED ON TITANIUM DIOXIDE
CONSISTING OF VARIOUS RUTILE/ANATASE RATIOS



Miss Kanyaluck Kontapakdee

A Thesis Submitted in Partial Fulfillment of the Requirements
for the Degree of Master of Engineering in Chemical Engineering
Department of Chemical Engineering

Faculty of Engineering
Chulalongkorn University

Academic Year 2005

ISBN 974-17-5740-9


Thesis Title SELECTIVE HYDROGENATION OF ACETYLENE
ON PALLADIUM CATALYSTS SUPPORTED ON
TITANIUM DIOXIDE CONSISTING OF VARIOUS
RUTILE/ANATASE RATIOS

By Miss Kanyaluck Kontapakdee

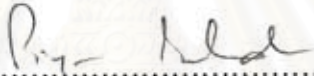
Field of Study Chemical Engineering

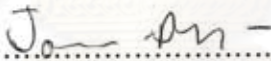
Thesis Advisor Assistant Professor Joongjai Panpranot, Ph.D.

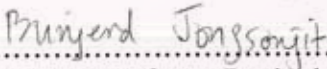
Accepted by the Faculty of Engineering, Chulalongkorn University in Partial
Fulfillment of the Requirements for the Master's Degree

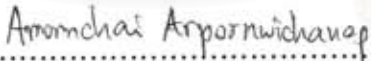

..... Dean of the Faculty of Engineering
(Professor Direk Lavansiri, Ph.D.)

THESIS COMMITTEE


..... Chairman
(Professor Piyasan Praserttham, Dr.Eng.)


..... Thesis Advisor
(Assistant Professor Joongjai Panpranot, Ph.D.)


..... Member
(Assistant Professor Bunjerd Jongsomjit, Ph.D.)


..... Member
(Amornchai Arpornwichanop, D.Eng.)

สถาบันวิทยบริการ
จุฬาลงกรณ์มหาวิทยาลัย

กัลยาลักษณ์ คนธภักดิ์: ปฏิกริยาไฮโดรจิเนชันแบบเลือกเกิดของอะเซทิลีนบนตัวเร่งปฏิกริยา
 แพลเลเดียมบนตัวรองรับไททาเนียมไดออกไซด์ ที่มีอัตราส่วนรูไทล์และ อนาเทส ต่างๆ
 (SELECTIVE HYDROGENATION OF ACETYLENE ON PALLADIUM CATALYSTS
 SUPPORTED ON TITANIUM DIOXIDE CONSISTING OF VARIOUS RUTILE/ANATASE
 RATIOS) อ. ที่ปรึกษา: ดร. จุงใจ ปั้นประณต 109 หน้า ISBN 974-17-5740-9

ทำการศึกษาผลกระทบของไททาเนียมไดออกไซด์ที่มีอัตราส่วนรูไทล์และอนาเทสต่างๆ ต่อการ
 นำไปใช้เป็นตัวรองรับของตัวเร่งปฏิกริยาแพลเลเดียมและ แพลเลเดียม-ซิลเวอร์ สำหรับปฏิกริยาไฮโดร
 จิเนชันแบบเลือกเกิดของอะเซทิลีน ไททาเนียมไดออกไซด์ ที่มีเปอร์เซ็นต์รูไทล์มากจะมีพื้นที่ผิว ปริมาณ
 Ti^{3+} และการกระจายตัวของแพลเลเดียมบนตัวรองรับลดลง เมื่อใช้ไททาเนียมไดออกไซด์ที่มี Ti^{3+} เป็นตัว
 รองรับของตัวเร่งปฏิกริยาแพลเลเดียม (0-44%รูไทล์) ในปฏิกริยาไฮโดรจิเนชันแบบเลือกเกิดอะเซทิลีน
 พบว่าความว่องไวและ การเลือกเกิดของเอทิลีนมีค่าสูง ในขณะที่การใช้ตัวรองรับของตัวเร่งปฏิกริยา
 แพลเลเดียมที่มีปริมาณรูไทล์ 85-100% ความว่องไวและ การเลือกเกิดของเอทิลีนมีค่าต่ำ การวิเคราะห์
 พื้นผิวด้วยวิธีอิเล็กตรอน สปิน เรโซแนนซ์ (ESR) และเอ็กซ์-เรย์ โฟโตอิเล็กตรอน สเปกโทรสโกปี
 (XPS) ยืนยันถึงการมี Ti^{3+} บนไททาเนียมไดออกไซด์ที่มี 0-44% รูไทล์ ทั้งนี้ Ti^{3+} ที่สัมผัสกับแพลเลเดียม
 อาจทำให้เกิดการดูดซับของเอทิลีนต่ำลง ส่งผลให้การเลือกเกิดเป็นเอทิลีนสูงขึ้น โดยที่ตัวเร่งปฏิกริยา
 แพลเลเดียมบนตัวรองรับที่มี 44%รูไทล์ ให้ค่าการเลือกเกิดของเอทิลีนสูงสุด นอกจากนี้ได้ทำการ
 สังเคราะห์ไททาเนียมไดออกไซด์เฟสอนาเทสด้วยวิธีโซลโวลเทอร์มอล และวิธีโซล-เจล นำมาใช้เป็นตัว
 รองรับโลหะแพลเลเดียมและ แพลเลเดียม-ซิลเวอร์ พื้นที่ผิวของไททาเนียมไดออกไซด์ที่เตรียมด้วยวิธี
 โซลโวลเทอร์มอล น้อยกว่าไททาเนียมไดออกไซด์ที่เตรียมด้วยวิธีโซลเจลและมีปริมาณ Ti^{3+} มากกว่า การ
 ใช้ไททาเนียมไดออกไซด์เฟสอนาเทสที่เตรียมด้วยวิธีโซลโวลเทอร์มอล เป็นตัวรองรับโลหะแพลเลเดียม ใน
 ปฏิกริยาไฮโดรจิเนชันแบบเลือกเกิดของอะเซทิลีน พบว่าความว่องไวและ การเลือกเกิดของเอทิลีนมีค่า
 ต่ำกว่าตัวเร่งปฏิกริยาบนตัวรองรับไททาเนียมไดออกไซด์ที่เตรียมด้วยวิธีโซลเจล เมื่อผสมโลหะซิลเวอร์
 บนตัวเร่งปฏิกริยาแพลเลเดียม พบว่าความว่องไวและ การเลือกเกิดของเอทิลีนมีค่าต่ำกว่าตัวเร่ง
 ปฏิกริยาแพลเลเดียมที่ไม่ผสมโลหะซิลเวอร์และมี Ti^{3+} ปรากฏ อย่างไรก็ตามโลหะซิลเวอร์สามารถ
 ปรับปรุงการเลือกเกิดของเอทิลีนให้สูงขึ้นบนตัวรองรับของตัวเร่งปฏิกริยาที่ไม่มี Ti^{3+} งานวิจัยนี้สามารถ
 สรุปได้ว่า ปริมาณ Ti^{3+} และ แรงกระทำระหว่างแพลเลเดียมและ ไททาเนียมไดออกไซด์ ส่งผลต่อทั้ง
 ความว่องไวและ การเลือกเกิดของตัวเร่งปฏิกริยาแพลเลเดียมและ แพลเลเดียม-ซิลเวอร์ในปฏิกริยา
 ไฮโดรจิเนชันแบบเลือกเกิดอะเซทิลีน

ภาควิชา.....วิศวกรรมเคมี.....
 สาขาวิชา.....วิศวกรรมเคมี.....
 ปีการศึกษา.....2548.....

ลายมือชื่อนิสิต.....ก้องภัสร์ภักดิ์.....คนธภักดิ์.....
 ลายมือชื่ออาจารย์ที่ปรึกษา.....ดร. จุงใจ ปั้นประณต.....

4770584421 : MAJOR CHEMICAL ENGINEERING

KEYWORDS: TITANIA POLYMORPH/ CRYSTALLINE PHASE COMPOSITION/ SOLVOTHERMAL METHOD/ SOL GEL METHOD/ SUPPORTED PALLADIUM CATALYSTS/ ACETYLENE HYDROGENATION

KANYALUCK KONTAPAKDEE: SELECTIVE HYDROGENATION OF ACETYLENE ON PALLADIUM CATALYSTS SUPPORTED ON TITANIUM DIOXIDE CONSISTING OF VARIOUS RUTILE/ANATASE RATIOS. THESIS ADVISOR: JOONGJAI PANPRANOT, Ph.D., 109 pp. ISBN 974-17-5740-9

Effect of titania consisting of various phase compositions on Pd and Pd-Ag catalysts for selective acetylene hydrogenation has been studied. Increasing amount of %rutile phase in the TiO_2 resulted in a decrease in BET surface areas, lower amount of Ti^{3+} sites, and lower Pd dispersion. Acetylene conversion was found to be merely dependent on Pd dispersion while ethylene selectivity appeared to be strongly affected by the presence of Ti^{3+} in the TiO_2 samples. When TiO_2 samples with 0-44% rutile were used, high ethylene selectivities were obtained whereas ethylene losses occurred for those supported on TiO_2 with rutile phase 85 or 100%. XPS and ESR experiments revealed that significant amount of Ti^{3+} existed in the TiO_2 samples composed of 0-44% rutile. The presence of Ti^{3+} in contact with Pd can probably lower adsorption strength of ethylene resulting in an ethylene gain. Among all the catalysts used in this study, the results for Pd/ TiO_2 -R44 suggest an optimum anatase/rutile composition of the TiO_2 used to obtain high selectivity of ethylene in selective acetylene hydrogenation. In addition, pure anatase titania has been prepared by solvothermal and sol-gel methods and employed as supports for Pd and Pd-Ag catalysts. BET surface area of the solvothermal TiO_2 was less than that of sol-gel TiO_2 . However, due probably to the different synthesis routes, the amount of Ti^{3+} sites on the TiO_2 prepared by solvothermal method were higher than the one prepared by sol-gel method. It was found that acetylene conversion and ethylene selectivity of Pd catalyst supported on solvothermal TiO_2 with higher Ti^{3+} sites were lower than those of sol-gel TiO_2 supported one. Acetylene conversion and ethylene selectivity of Pd-Ag catalyst were found to be lower than that of single metal Pd catalyst supported on TiO_2 containing Ti^{3+} . However, the presence of Ag improved significantly ethylene selectivity of the catalysts without Ti^{3+} presented. In conclusion, this study reveal both Ti^{3+} and the strong-metal support interaction (SMSI) presented in Pd and Pd-Ag supported on TiO_2 significantly affect the catalyst performance in selective hydrogenation of acetylene.

สถาบันวิทยบริการ
จุฬาลงกรณ์มหาวิทยาลัย

Department Chemical Engineering
Field of Study Chemical Engineering
Academic year 2005

Student's signature *กัญญาลักษณ์ หนองบัว*
Advisor's signature *Joongjai Panpranot*

ACKNOWLEDGEMENTS

The author would like to express her sincere gratitude and appreciation to her advisor, Dr. Joongjai Panpranot, for her invaluable suggestions, encouragement during her study, useful discussions throughout this research and especially, giving her the opportunity to present her research at RSCE conference in Vietnam. In addition, the author would also be grateful to Professor Piyasan Prasertdam, as the chairman, Assistant Professor Bunjerd Jongsomjit, and Dr. Amornchai Arpornwichanop as the members of the thesis committee. The financial supports of the Thailand Research Fund (TRF), TJTTP-JBIC, and the Graduate School of Chulalongkorn University are gratefully acknowledged.

Most of all, the author would like to express her highest gratitude to her parents who always pay attention to her all the times for suggestions and listen her complain. The most success of graduation is devoted to my parents.

Finally, the author wishes to thank the members of the Center of Excellence on Catalysis and Catalytic Reaction Engineering, Department of Chemical Engineering, Faculty of Engineering, Chulalongkorn University for friendship. To the many others, not specifically named, who have provided her with support and encouragement, please be assured that she thinks of you.

สถาบันวิทยบริการ
จุฬาลงกรณ์มหาวิทยาลัย

CONTENTS

	Page
ABSTRACT (IN THAI)	iv
ABSTRACT (IN ENGLISH)	v
ACKNOWLEDGMENTS	vi
CONTENTS	vii
LIST OF TABLES	x
LIST OF FIGURES	xii
CHAPTER	
I INTRODUCTION	1
II LITERATURE REVIEWS	3
2.1 Synthesis of nanocrystalline titania by solvothermal method	5
2.2 Synthesis of nanocrystalline titania by sol-gel method.....	8
2.3 Supported Pd catalyst in selective hydrogenation reaction.....	11
2.4 Role of titania in the selective hydrogenation on Pd catalysts....	12
2.5 Comments on the previous studies.....	15
III THEORY	16
3.1 Acetylene Hydrogenation Reaction.....	16
3.2 Titanium (IV)oxide.....	19
3.3 Solvothermal method.....	22
3.4 Sol-gel method.....	23
3.5 Promoters	23
IV EXPERIMENTS	24
4.1 Chemicals.....	24
4.2 Preparation of TiO ₂ supports.....	25
4.2.1 Preparation of TiO ₂ supports consisting of various phase compositons.....	25
4.2.2 Preparation TiO ₂ using the solvothermal method.....	26
4.2.3 Preparation TiO ₂ using the sol-gel method.....	28
4.3 Palladium and Palladium –Silver loading.....	28
4.4 Catalyst Characterization.....	29
4.4.1 X-ray diffraction	29
4.4.2 BET Surface Area	29

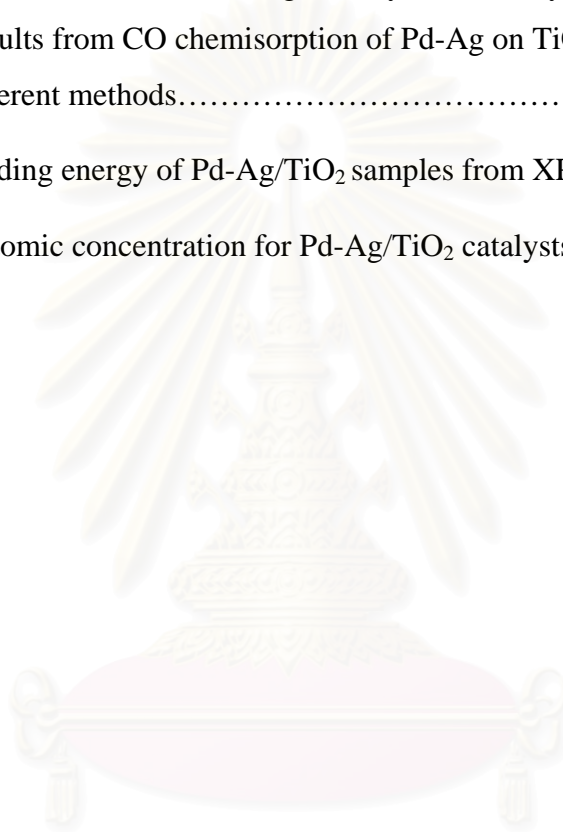
	Page
4.4.3 CO-pulse chemisorption	30
4.4.4 Scanning electron microscopy (SEM)	30
4.4.5 Transmission electron microscopy (TEM)	30
4.4.6 Electron Spin Resonance (ESR.).....	31
4.4.7 X-ray photoelectron spectroscopy (XPS).....	31
4.4.8 Temperature Programmed Desorption	31
4.5 Reaction study in acetylene hydrogenation	31
V RESULTS AND DISCUSSION.....	35
5.1 TiO ₂ consisting of various crystalline phase compositions	35
5.1.1 Properties of TiO ₂ support consisting of various phase compositions	35
5.2 1% Pd over TiO ₂ catalysts	49
5.2.1 Properties of 1% Pd over TiO ₂ catalysts.....	49
5.2.2 The catalytic activities of Pd/TiO ₂ catalysts in selective acetylene hydrogenation.....	57
5.2.3 Temperature programmed desorption study	61
5.3 Pd-Ag/TiO ₂ catalysts consisting of various TiO ₂ phase compositions.....	62
5.3.1 Catalyst Characterization of Pd-Ag catalysts.....	62
5.3.2 The catalytic activities of Pd-Ag/TiO ₂ catalysts in selective acetylene hydrogenation.....	67
5.4 Proposed mechanism for selective acetylene hydrogenation on the various phase composition of TiO ₂ supported Pd catalysts.....	68
5.5 Solvothermal and sol gel – derived TiO ₂	70
5.6 1% Pd catalysts on TiO ₂ synthesized by the different methods	76
5.6.1 Properties of 1% Pd on supported TiO ₂ catalysts.....	76
5.6.2 The catalytic activities of Pd/TiO ₂ catalysts in selective acetylene hydrogenation.....	80
5.7 1%Pd- 3%Ag over TiO ₂ catalysts synthesized TiO ₂ using the different methods.....	82
5.7.1 Catalyst Characterization of Pd-Ag catalysts.....	82

	Page
5.7.2 The catalytic activities of Pd-Ag/TiO ₂ catalysts in selective acetylene hydrogenation.....	86
VI CONCLUSION AND RECOMMENDATION	87
6.1 Conclusions.....	87
6.2 Recommendation.....	88
REFERENCES	89
APPENDICES	97
APPENDIX A: CALCULATION FOR CATALYST PREPARATION	98
APPENDIX B: CALCULATION FOR THE CRYSTALLITE SIZE	100
APPENDIX C: CALCULATION FOR METAL ACTIVE SITES AND DISPERSION	103
APPENDIX D: CALIBRATION CURVES	104
APPENDIX E: CALCULATION OF CONVERSION AND SELECTIVITY	107
APPENDIX F: LIST OF PUBLICATIONS	108
VITAE	109

LIST OF TABLES

TABLE		Page
3.1	Crystallographic properties of anatase, brookite, and rutile.....	21
4.1	Chemicals used in the experiment.....	25
4.2	Operating conditions of gas chromatograph for selective hydrogenation of acetylene.....	33
5.1	BET surface area of TiO ₂ samples consisting of various % rutile phase.....	38
5.2	% atomic concentration of Ti and O on TiO ₂ surface from XPS ...	44
5.3	BET surface area of Pd catalysts.....	50
5.4	Results from CO chemisorption of 1%Pd supported on TiO ₂ consisting of various %rutile (reduced at 500 °C).....	51
5.5	Results from CO chemisorption of 1%Pd supported on TiO ₂ consisting of various %rutile (reduced at room temperature).....	51
5.6	XPS binding energies and surface compositions of Pd catalysts ...	55
5.7	% atomic concentration of Ti and O on TiO ₂ surface from XPS ...	56
5.8	BET surface area of Pd-Ag catalysts.....	63
5.9	Results from pulse CO chemisorption Pd-Ag catalysts	65
5.10	XPS binding energies and surface compositions of Pd-Ag catalysts	66
5.11	% atomic concentration of Pd and Ag on Pd-Ag catalysts from XPS results.....	66
5.12	BET surface area and average crystallite size of TiO ₂ synthesized by solvothermal and sol- gel method.....	72
5.13	Binding energy and atomic concentration of TiO ₂ samples from XPS results.....	74
5.14	BET surface area Pd/TiO ₂ synthesized by different methods.....	78

TABLE		Page
5.15	Results from CO chemisorption of 1%Pd on TiO ₂ synthesized by different methods.....	78
5.16	Binding energy of Pd/TiO ₂ samples from XPS results.....	79
5.17	%atomic concentration for Pd/TiO ₂ catalysts from XPS results....	79
5.18	BET surface area of Pd-Ag/TiO ₂ synthesized by different methods	83
5.19	Results from CO chemisorption of Pd-Ag on TiO ₂ synthesized by different methods.....	84
5.20	Binding energy of Pd-Ag/TiO ₂ samples from XPS results.....	84
5.21	%atomic concentration for Pd-Ag/TiO ₂ catalysts from XPS results	85



สถาบันวิทยบริการ
จุฬาลงกรณ์มหาวิทยาลัย

LIST OF FIGURES

FIGURE		Page
2.1	Reaction between a species (G^*) and an adsorbed molecule R.....	9
3.1	Major reaction path of acetylene hydrogenation system.....	18
3.2	Crystal structure of TiO_2	20
4.1	Autoclave reactor.....	27
4.3	A schematic of acetylene hydrogenation system.....	34
5.1	XRD patterns of TiO_2 consisting of different % rutile phase.....	37
5.2	SEM micrographs of various TiO_2 samples.....	39
5.3	ESR spectra of TiO_2 consisting various % rutile phase	42
5.4	XPS survey spectra of TiO_2 samples.....	44
5.5	XPS Ti 2p spectra of TiO_2 samples.....	45
5.6	XPS O 1s spectra of TiO_2 samples.....	45
5.7	XPS C 1s spectra of TiO_2 samples.....	46
5.8	XPS Ti 2p spectra of TiO_2 samples after 2 min etching by Ar^+	47
5.9	XPS Ti 2p spectra of TiO_2 -R100 sample after 2, 5, and 10 mins etching by Ar^+	48
5.10	TEM micrographs of Pd/ TiO_2 -R0 reduced at 500°C and reduced at room temperature.....	53
5.11	XPS survey spectra of various Pd catalysts.....	56
5.12	Catalytic performances of various Pd/ TiO_2 catalysts in selective acetylene hydrogenation.....	60
5.13	Temperature programmed desorption of (A) CO and (B) C_2H_4 for the various Pd/ TiO_2 catalysts.....	62
5.14	XRD pattern of various Pd-Ag/ TiO_2 catalysts.....	64

FIGURE		Page
5.15	Catalytic performances of various Pd-Ag/TiO ₂ catalysts in various phase composition acetylene hydrogenation.....	68
5.16	A conceptual model for selective acetylene hydrogenation mechanism on Pd/TiO ₂ catalysts.....	69
5.17	A conceptual model demonstrating for selective acetylene hydrogenation mechanism on Pd-Ag/TiO ₂ catalysts.....	70
5.18	XRD patterns of the solvothermal and sol gel - titania supports....	71
5.19	SEM images of titania products synthesized by (A) solvothermal and (B)sol-gel methods.....	73
5.20	XPS survey spectra of TiO ₂ synthesized by the solvothermal and sol gel methods.....	75
5.21	ESR results of the solvothermal and sol gel TiO ₂ supports.....	76
5.22	XRD patterns of Pd/TiO ₂ synthesized by the solvothermal and sol gel methods.....	77
5.23	XPS survey spectra of Pd/TiO ₂ synthesized by the solvothermal and sol gel methods.....	80
5.24	Catalytic performances of Pd catalysts in different synthesized methods in acetylene hydrogenation.....	81
5.25	XRD patterns of Pd-Ag/TiO ₂ synthesized by the solvothermal and sol gel methods.....	82
5.26	XPS survey spectra of Pd-Ag/TiO ₂ synthesized by the solvothermal and sol gel methods.....	85
5.27	Catalytic performances of Pd-Ag catalysts in different synthesized methods in acetylene hydrogenation.....	86

CHAPTER I

INTRODUCTION

1.1 Rationale

Ethylene is an important raw material for industrial products, particularly for polyethylene production. Typically ethylene stream from a naphtha cracker unit contains about 0.1-1% of acetylene as an impurity; this must be removed to a level of less than 5 ppm because it poisons the catalyst used in subsequent ethylene polymerization process and eventually degrades selectivity at high acetylene conversion and degrades the quality of the produced polyethylene (Kim, W.J. et al., 2004). There have been two general methods to reduce the amount of acetylene to 5 ppm. One is separation of acetylene from ethylene through adsorption, using zeolite, however, this technique is difficult and very costly. The other method is selective catalytic hydrogenation reaction of acetylene to ethylene which is the preferred route (Kang, J.H. et al., 2000). This reaction is usually performed on a supported palladium catalyst (Shin, E.W. et al., 1998, Kim, J.W. et al., 2003 and Ngamsom, B. et al., 2004).

Due to poor selectivity at high acetylene conversion, oligomer formation during acetylene hydrogenation (Ngamsom, B. et al., 2004) and the demand for high purity ethylene, considerable attention has been focused on the factors which improve activity and selectivity of acetylene hydrogenation catalysts. Several second metals especially the metals of group IB such as Ag (Praserthdam, P. et al., 2002 and Ngamsom, B. et al., 2004), K (Kim, W.J. et al., 2004), Si (Shin, E.W. et al., 1998, Shin, E.W. et al., 2002 and Kim, W.J. et al., 2003), Au (Sarkany, A. et al., 2002), Ti (Kang, J.H. et al., 2000 and Kang, J.H. et al., 2002), Nb (Kang, J.H. et al., 2000), Ce (Kang, J.H. et al., 2000) have been incorporated into palladium catalysts. Substantial improvement of the performance of the Pd catalysts particularly in achieving a high selectivity for ethylene production as well as reduction in green oil formation have been reported with supported Pd-Ag catalysts (Praserthdam, P. et al., 2002 and Ngamsom, B. et al., 2004).

Generally, the catalyst support must present a good stability to high temperature and a sufficiently large specific surface area. They can interact more or less with the active metal and can possess other functions, such as acidity or basicity (Guimon, C. et al., 2003). Among different supports used in preparation of supported palladium catalysts for selective hydrogenation of acetylene, one of the most interesting supports is probably titanium dioxide because it possesses a large surface area and it exhibits a strong metal-support interaction (SMSI). The strong interaction between titanium dioxide and palladium has been shown to modify the active palladium surface and resulted in higher ethylene selectivity during selective acetylene hydrogenation.

Support effects in selective hydrogenation of acetylene have been investigated (Shin, E.W. et al., 1998; Kim, W.J. et al., 2003; and Ngamsom, B. et al., 2004). The commonly used supports for palladium are α -alumina and silica. However, it has recently been reported that Pd/TiO₂ catalysts exhibited higher activities and selectivities in selective acetylene hydrogenation than Pd/Al₂O₃ catalyst (Chu, W. et al., 2004). It is well known that metal catalyst supported on titania exhibits “the strong metal-support interaction” (SMSI) phenomenon after reduction at high temperatures due to the decoration of the metal surface by partially reducible metal oxides (Santos, J. et al., 1983 and Raupp, G.B. et al., 1985) or by an electron transfer between the support and the metals (Herrmann, J.M. et al., 1987 and Chou, P. et al., 1987). Recently, Kang, J.H. et al., (2002) reported that during the selective hydrogenation of acetylene to ethylene on Pd/TiO₂ catalysts, charge transfer from Ti species to Pd weakened the adsorption strength of ethylene on the Pd surface hence higher ethylene selectivity was obtained.

This thesis focuses on investigation of characteristics and catalytic properties for titania-supported Pd and Pd- Ag catalysts. In this investigation, vary crystalline titania- supports can be identified as 2 parts, commercial titania- supports are various rutile/ anatase phase ratios, the other is comparable the preparation method of titania between solvothermal and sol- gel method. Moreover, the effect of defective structures in titania on the catalytic performances of the titania supported Pd and Pd-Ag catalysts in acetylene hydrogenation was investigated.

1.2 Objectives

The objectives of this research are

1. To investigate the effects of various ratios of rutile to anatase phase of titania support on the characteristics and the catalytic properties of titania supported Pd and Pd-Ag catalysts for selective acetylene hydrogenation
2. To synthesis titania from different method, titania are prepared by solvothermal method and sol- gel method.
3. To investigate the characteristics and catalytic properties of solvothermal and sol-gel derived titania supported Pd and Pd-Ag catalysts for selective acetylene hydrogenation.

1.3 Research Scopes

1. Preparation of various ratios of rutile to anatase phase of titania by calcination pure anatase of titania (900- 1010°C, 10°C/ min, 4 h, in air)
2. Preparation of titania using solvothermal techniques in 1, 4- butanediol.
3. Preparation of titania using sol- gel method of titanium ethoxide.
4. Preparation of various ratio of rutile to anatase phase of titania, solvothermal- derived titania supported, sol- gel derived titania supported Pd (1wt% Pd) and Pd-Ag catalysts (1 wt%Pd-3 wt%Ag) using the incipient wetness impregnation method.
5. Characterization of the catalyst sample using atomic absorption X- ray diffraction (XRD), BET surface area, X-ray photoelectron spectroscopy (XPS) Scanning electron microscopy (SEM), Transmission electron microscopy (TEM), pulse CO chemisorption, Electron spin resonance (ESR) and Temperature programmed desorption study (TPD).
6. Reaction study of the catalyst samples in selective acetylene hydrogenation at 40°C and 1 atm using a fixed-bed quartz reactor.

CHAPTER II

LITERATURE REVIEWS

Selective hydrogenation of acetylene to ethylene is a well-known catalytic reaction used to purify ethylene feedstocks for the production of polyethylene. Typically, supported palladium catalyst is employed for this process due to its good activity and selectivity. Nevertheless, various factors have shown to affect the performance of Pd catalysts for the selective hydrogenation of acetylene such as addition of a second metal, pretreatment with oxygen-containing compounds, H₂ spill-over and support effects. This chapter summarizes the recent reports on (1) synthesis of nanocrystalline titania using solvothermal method, (2) synthesis of nanocrystalline titania using sol-gel method, (3) supported Pd catalysts in selective hydrogenation reaction, (4) role of titania in the selective hydrogenation on Pd catalysts, and comments on previous studies which are given in section 2.1-2.5, respectively.

2.1 Synthesis of nanocrystalline titania by solvothermal method

Solvothermal method (Kominami, H. et al., 1999) has been developed for synthesis of metal oxide and binary metal oxide by using solvent as the reaction medium. Use the solvent instead of the water in the hydrothermal method produce the different forms of intermediate phase and the stability of such intermediate phase was not strong. Instability of the intermediate phase gives a large driving force to the formation of product under quite mild condition.

Kim, C. S. et al., (2003) synthesized TiO₂ nanoparticles in toluene solutions with isopropoxide (TIP) as precursor by a solvothermal synthetic method. Weight ratios of precursor to solvent prepared in the mixture are 5/100, 10/100, 20/100, 30/100 and 40/100. At the weight ratio of 10/100, 20/100 and 30/100, TiO₂ nanocrystalline particles were obtained after synthesis at 250°C for 3 h in an autoclave. TiO₂ particles are formed and they have a uniform anatase structure with average particle size below 20 nm. As the composition of TIP in the solution increases, the particle size of TiO₂ powder tends to increase. For the products

obtained from the solution of 5/100 and 40/100, crystalline particles cannot be obtained. The 5/100 of TIP in the mixture may be too small amount to synthesize TiO₂ nanoparticles at 250°C and longer time is also needed to obtain adequate size of the particle. In the mixture of 40/100 TIP the synthetic process of TiO₂ particles may be hindered by agglomeration of the reactants due to surplus of precursor.

Kominami, H. et al., (2003) studied thermal treatment of titanium (IV) butoxide dissolved in 2-butanol at 573 K under autogenous pressure (alcoholthermal treatment) yielded microcrystalline anatase-type titanium (IV) oxide (TiO₂). Thermal treatment of oxobis (2,4-pentanedionato-O,O') titanium (TiO(acac)₂) in ethylene glycol (EG) in the presence of sodium acetate and a small amount of water at 573 K yielded microcrystalline brookite-type TiO₂. Tungsten (VI) oxide (WO₃) powders of monoclinic crystal structure with high crystallinity were synthesized by hydrothermal treatment (HTT), at 523 or 573 K, of aqueous tungstic acid (H₂WO₄) solutions prepared from sodium tungstate by ion-exchange (IE) with a proton-type resin. Anatase and brookite TiO₂ products were calcined at various temperatures and then used for photocatalytic mineralization of acetic acid in aqueous solutions under aerated conditions and dehydrogenation of 2-propanol under deaerated conditions. Almost all the anatase-type TiO₂ samples showed the activities more than twice higher than those of representative active photocatalysts, Degussa P-25 and Ishihara ST-01 in both reactions. A brookite sample with improved crystallinity and sufficient surface area obtained by calcination at 973 K exhibited the hydrogen evolution rate almost equal to P-25. HTT WO₃ powders with various physical properties were used as photocatalyst for evolution of oxygen (O₂) from an aqueous silver sulfate solution. WO₃ powder of high crystallinity, e.g., IE-HTT-WO₃ synthesized at 573 K, gave much higher O₂ yield than commercially available WO₃ samples.

Payakgul, W. et al., (2005) synthesized titania using thermal decomposition of titanium (IV) n-butoxide (TNB) in organic solvents yields nanosized anatase titania without the contamination of other phases. From the characteristic, it is suggested that anatase titania synthesized in 1, 4-butanediol is the result from direct crystallization while titania synthesized in toluene is transformed from precipitated amorphous intermediate. Thermal stability of products investigated by calcination at various

temperatures and photocatalytic activity evaluated from ethylene decomposition reaction suggest that amount of defect structures in titania synthesized depends upon the solvent used.

2.2 Synthesis of nanocrystalline titania by sol- gel method

Manzini, I. et al., (1995) studied sol-gel derived bulk amorphous and the crystalline phase TiO_2 obtained by heat treatment are investigated by X-ray absorption spectroscopy. The environment of Ti atoms in the amorphous phase shows a residual from the alkoxide precursor and the presence of anatase crystallites. The thermal treatment up to 350°C give crystalline anatase and the pure rutile phase is obtained at 750°C . Near- edge absorption measurements confirm the octahedral coordinate of Ti in all the phase investigated.

Ding, X. et al., (1996) studied grain growth process in gel-derived nanocrystalline titania powders during various heat-treatment programs was monitored by the X- ray diffraction line profile analysis process method, was found that grain growth in these powders can be significantly enhanced by the anatase to rutile phase transformation. This enhancement effect on grain growth was qualitatively ascribed to the higher mobility atoms because of the bond breakage during the transformation.

Riedy, D.J. et al., (2005) studied a series of titania and doped titania materials have been prepared sol- gel methods using a titanium isopropoxide precursor. Power X- ray diffraction (PXRD) and secondary electron microscopy (SEM) have been used to follow the anatase to rutile transformation phase. PXRD was used to estimated the relative amounts of each phase and the average particle size at series temperatures. Importantly, very careful choice of reaction precursors were made so that a wide range of similar samples could be compared, thus removing effects due to preparation. It was found that doping with Si, Zr, Al and tertiary mixtures these produced an elevated ART temperature whilst Co, Mn, V had the opposite effect. The most likely explanation for the elevation in the ART temperature is the presence of dopant strain fields, which limit mass transport routes. It was also found that in the majority of samples, the mechanism for phase change was related to attaining a critical particle size. This was measured at around 450°A independent of the dopant used.

2.3 Supported Pd catalyst in selective hydrogenation reaction

Sárkány, A. and coworker (Sárkány, A. et al., 1984) studied the hydrogenation of a mixture of 0.29 mole% C_2H_2 , 0.44 mole% H_2 and C_2H_4 up to 100%, a so-call tail-end mixture, on palladium black and several Pd/ Al_2O_3 catalysts. Hydrogenation of C_2H_4 increased with time on stream for all the Al_2O_3 -supported catalysts; the opposite behaviour was noted with palladium black. Polymer formation was noted for all catalysts studied and also increased with time. It was recognized that a small number of C_2H_4 hydrogenation sites were located on the metal but the majority were on the polymer-covered support. The authors proposed that C_2H_4 adsorbed on the support and was hydrogenated there. Spill-over hydrogen was tentatively identified as the source of hydrogen. Because of the parallelism between polymer formation and ethylene hydrogenation, it was proposed that the surface polymer served as a hydrogen pool or facilitated diffusion of hydrogen from Pd to the support.

Hydrogen spill-over (Hodnett, B.K. et al., 1986) is the deal of evidence used to suggest the surface-mobile species. It can play a role in catalytic reaction involving hydrogen. However, spill-over hydrogen is elusive it has never been detected by physico-chemical means under condition similar to those prevailing during catalysis. It is therefore difficult to determine the real role of this species in catalytic hydrogenation, hydrogenolysis and other hydrotreating reactions. The effects attributed to spill-over are usually chemical effect, e.g., hydrogenation by spill-over hydrogen of species adsorbed on a support, removal of carbonaceous deposits, occurrence or enhancement of a given reaction and, more generally, change in catalytic activity. These phenomena are frequency anomalous and can often be explained only by invoking surface mobility and spill-over from one phase to another. The hydrogen spill-over phenomenon is described in Figure 3.2. Essentially a hydrogen species is formed on one phase (usually a metal) and spilled over to react on the other phase.

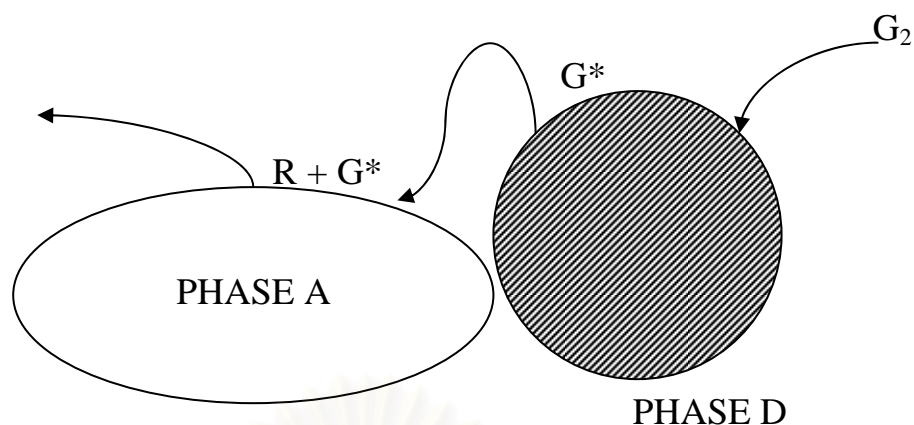


Figure 2.1 Reaction between a species (G^*), formed on phase D, and then transferred to phase A by spill-over and surface diffusion, where it reacts with an adsorbed molecule R. (re-drawn from Hodnett, B. K. et al., 1986)

Asplund, S. et al., (1996) studied the catalyst aging by coke formation for the selective hydrogenation of acetylene in the presence of excess ethylene on supported palladium catalyst. He found that the deposited coke have a substantial influence on the effective diffusivity, which decreased about one order of magnitude during 100 h of operation. He also observed previously the selectivity for the undesired ethane was higher on aged catalysts, while the activity for acetylene hydrogenation was almost constant. However, these effects were strongly dependent on the catalyst particle size, although the behavior of fresh catalysts was unaffected by mass transfer limitations. When the catalyst used was Pd/Al₂O₃ the change in selectivity with aging could be explained solely as a consequence of the increased diffusion resistance. The mass transfer effects were important also on Pd/Al₂O₃, but on this catalyst there was an additional increase in ethane selectivity that could not be attributed to diffusion limitations. Calculations and experimental tests showed that the observed phenomena are relevant also for the shell-type catalysts normally used industrially. The coke formation itself was about four to five times faster on Pd/ α -Al₂O₃ compared to the α -Al₂O₃ supported catalyst. The coke was generally concentrated towards the pellet periphery showing the influence of diffusion resistance also on the coke-forming reactions.

Shin, E.W. et al., (1998) synthesized supported Pd catalysts modified with Si deposited on the support by silane decomposition when used in acetylene

hydrogenation; the Si-modified catalysts show higher selectivity for ethylene and produce less amount of green oil than the unmodified Pd catalysts. They suggested that Si covers the Pd surface as Si or SiO₂ patches. The Pd surface is diluted with the deposited Si. However, the electronic property of the Pd surface seems to be unaffected by the Si species. They conclude that improved performance of the Si modified catalysts comes mostly from geometric modification of the Pd surface by Si.

Kang, J.H. et al., (2000) studied the effect of transition-metal oxides as promoters of the Pd catalyst for acetylene hydrogenation. Transition-metal oxides added to Pd/SiO₂ improve significantly the activity and the ethylene selectivity of the catalyst in acetylene hydrogenation, which is caused by the interaction between the oxides and the Pd surface similar to the case of the oxide-supported catalysts. They confirmed that metal oxide spread on and modify both geometrically and electronically the Pd surface after the catalyst is reduced at 500°C. Such a behavior of metal oxides in the catalyst is correlated well with their promotional effect on the catalyst performance. They found that the oxide on the Pd surface retard the sintering of the dispersed Pd particles, suppresses the adsorption of ethylene in the multiply-bound mode, and facilitates the desorption of ethylene produced by acetylene hydrogenation. Among the three metal oxides examined in this study, titanium oxide is found to have the most promotional effect.

Zhang, Q. et al., (2000) studied an alloy of palladium and silver dispersed on Al₂O₃ for the selective hydrogenation of acetylene. They reported that the activity of Pd–Ag catalyst is lower than that of pure metal Pd catalyst. But the selectivity of Pd–Ag catalyst is higher and less impaired by temperature increase than that of Pd catalyst. They also found that metal Pd and Ag can form an alloy on the surface of alumina. There is a synergetic effect in the hydrogenation of acetylene over Pd–Ag catalyst. Addition of Ag to Pd catalyst decreases the quantity of absorption hydrogen, and reduces absorption hydrogen spill over from the bulk of the metals to react with acetylene, which increases the selectivity of acetylene hydrogenation to ethylene.

Sárkány, A. et al., (2002) investigated acetylene hydrogenation and formation of surface deposits on two series of Pd and Pd-Au/SiO₂ catalysts differing in metal particle size ($D = 0.47$ and 0.08). Gold was deposited via ionization of pre adsorbed

hydrogen over pre-reduced Pd/SiO₂ in order to ensure selective poisoning of the Pd surface. The non-steady-state regime of operation and the accumulation of hydrocarbonaceous over layer were tested in pulse-flow experiments. They determined concentration of surface hydrocarbonaceous deposits accumulated during different treatments by temperature programmed oxidation (TPO). They also observed hydrocarbon over layer to form immediately and its presence appeared to be a necessary requisite to get steady-state conversion and selectivity data. They suggested that a large excess of hydrogen suppressed the formation of carbonaceous layer and increased the over-hydrogenation of acetylene. Presence of Au decreased the carbon coverage and improved the ethylene selectivity. Decoration of Pd by Au and the morphology of particles explain the ethylene selectivity improvement.

Shin, E.W. et al., (2002) studied the origin of the selectivity improvement over the supported Pd catalyst modified with Si, which is deposited selectively on Pd by silane decomposition and subsequently oxidized in oxygen, by observing the adsorption and desorption behavior of acetylene, ethylene, and hydrogen on the Pd surface. They reported that the adsorption strength of ethylene on Pd becomes weak and the amount of adsorbed hydrogen decreases when the Pd catalyst is modified with Si. The Si modification also reduces the amounts of surface hydrocarbons or carbonaceous species that are deposited on the catalyst either during the temperature programmed desorption (TPD) of ethylene or by surface reactions between co-adsorbed acetylene and hydrogen. The hydrocarbon species deposited on the Si modified catalyst have a shorter chain length than those produced on the Pd-only catalyst. All these results are consistent with the improvement in ethylene selectivity on the Si-modified Pd catalyst, which has been explained based on the reaction mechanism of acetylene hydrogenation.

Sárkány, A. et al., (2003) synthesized Pd/SiO₂ (1.08 wt.%) catalyst via sol-derived route using poly(diallyldimethylammonium chloride) (PDDA) polycation as ionic stabiliser. The immobilised sol (monomer/ Pd²⁺ = 1.25) fixed at pH = 8.5 onto Aerosil 200 contains Pd particles of 3.1 nm number-mean diameter. The immobilised sol showed good thermal stability but oxidation of PDDA to get “polymer free” sample causes sintering of Pd particles. They reported that the immobilised sample

even in “as prepared state” possesses hydrogenation activity. Treatments at different temperatures in H₂ or Ar enhance the catalytic activity suggesting an increase in space around the metal particle. They suggested that the PDDA modified sample exhibits better competition selectivity than the “polymer free” sample pointing to surface structure variations caused by geometric/steric effects.

Kim, W.J. et al., (2003) studied the deactivation behavior of Si-modified Pd catalysts in acetylene hydrogenation. They reported that TGA and IR analyses of green oil produced on the catalyst indicate that it is produced in smaller amounts and its average chain length is shorter on a Si-modified catalyst than on an unmodified one. The above findings are due to deposition of Si species on the Pd surface; such deposits effectively block multiply-coordinated adsorption sites on the catalyst and suppress the formation of green oil on the catalyst surface, specifically on or in the vicinity of Pd. The Si species also retard the sintering of Pd crystallites during the regeneration step and allow for the slow deactivation of the catalyst during acetylene hydrogenation, after regeneration. They also suggested that the improvement in the deactivation behavior of the Si-modified catalyst is believed to arise from the geometric modification of the Pd surface with small clusters of the Si species.

2.4 Role of titania in the selective hydrogenation on Pd catalysts

Kang, J.H. et al., (2002) investigated the performance of TiO₂-modified Pd catalysts, containing TiO₂ either as an additive or as a support, in the selective hydrogenation of acetylene was investigated using a steady-state reaction test. They reported that the TiO₂ added Pd catalyst reduced at 500°C (Pd-Ti/SiO₂/500°C) showed a higher selectivity for ethylene production than either the Pd/TiO₂ or Pd/SiO₂ catalyst. The amounts of chemisorbed H₂ and CO were significantly reduced and, in particular, the adsorption of multiply coordinated CO species was suppressed on Pd-Ti/SiO₂/500°C, which is characteristic of the well-known strong-metal-support-interaction (SMSI) phenomenon that has been observed with the TiO₂-supported Pd catalyst reduced at 500°C, Pd/TiO₂/500°C. Moreover, XPS analyses of Pd-Ti/SiO₂/500°C suggested an electronic modification of Pd by TiO₂, and the TPD of ethylene from the catalyst showed the weakening in ethylene adsorption on the Pd surface. The 1, 3-Butadiene was produced in smaller amounts when using Pd-

Ti/SiO₂/500°C than when using Pd/SiO₂/500°C, indicating that the polymerization of C₂ species leading to catalyst deactivation proceeds at slower rates on the former catalyst than on the latter. They also suggested that the enhanced ethylene selectivity on Pd–Ti/SiO₂/500°C may be explained by correlating the catalyst surface properties with the mechanism of acetylene hydrogenation.

Kim, W. J. et al., (2004) studied the deactivation behavior of a TiO₂-added Pd catalyst, reduced at 773 K, for the selective hydrogenation of acetylene showed that the added TiO₂ to a Pd catalyst, reduces the amount of green oil deposited on and in the vicinity of Pd sites and maintains the average number of carbon atoms per green oil molecule was smaller for the TiO₂-added catalyst than for the Pd-only catalyst because multiply coordinated Pd sites were suppressed on the TiO₂-added catalyst so TiO₂ improved the lifetime of the catalyst. Accordingly, the TiO₂-added Pd catalyst becomes deactivated at slower rates than the Pd-only catalyst and the deactivation of the former catalyst was nearly unaffected by the regeneration.

Li, Y. et al., (2003) investigated in situ EPR by using CO as probe molecules shows that even pre-reduced by H₂ at lower temperature results in SMSI for anatase titania supported palladium catalyst, but not for rutile titania supported palladium catalyst, which is attributed that the Ti³⁺ ions produced by reduction of Ti⁴⁺ by the dissociatively chemisorbed hydrogen on palladium diffusing from Pd to TiO₂ are fixed in the surface lattice of TiO₂, as rutile titania is more thermodynamically and structurally stable than anatase titania so that the Ti³⁺ ions fixed in the surface lattice of anatase TiO₂ is easier to diffuse to surface of palladium particle than one in the surface lattice of rutile TiO₂. The reason why the pre-reduction of both anatase and rutile supported palladium catalyst at higher temperature results in SMSI between Ti³⁺ and Pd is attributed that the thermal diffusion of produced Ti³⁺ ion at higher temperature is much easier than at lower temperature so that it could overcome the binding of surface lattice of both anatase and rutile titania to move to the surface or surrounding of palladium particle. The very different catalytic properties between 0:075%Pd/TiO₂ (R) and 0:075%Pd/TiO₂ (A) catalyst pre-reduced at lower temperature, and the rapid change of conversion and selectivity of 0:075%Pd/TiO₂ (A) and 0:075%Pd/TiO₂ (R) with the elevation of pre-reduction temperature further confirm the presence of SMSI both for anatase titania supported palladium catalyst

pre-reduced at lower temperature, and titania (rutile and anatase) supported palladium catalyst pre-reduced at higher temperature.

Kim, W. J. et al., (2004) investigated the effect of potassium (K) addition on the performance of a TiO₂-modified Pd catalyst in the hydrogenation of acetylene. When potassium was added to Pd-Ti/SiO₂, the resulting catalyst showed an improved selectivity for ethylene production over a wide range of conversions, when the catalyst was reduced at 300°C. This is in contrast with the case of K-free Pd-Ti/SiO₂, which showed an improved selectivity only when the catalyst was reduced at high temperatures, e.g. 500°C. They found that k-containing Pd surface is modified with the Ti species after the catalyst is reduced at relatively low temperatures. The origin of the facilitated modification is the formation of potassium titanates, which have a lower melting point than that of TiO₂ and therefore migrate onto the Pd surface after the catalyst, is reduced at lower temperatures compared to the case of TiO₂.

Li, Y. et al., (2004) investigated in situ EPR and IR by using CO as probe molecules show that even pre-reduced by H₂ at lower temperature results in SMSI for anatase titania supported palladium catalyst, but not for rutile titania supported palladium catalyst. This deference is attributed that the Ti³⁺ ions produced by reduction of Ti⁴⁺ are fixed in the surface lattice of TiO₂, as rutile titania is more thermodynamically and structurally stable than anatase titania so that the Ti³⁺ ions fixed in the surface lattice of anatase TiO₂ is easier to diffuse to surface of palladium particle than one in the surface lattice of rutile TiO₂. The reason why the pre-reduction of both anatase and rutile supported palladium catalyst at higher temperature results in SMSI between Ti³⁺ and Pd is attributed that the thermal diffusion of produced Ti³⁺ ion at higher temperature is much easier than at lower temperature so that it could overcome the binding of surface lattice of both anatase and rutile titania to move to the surface or surrounding of palladium particle. The anatase titania supported palladium catalyst 0.075% Pd/TiO₂ (A) reduced at lower temperature has higher selectivity of alkenes than rutile titania supported palladium catalysts 0.075% Pd/TiO₂ (R). For titania (rutile or anatase) supported palladium catalysts, the elevation of pre-reduction temperature from 200 to 450°C gives rise to sharp change of catalytic properties, especially for selectivity of alkenes. The very different catalytic properties between 0.075% Pd/TiO₂ (R) and 0.075% Pd/TiO₂ (A)

catalyst pre-reduced at lower temperature, and the rapid change of conversion and selectivity of 0.075% Pd/TiO₂ (A) and 0.075% Pd/TiO₂ (R) with the elevation of pre-reduction temperature are reasonably explained by the presence of SMSI both for anatase titania supported palladium catalyst pre-reduced at lower temperature, and titania (rutile and anatase) supported palladium catalyst pre-reduced at higher temperature.

Panpranot, J. *et al.*, (2005) prepared nanocrystalline titania by thermal decomposition of titanium (IV) *n*-butoxide in two different solvents (toluene and 1,4-butanediol) at 320°C and employed as supports for Pd and Pd-Ag catalysts for selective acetylene hydrogenation. The titania products obtained from both solvents showed only anatase phase with similar crystallite sizes and BET surface areas. However, due probably to the different crystallization pathways, the number of Ti³⁺ defective sites as shown by ESR results of the titania prepared in toluene were much higher than the ones prepared in 1,4-butanediol. It was found that the use of anatase titania with higher Ti³⁺ defective sites as a support for Pd catalysts resulted in lower activity and ethylene selectivity in selective acetylene hydrogenation. However, this effect was suppressed by Ag promotion.

2.5 Comments on previous studies

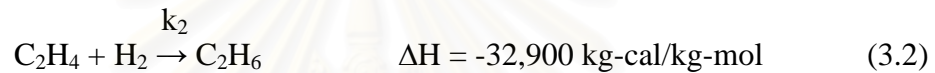
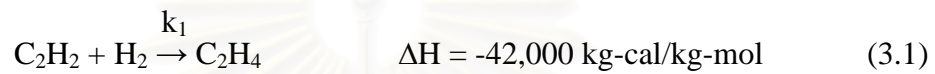
From the previous studies, it was found that titania existing in different crystalline phases such as anatase and rutile exhibited different physical properties. For example, Li, Y. *et al.*, (2003) and Li, Y. *et al.*, (2004) have shown the effect of pure anatase and rutile phase of titania supported palladium catalyst, in selective hydrogenation of long chain alkadienes. Moreover, containing TiO₂ either as additive or as a support of Pd catalysts has shown to improve the reactivity for selective hydrogenation of acetylene due to the decoration of Pd surface by Ti species lower the adsorption strength of ethylene on Pd (Shin, E.W. *et al.*, 2002). There is no report on the role of crystalline phase composition of titania on the catalytic performance during selective hydrogenation of acetylene. Thus, it is interesting to study the different crystalline phase of titania supports on the catalytic properties during selective hydrogenation of acetylene on Pd/ TiO₂ catalysts.

CHAPTER III

THEORY

3.1 Acetylene Hydrogenation Reaction

Generally, there are two primary reactions proceeding during acetylene hydrogenation:



The first reaction (3.1) is the desired reaction whereas the second reaction (3.2) is an undesired side reaction due to the consumption of ethylene product. There is also a third reaction occurring during normal operation, which adversely affects the catalyst performance, i.e., the polymerization reaction of C_2H_2 with itself to form a longer chain molecule, commonly called “green oil”.



According to the above reactions involving acetylene hydrogenation, two influencing parameters on the desired reaction can be assigned. The first parameter is reaction temperature, which has a direct relationship with the kinetics of the system. However, it affects not only the reaction rate of the desired reaction (k_1), but also the rate of ethylene hydrogenation (k_2). The rate of polymerisation (k_3) also increases with temperature and the resulting green oil can affect catalyst activity by occupying active sites. When the catalyst is new or has just been regenerated, it has high activity. With time on stream, activity declines as the catalyst becomes fouled with green oil and other contaminants. By the end-of-run (EOR), the inlet temperature must be increased (25-40°C) over start-of-run (SOR) inlet temperature in order to maintain enough activity for complete acetylene removal. In order to selectively hydrogenate

acetylene to ethylene, it is critical to maintain the differential between the activation energies of reaction (eq. 3.1) and (eq. 3.2). However, it is desirable that the ethylene remains intact during hydrogenation. Once energy is supplied to the system over a given catalyst by increasing the temperature, the differential between the activation energies disappears and complete removal of acetylene, which generally has the lower partial pressure, becomes virtually impossible. In other words, higher temperature reduces selectivity; more hydrogen is used to convert ethylene to ethane, thereby increasing ethylene loss. The inlet temperature should therefore be kept as low as possible while still removing acetylene to specification requirements. Low temperatures minimise the two undesirable side reactions and help optimise the converter operation.

Another crucial parameter affecting the selectivity of the system is the ratio between hydrogen and acetylene ($H_2:C_2H_2$). Theoretically, the $H_2:C_2H_2$ ratio would be 1:1, which would mean that no hydrogen would remain for the side reaction (eq. 3.2) after acetylene hydrogenation (eq. 3.1). However, in practice, the catalyst is not 100% selective and the $H_2:C_2H_2$ ratio is usually higher than 1:1 to get complete conversion of the acetylene. As hydrogen is one of the reactants, the overall acetylene conversion will increase with increasing hydrogen concentration. Increasing the $H_2:C_2H_2$ ratio from SOR to EOR can help offset the decline in catalyst activity with time on stream. However, this increased acetylene conversion with a higher $H_2:C_2H_2$ ratio can have a cost in selectivity which leads to ethylene loss. Typically, the $H_2:C_2H_2$ ratio is between 1.1 and 2.5 (Derrien, M.J. et al., 1986 and Molnár, A *et al.*, 2001).

The mechanism of acetylene hydrogenation involves four major paths as shown in Fig. 3.1. Path I is the partial hydrogenation of acetylene to ethylene, which is either desorbed as a gaseous product or further hydrogenated to ethane via Path II. It previously was proposed that Path I proceeds mostly on Pd sites, which are covered to a great extent with acetylene under typical industrial reaction conditions, and Path II occurs on support sites, particularly those covered with polymer species.

Consequently, selectivity may be improved by reducing both the strength of ethylene adsorption on Pd and the amount of polymer, which accumulates on the

catalyst. One of the methods for improving selectivity is to maintain a low H_2 /acetylene ratio in the reactant stream such that the low hydrogen concentration on Pd retards the full hydrogenation of the ethylenic species on the Pd surface. However, this method has the drawback of accelerating the polymer formation and therefore the H_2 /acetylene ratio must be managed deliberately or sometimes controlled in two steps. Path III, which allows for the direct full hydrogenation of acetylene, becomes negligible at high acetylene coverage and low hydrogen partial pressures. Ethylidyne was suggested as an intermediate in Path III but was later verified to be a simple spectator of surface reactions. Path IV, which allows for the dimerization of the C_2 species, eventually leads to the production of green oil and the subsequent deactivation of the catalyst. Polymer formation lowers ethylene selectivity because it consumes acetylene without producing ethylene and, in addition, the polymer species, which is usually located on the support, acts as a hydrogen pool, thus promoting ethane formation (Kang, J.H. et al., 2002).

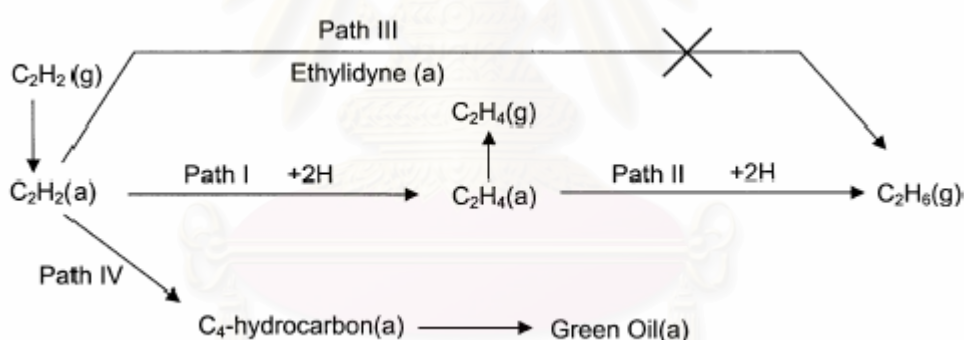


Figure 3.1 Major reaction path of acetylene hydrogenation (Kang, J.H. et al., 2002)

Considering the mechanism of acetylene hydrogenation described above, it was found that ethylene selectivity is improved when the C_2 species produced by Path I is readily desorbed from the catalyst surface and the other paths are simultaneously retarded.

3.2 Titanium (IV) oxide (Othmer, K. et al., 1991 and Fujishima, A. et al., 1999)

Physical and chemical properties

Titanium dioxide may take on any of the following three crystal structures: rutile, which tends to be more stable at high temperatures and thus is sometimes found in igneous rocks, anatase, which tends to be more stable at lower temperatures (both belonging to the tetragonal crystal system), and brookite, which is usually found only in minerals and has a structure belonging to the orthorhombic crystal system. The titanium dioxide use in industrial products, such as paint, is almost a rutile type. These crystals are substantially pure titanium dioxide but usually amount of impurities, e.g., iron, chromium, or vanadium, which darken them. A summary of the crystallographic properties of the three varieties is given in Table 3.1

Although anatase and rutile are both tetragonal, they are not isomorphous (Figure 2.2). The two tetragonal crystal types are more common because they are easy to make. Anatase occurs usually in near-regular octahedral, and rutile forms slender prismatic crystal, which are frequently twinned. Rutile is the thermally stable form and is one of the two most important ores of titanium.

The three allotropic forms of titanium dioxide have been prepared artificially but only rutile, the thermally stable form, has been obtained in the form of transparent large single crystal. The transformation from anatase to rutile is accompanied by the evolution of ca. 12.6 kJ/mol (3.01 kcal/mol), but the rate of transformation is greatly affected by temperature and by the presence of other substance which may either catalyze or inhibit the reaction. The lowest temperature at which conversion of anatase to rutile takes place at a measurable rate is ca. 700°C, but this is not a transition temperature. The change is not reversible; ΔG for the change from anatase to rutile is always negative.

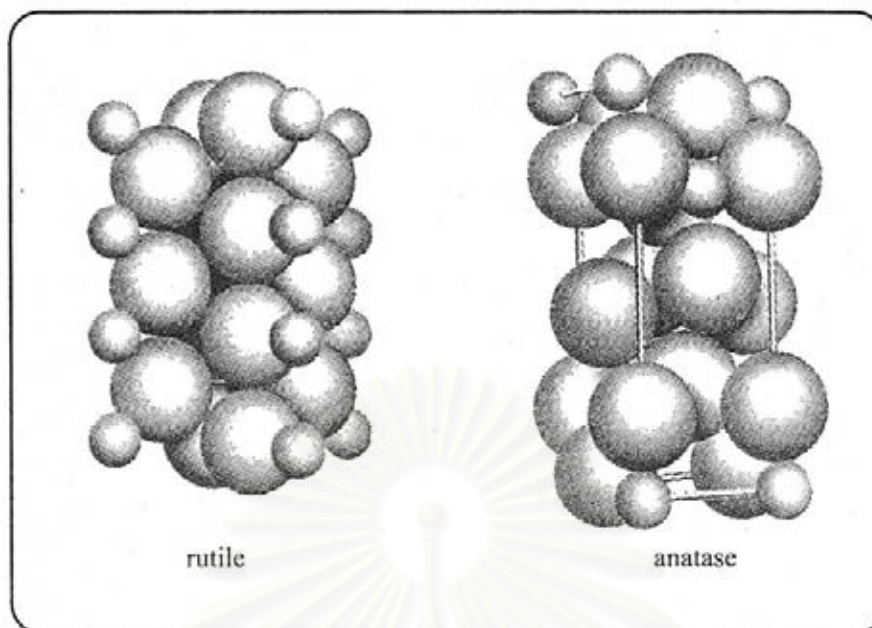


Figure 3.2 Crystal structure of TiO₂. (Fujishima, A. *et al.*, 1999)

Heating amorphous titanium (IV) oxide, prepared from alkyl titanates of sodium titanate with sodium or potassium hydroxide in an autoclave at 200 to 600°C for several days has produced brookite. The important commercial forms of titanium dioxide are anatase and rutile, and these can readily be distinguished by X-ray diffraction spectrometry.

Since both anatase and rutile are tetragonal, they are both anisotropic, and their physical properties, e.g. refractive index, vary according to the direction relative to the crystal axes. In most applications of these substances, the distinction between crystallographic direction is lost because of the random orientation of large numbers of small particles, and it is mean value of the property that is significant.

Table 3.1 Crystallographic properties of anatase, brookite, and rutile.

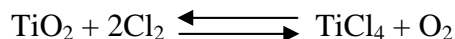
Properties	Anatase	Brookite	Rutile
Crystal structure	Tetragonal	Orthorhombic	Tetragonal
Optical	Uniaxial, negative	Biaxial, positive	Uniaxial, negative
Density, g/cm ³	3.9	4.0	4.23
Harness, Mohs scale	5 ^{1/2} – 6	5 ^{1/2} – 6	7 – 7 ^{1/2}
Unit cell	D _{4h} ¹⁹ .4TiO ₂	D _{2h} ¹⁵ .8TiO ₂	D _{4h} ¹² .3TiO ₂
Dimension, nm			
a	0.3758	0.9166	0.4584
b		0.5436	
c	0.9514	0.5135	2.953

Measurement of physical properties, in which the crystallographic directions are taken into account, may be made of both natural and synthetic rutile, natural anatase crystals, and natural brookite crystals. Measurements of the refractive index of titanium dioxide must be made by using a crystal that is suitably orientated with respect to the crystallographic axis as a prism in a spectrometer. Crystals of suitable size of all three modifications occur naturally and have been studied. However, rutile is the only form that can be obtained in large artificial crystals from melts. The refractive index of rutile is 2.75. The dielectric constant of rutile varies with direction in the crystal and with any variation from the stoichiometric formula, TiO₂; an average value for rutile in powder form is 114. The dielectric constant of anatase powder is 48.

Titanium dioxide is thermally stable (mp 1855°C) and very resistant to chemical attack. When it is heated strongly under vacuum, there is a slight loss of oxygen corresponding to a change in composition to TiO_{1.97}. The product is dark blue but reverts to the original white color when it is heated in air.

Hydrogen and carbon monoxide reduce it only partially at high temperatures, yielding lower oxides or mixtures of carbide and lower oxides. At ca. 2000°C and

under vacuum, carbon reduces it to titanium carbide. Reduction by metal, e.g., Na, K, Ca, and Mg, is not complete. Chlorination is only possible if a reducing agent is present; the position of equilibrium in the system is



The reactivity of titanium dioxide towards acids is very dependent on the temperature to which it has been heated. For example, titanium dioxide that has been prepared by precipitation from a titanium (IV) solution and gently heated to remove water is soluble in concentrated hydrochloric acid. If the titanium dioxide is heated to ca. 900°C, then its solubility in acids is considerably reduced. It is slowly dissolved by hot concentrate sulfuric acid, the rate of salvation being increased by the addition of ammonium sulfate, which raises the boiling point of the acid. The only other acid in which it is soluble is hydrofluoric acid, which is used extensively in the analysis of titanium dioxide for trace elements. Aqueous alkalies have virtually no effect, but molten sodium and potassium hydroxides, carbonates, and borates dissolve titanium dioxide readily. An equimolar molten mixture of sodium carbonate and sodium borate is particularly effective as is molten potassium pyrosulfate.

3.3 Solvothermal Method (Kominami, H. et al., 2003)

Solvothermal method have been developed for synthesis of metal oxide and binary metal oxide with large surface area, high crystallinity and high thermal stability (Payakgul et al 2005) by using solvent as the reaction medium. Use the solvent instead of the water in the hydrothermal method produce the different forms of intermediate phase and the stability of such intermediate phase was not strong. Instability of the intermediate phase gives a large driving force to the formation of product under quite mild condition. Titanium precursor such as titanium alkoxide, was used as starting material for titania synthesis. Titanium precursor was first suspended in organic solvent in a test tube of autoclave. The crystalline titania was formed at temperature in the rang of 200-320 °C in autoclave. Autogeneous pressure during the reaction gradually increased as the temperature was raised. It has

been reported that physiochemical properties of the synthesized titania depend on the reaction conditions as well as the calcination temperature.

3.4 Sol – gel method

This method can be performed at relatively low temperature. The steps of this method starting at titania alkoxide was mixed with alcohol . The mixture of water and acid was added to first mixture (Jung, K.Y. et al., 1999) . The sol-gel was formed by hydrothermal process. This technique can be applied by using ultrasonication to aid dispersion and the efficiency of titania with higher surface area , better thermal stability than stirring method. The average crystal size of titania by this method were in the range of 4 – 8 nm and BET surface area were in the range of 91-120 m²/g depend on calcined temperature. However the limit of this method are the strong reactivity of alkoxide toward H₂O often results in an uncontrolled precipitation.

3.5 Promoters

There are two kinds of promoters such as textural and chemical promoters. Textural promoters are used to facilitate the dispersion of metal phase during preparation and/or reaction conditions. Chemical promoters are used to enhance the activity and/or selectivity of catalysts. Generally, noble, alkali and alkaline earth metals are considered to be chemical promoters, which play important roles on catalyst performance to date.

The effect of promoter such as Ag (Praserthdam, P. et al., 2002 and Ngamsom, B. et al., 2004), K (Kim, W.J. et al., 2004), Si (Shin, E.W. et al., 1998; Shin, E.W. et al., 2002 and Kim, W.J. et al., 2003), Au (Sárkány, A. et al., 2002), Ti (Kang, J.H. et al., 2000; Lee, D.C. et al., 2003; Kim, W.J. et al., 2004; and Kang, J.H. et al., 2002), Nb (Kang, J.H. et al., 2000), Ce (Kang, J.H. et al., 2000) incorporated into palladium catalysts for the selective acetylene hydrogenation reaction were studied. They reported that these metal promoters can improve activity and selectivity of acetylene hydrogenation catalysts.

CHAPTER IV

EXPERIMENTAL

This chapter consists of experimental systems and procedures used in this work which is divided into five parts. The chemicals and preparation of TiO₂ supports are shown in sections 4.1 and 4.2 respectively. Section 4.3 describes the procedures for catalyst preparation including preparation of titania supports, palladium loading, and palladium-silver loading. The fourth part (section 4.4) explains the details of catalyst characterization by various techniques such as XRD, BET surface area, XPS, CO-pulse chemisorption, SEM, TEM, ESR, CO-TPD and C₂H₄-TPD. The last part (section 4.5) describes the catalyst evaluation in term of catalytic activity measurement in selective acetylene hydrogenation.

4.1 Chemicals

The details of chemicals for preparation of TiO₂ supports consisting various phase compositions, TiO₂ supports synthesized by sol-gel and solvothermal methods, and these TiO₂ employed as supports for Pd and Pd-Ag catalysts in acetylene selective hydrogenation were shown in table 4.1

สถาบันวิทยบริการ
จุฬาลงกรณ์มหาวิทยาลัย

Table 4.1 Chemicals used in the experiment

Chemical	supplier
Titanium (IV) tert-butoxide (97% TNB, $\text{Ti}[\text{O}(\text{CH}_2)_3\text{CH}_3]_4$)	Aldrich
Titanium dioxide (pure anatase)	Aldrich
Titanium isopropoxide	Aldrich
1,4-butanediol (1,4-BG, $\text{HO}(\text{CH}_2)_4\text{OH}$)	Aldrich
Palladium (II) nitrate hydrate	Aldrich
Methyl alcohol	Aldrich
Ethyl alcohol	Mallinckrodt
Silver nitrate	APS Finechem

4.2 Preparation of TiO_2 supports

4.2.1 Preparation of TiO_2 supports consisting of various phase compositions

The various ratios of rutile:anatase in titania support will be prepared by calcination pure anatase of TiO_2 supports in air at temperatures between 900-1010°C at the rate of 10 °C/min and held at that temperature for 4 hours. The ratios of rutile:anatase will be determined by XRD according to the method described by Jung et al., 1999 as follows:

$$\% \text{ Rutile} = \frac{1}{[(A/R)0.884 + 1]} \times 100 \quad (1)$$

Where, A and R are the peak area for major anatase ($2\theta = 25^\circ$) and rutile phase ($2\theta = 28^\circ$), respectively.

4.2.2 Preparation TiO₂ using the solvothermal method

Titanium dioxide was prepared using 25 g of TNB. The starting material was suspended in 100 ml of solvent (1,4-butanediol) in a test tube and then set up in an autoclave. In the gap between the test tube and autoclave wall, 30 ml of solvent was added. After the autoclave was completely purged with nitrogen, the autoclave was heated to desired temperature (320°C) at the rate of 2.5°C min⁻¹ and held at that temperature for 6 hours. Autogeneous pressure during the reaction gradually increased as the temperature was raised. After the reaction, the autoclave was cooled to room temperature. The resulting powders were collected after repeated washing with methanol by centrifugation. They were then air-dried at room temperature. All equipments used in this study are consisted of:

4.2.2.1 Autoclave reactor

- Made from stainless steel
- Volume of 1000 cm³
- 10 cm inside diameter
- Maximum temperature of 350°C
- Pressure gauge in the range of 0-140 bar
- Relief valve used to prevent runaway reaction
- Iron jacket was used to reduce the volume of autoclave to be 300 cm³
- Test tube was used to contain the reagent and glycol

The autoclave reactor is shown in Figure 4.1

4.2.2.2 Temperature program controller

A temperature program controller CHINO DB1000F was connected to a thermocouple with 0.5 mm diameter located inside the autoclave.

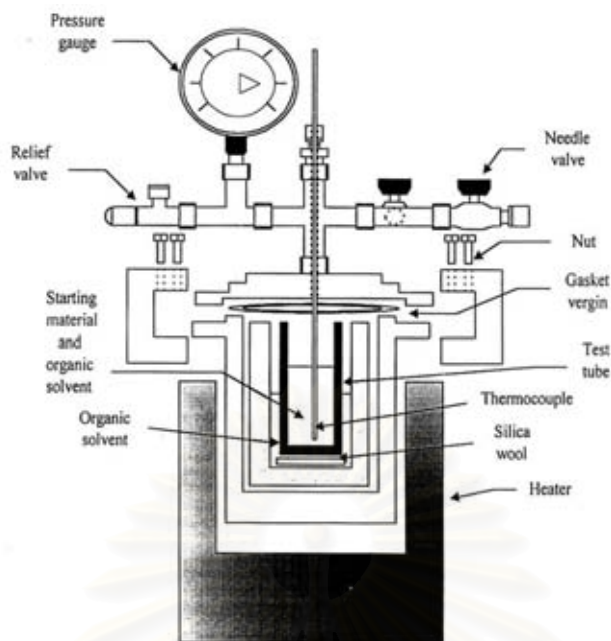


Figure 4.1 Autoclave reactor

4.2.2.3 Electrical furnace (Heater)

Electrical furnace was used to supply the required heat to the autoclave for the reaction.

4.2.2.4 Gas controlling system

Nitrogen was set with a pressure regulator (0-150 bar) and needle valves are used to release gas from autoclave. The diagram of the reaction equipment is shown in Figure 4.2

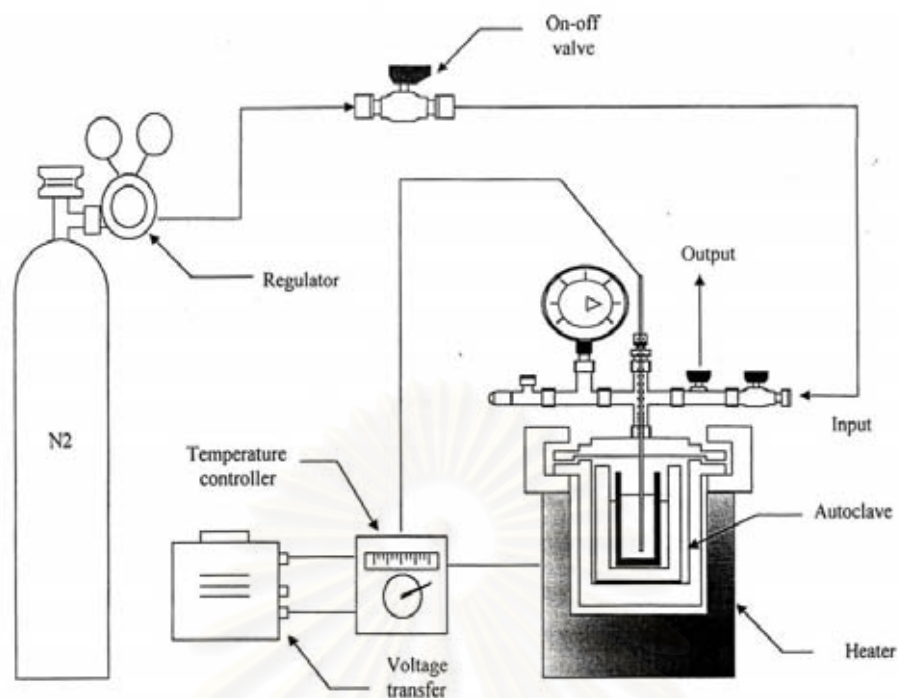


Figure 4.2 Diagram of the reaction equipment for the catalyst preparation.

4.2.3 Preparation of TiO₂ using the sol-gel method

Titania nanocrystals were synthesized via sol-gel process of titanium ethoxide (Ti -20%, Aldrich). A specific amount of precursor was dissolved in ethanol, and mixed with a water-ethanol solution at water to alkoxide molar ratio equal to 165. A precursor solution was added dropwise to the aqueous solution and was stirred by ultrasonic vibration at room temperature. White precipitates of hydrous oxides formed instantly and the mixture was stirred for at least two more hours. The amorphous precipitates were separated from the mother liquor by centrifugation and were redispersed in ethanol for five times to minimize particle agglomeration. The resulting materials were then dried and calcined at 450°C in flowing oxygen for 2 hours and the heating rate was at 10°C/min (Suriye, K. et al., 2005)

4.3 Palladium and Palladium –Silver loading

1wt%Pd and 1wt%Pd-3wt%Ag over TiO₂ supports were prepared by the sequential impregnation technique detailed as follows:

(1) Titanium dioxide supports were impregnated with a solution of palladium by the incipient wetness technique. Using the water capacity measurement obtained previously for the titanium dioxide particles, a sufficient amount of the palladium salt was added to obtain a 1% weight of palladium.

(2) The impregnated support was left to stand for 6 hours to assure adequate distribution of metal complex. The support was subsequently dried at 110°C in air overnight.

(3) The dried impregnated support was calcined under 60 ml/min nitrogen with the heating rate of 10°C/min until the temperature reached 500°C. 100ml/min of flowing air was then switched into the reactor to replace nitrogen and the temperature was held at 500°C for 2 hours.

(4) The palladium impregnated sample was re-impregnated with silver complex using a similar procedures with the exception that the calcination were performed at 370°C and held at the temperature for 1 hours.

(5) The calcined sample was finally cooled down and stored in a glass bottle in a desiccator for later use.

4.4 Catalyst Characterization

4.4.1 X-Ray Diffraction (XRD)

XRD was performed to determine the bulk phase of catalysts by SIEMENS D 5000 X-ray diffractometer using CuK_α radiation with Ni filter in the 2θ range of 20-80 degrees resolution 0.04°

4.4.2 BET Surface Area

The BET surface area of samples were measured by N_2 physisorption, with nitrogen as the adsorbate using a micromeritics model ASAP 2000 automated system degassing at 200°C for 1 h prior to N_2 physisorption

4.4.3 CO-Pulse Experiment

Palladium dispersion was determined by pulsing carbon monoxide over the reduce catalyst. The amounts of CO chemisorbed on the catalysts were measured using a Micromeritic Chemisorb 2750 automated system attached with ChemiSoft TPx software at room temperature. The number of metal active sites was measured in the basic assumption that only one CO molecule adsorbed on one metal active site (Vannice, M.A. et al., 1981; Anderson, A.B. et al., 1985; Ali, S.H. et al., 1998 and Mahata, N. et al., 2000).

Approximately 0.2 g of catalyst was filled in a quartz tube, incorporated in a temperature-controlled oven and connected to a thermal conductivity detector (TCD). He was introduced into the reactor at the flow rate of 30 ml/min in order to remove remaining air. Prior to chemisorption, the samples were reduced in a H₂ flow rate at 50 ml/min with heated at an increasing rate of 10 °C/min from room temperature to 500°C and held at this temperature for 1 h after that cooled down to ambient temperature in a He flow, then CO was plused into the catalyst bed at room temperature. Carbon monoxide that was not adsorbed was measured using thermal conductivity detector. Pulsing was continued until no further carbon monoxide adsorption was observed. Calculation details of %metal dispersion are given in Appendix C.

4.4.4 Scanning Electron Microscopy (SEM)

Catalyst granule morphology and elemental distribution were obtained using a JEOL JSM-35F scanning electron microscope. The SEM was operated using the back scattering electron (BSE) mode at 20 kV at the Scientific and Technological Research Equipment Center, Chulalongkorn University (STREC)

4.4.5 Transmission Electron Microscopy (TEM)

The palladium oxide particle size and distribution of palladium on silica supported were observed using JEOL-JEM 200CX transmission electron microscope operated at 100 kV at National Metal and Materials Technology Center, MTEC

4.4.6 Electron Spin Resonance (ESR.)

ESR was performed to determine the defect of surface catalysts by JEOL model JES-RE2X at the Scientific and Technological Research Equipment Center, Chulalongkorn University (STREC)

4.4.7 X-ray photoelectron spectroscopy (XPS)

The XPS analysis was performed using an AMICUS photoelectron spectrometer equipped with a Mg K_{α} X-ray as a primary excitation and a KRATOS VISION2 software. XPS elemental spectra were acquired with 0.1 eV energy step at a pass energy of 75 kV. The C 1s line was taken as an internal standard at 285.0 eV.

4.4.8 Temperature Programmed Desorption

Temperature programmed desorption (TPD) study was performed in a Micromeritic ChemiSorb 2750 automated system attached with ChemiSoft TPx software. The amount of C_2H_4 or CO adsorbed on the surface was determined by temperature programmed desorption with a temperature range from 35 to 500 °C. The thermal conductivity detector was used to measure the amount of C_2H_4 .

Approximately 0.05 g of a calcined catalyst was placed in a quartz tube in a temperature-controlled oven and reduced by hydrogen flowing over catalyst at the rate of 50 ml/min for 1 h at 500 °C using a ramp rate of 10 °C and cooled down to the room temperature by helium flow. The catalyst surface was adsorbed with ethylene or CO by applying a high purity grade ethylene or CO at 60 ml/min for 1 h ensuring the saturated catalyst. Then the samples were flushed with helium at flow rate of 30 ml/min down to room temperature for about 1 h. The temperature-programmed desorption was performed with a constant heating rate of ca. 10 °C/min from 35 °C to 500 °C. The amount of desorbed ethylene or CO was measured by analyzing the effluent gas with a thermal conductivity detector.

4.5 Reaction study in acetylene hydrogenation

Selective acetylene hydrogenation was performed in a quartz tube reactor (ID 9 mm). Feed gas composed of 1.46% C₂H₂, 1.71% H₂, 15.47% C₂H₆ and balanced C₂H₄ (Rayong Olefin Co., Ltd) and a GHSV of 2,8818.88 h⁻¹ were used. The composition of product and feed stream were analyzed by a Shimadzu GC 8A equipped with TCD and FID detectors (molecular sieve-5A and carbosieve S2 columns, respectively). The operating conditions for each instrument are summarized in table 4.2

Approximately 0.2 g of catalyst was packed in a quartz tubular down flow reactor. The catalyst bed length was about 0.3 cm. The reactor was placed into the furnace and argon was introduced into the reactor in order to remove remaining air. Prior to reaction, the catalyst was reduced with 100 ml/min hydrogen flow at a temperature of 500°C and held at that temperature for 1 h. Afterwards, argon was switched in to replace hydrogen for cooling down to the reaction temperature, 40°C. The reactant gases was introduced at temperature from 40 and 1 atm, sampling was undertaken when the steady state of the system was reached, which was approximately within 1 h. Effluent gases were sampled to analyze the concentration of CH₄, C₂H₂, C₂H₄ and C₂H₆ using GC-9A, whereas H₂ concentration was analyzed by GC-8A. System of acetylene hydrogenation is shown in Figure 4.3. The Details of the calculation of the catalyst activity to convert acetylene and the selectivity are given in Appendix E.

Table 4.2 Operating conditions of gas chromatograph for selective hydrogenation of acetylene

Gas Chromatograph	SHIMADZU FID GC 9A	SHIMADZU TCD GC 8A
Detector	FID	TCD
Packed column	Carbosieve column S-II	Molecular sieve 5A
Carrier gas	Ultra high purity N ₂	Ultra high purity Ar
Carrier gas flow rate (ml/min)	30	30
Injector temperature (°C)	185	80
Detector temperature (°C)	185	80
Initial column temperature (°C)	100	50
Initial holding time (min)	50	-
Programmed rate (°C/min)	10	-
Final column temperature (°C)	160	50
Final holding time (min)	160	-
Current (mA)	-	70
Analyzed gas	CH ₄ , C ₂ H ₂ , C ₂ H ₄ , C ₂ H ₆	H ₂

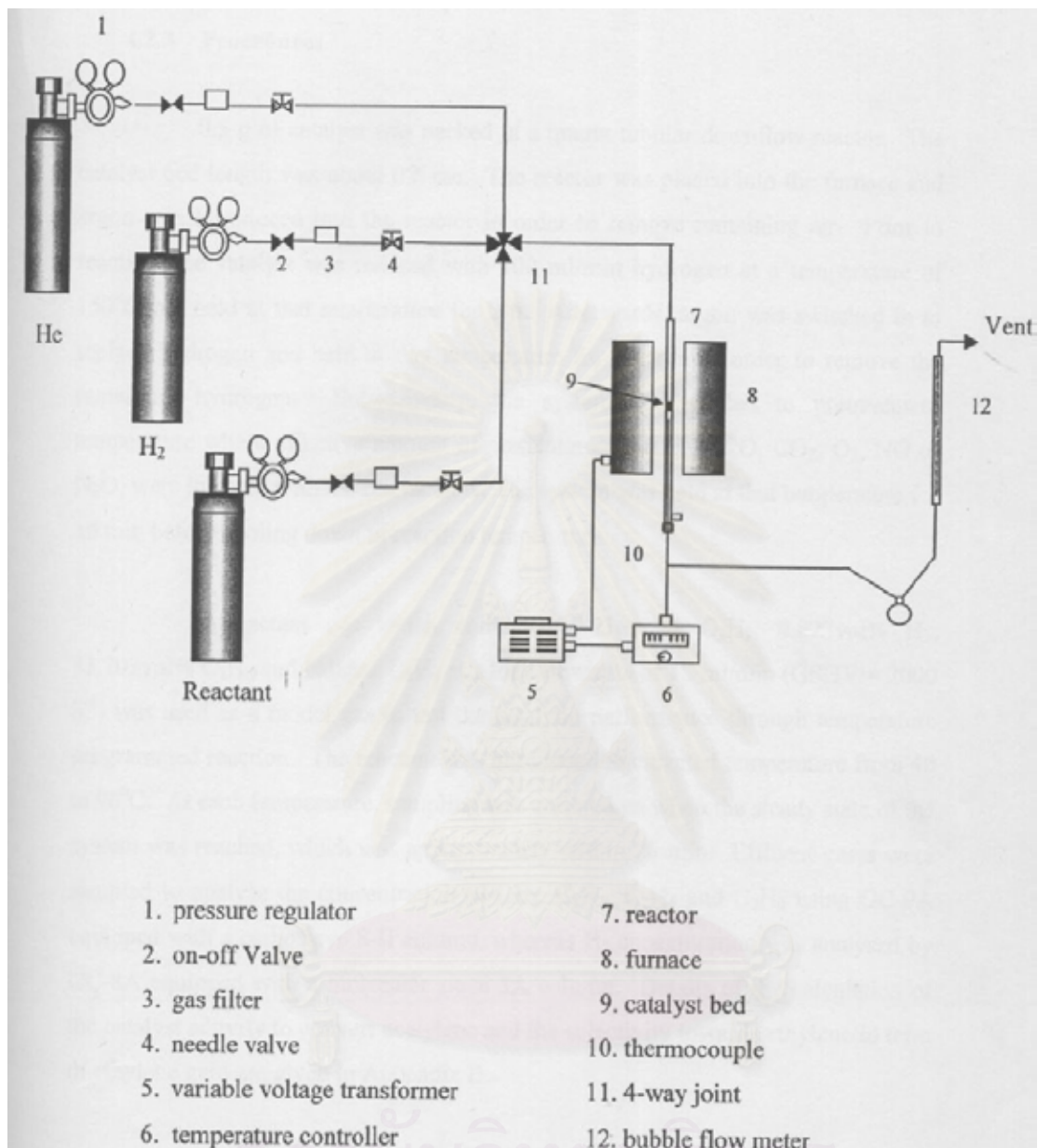


Figure 4.3 A schematic of acetylene hydrogenation system.

CHAPTER V

RESULTS AND DISCUSSION

The study was conducted in order to investigate the physicochemical properties of TiO_2 , 1%Pd/ TiO_2 , and 1%Pd- 3%Ag/ TiO_2 in which TiO_2 was either commercially obtained and prepared with various rutile/anatase phase compositions or synthesized in laboratory by different methods (sol-gel and solvothermal). The catalytic properties were evaluated using selective hydrogenation of acetylene in excess ethylene as probe reaction. The results in this chapter are divided into two major parts. The first part describes the characteristics of commercial TiO_2 consisting of various phase compositions (section 5.1), the catalytic properties and activities of Pd/ TiO_2 (section 5.2) and Pd-Ag/ TiO_2 (section 5.3), the proposed mechanism for selective acetylene hydrogenation on TiO_2 supported Pd and Pd-Ag catalysts (section 5.4). The other part describes the characteristics of the synthesized TiO_2 (section 5.5) and the catalytic properties and activities of Pd/ TiO_2 (section 5.6), and Pd-Ag/ TiO_2 (section 5.7) in selective acetylene hydrogenation.

5.1 TiO_2 consisting of various crystalline phase compositions

TiO_2 has three main crystal structures: anatase, which tends to be more stable at low temperature; brookite, which is usually found in minerals and has an orthorhombic crystal structure; and rutile, which is the stable form at higher temperature (Rao, C.N.R. et al., 1961). The different phase compositions of titania could play an important role on the catalytic properties.

5.1.1 Properties of TiO_2 support consisting of various phase compositions

5.1.1.1 X-ray diffraction (XRD)

Pure anatase Titania was gradually transformed into titania by calcinations in air under different temperatures. XRD patterns of the calcined TiO_2 samples are

shown in Figure 5.1. For the pure anatase titania, XRD peaks at 25° , 37° , 48° , 55° , 56° , 62° , 71° , and 75° 2θ were evident. XRD peaks for rutile phase at 28° (major), 36° , 42° , and 57° appeared after calcinations. The amount of rutile phase formed during calcinations depended on the temperature used and was calculated using the areas of the major anatase and rutile XRD peaks according to the method described by Jung, K.Y. et al., 1999 as follows:

$$\% \text{Rutile} = \frac{1}{\left[\left(\frac{A}{R} \right) 0.884 + 1 \right]} \times 100$$

where A and R are the peak areas for major anatase ($2\theta = 25^\circ$) and rutile phase ($2\theta = 28^\circ$), respectively.

The titania samples consisting of 0, 17, 44, 85, and 100% rutile phase were named as TiO₂-R0, R17, R44m R85, and R100, respectively.

5.1.1.2 BET surface areas

The most common procedure for determining surface area of a solid is based on adsorption and condensation of nitrogen at liquid nitrogen temperature using static vacuum procedure. This method is also called BET (Brunauer Emmett Teller) method.

The BET surface areas of samples are shown in Table 5.1, After being subjected to the thermal treatment (calcination), BET surface areas of the TiO₂ samples decreased essentially from 64.4 for R0 (pure anatase) to 18.3 m²/g for R100 (pure rutile).

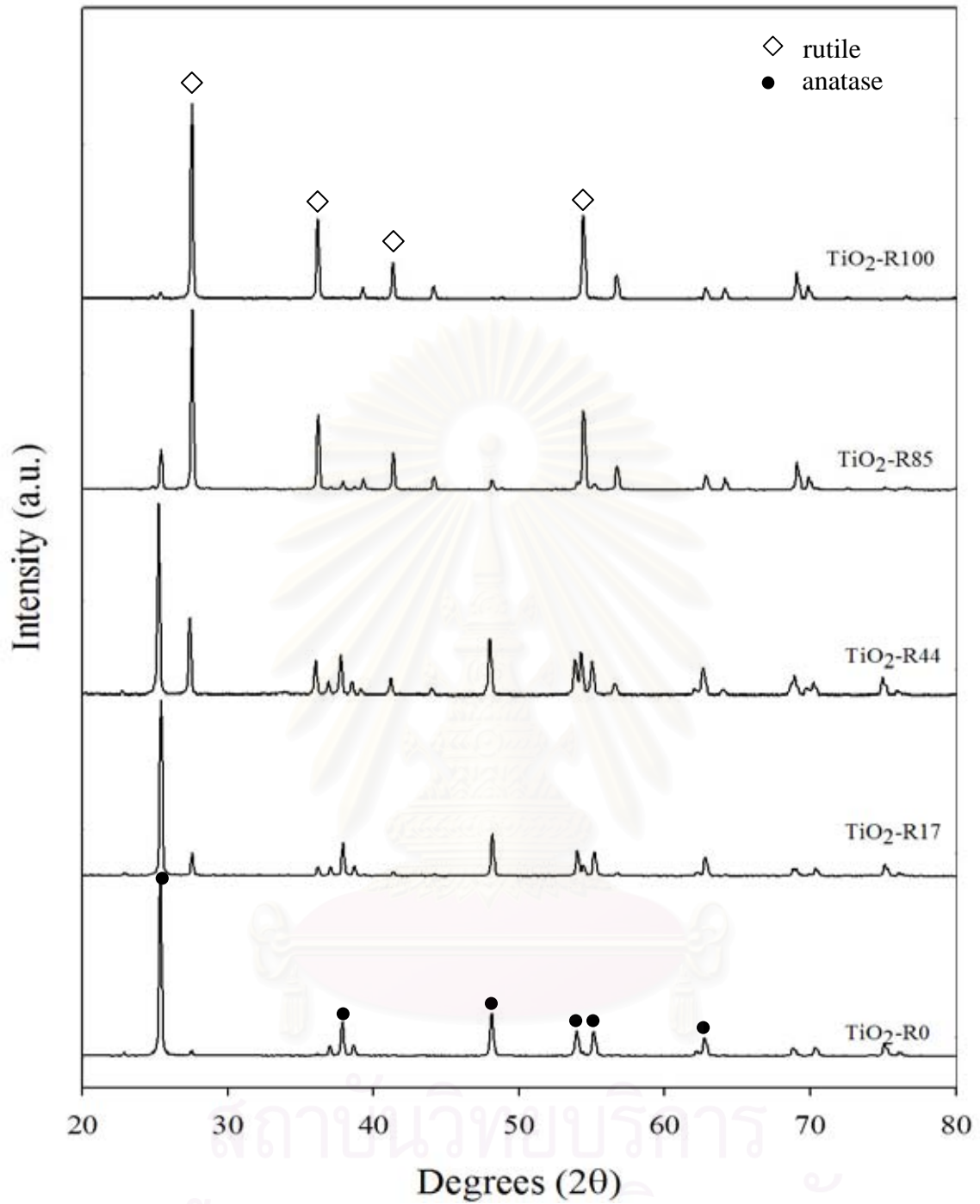


Figure 5.1 XRD patterns of TiO₂ samples consisting of different % rutile phase.

Table 5. 1 TiO₂ samples consisting of various % rutile phase

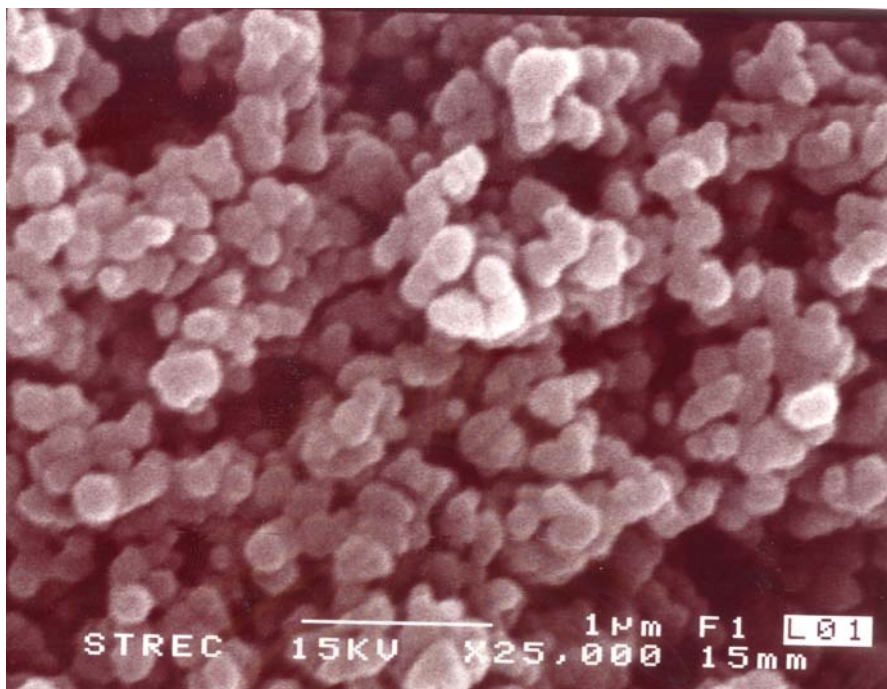
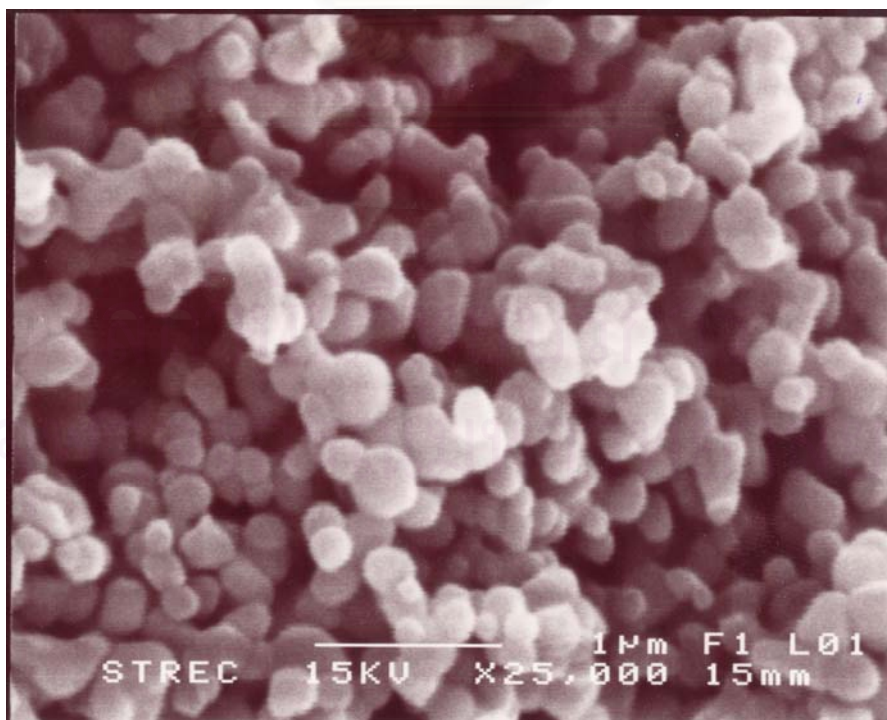
Sample	%Rutile	BET S.A. (m ² /g)
TiO ₂ -R0	0	64.4
TiO ₂ -R17	17	38.6
TiO ₂ -R44	44	25.0
TiO ₂ -R85	85	23.5
TiO ₂ -R100	100	18.3

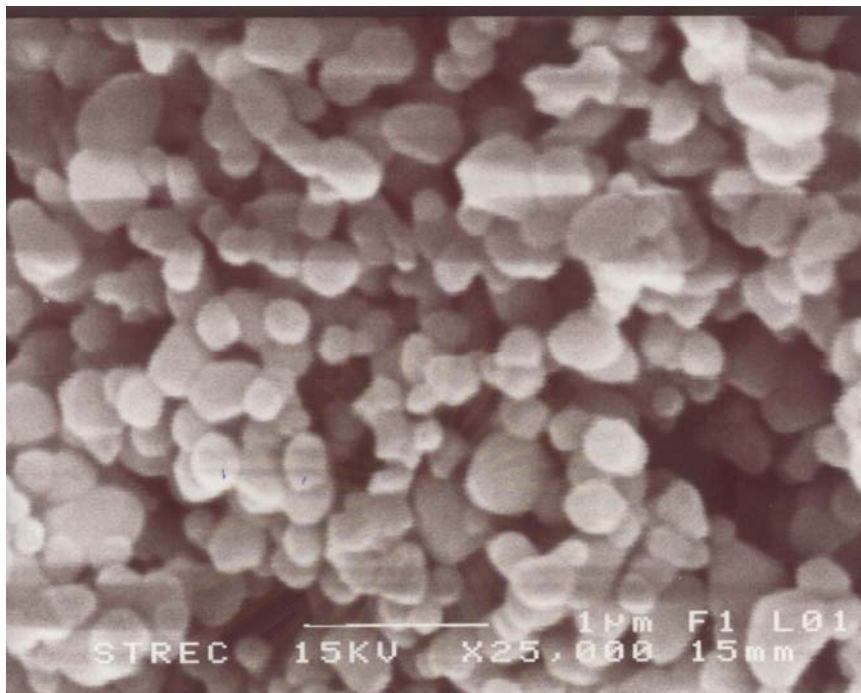
5.1.1.3 Scanning electron microscopy (SEM)

Scanning electron microscopy (SEM) is a powerful tool for observing directly surface texture, morphology and particle granule size of catalyst materials. In the backscattering mode (SEM), the electron beam focused on the sample is scanned by a set of deflection coil. Backscattered electrons or secondary electrons emitted from the sample are detected.

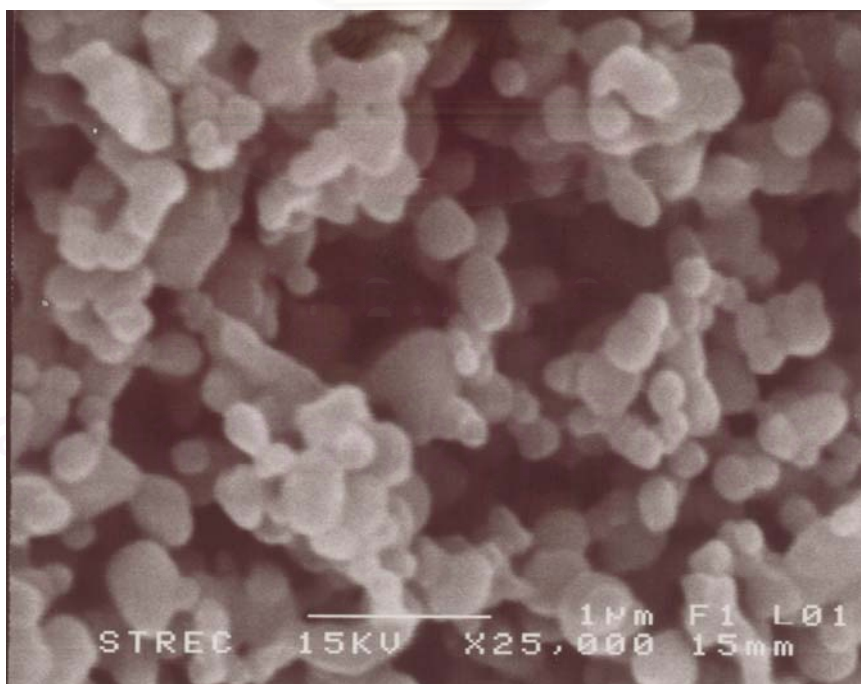
The SEM micrographs of various titania samples are shown in Figure 5.2. The morphology of the titania particles was found to be clearly seen more agglomeration of the particles with increasing % rutile phase in the TiO₂ samples.

สถาบันวิทยบริการ
จุฬาลงกรณ์มหาวิทยาลัย

(A) TiO₂-R0(B) TiO₂-R17



(C) TiO₂-R44



(D) TiO₂-R85

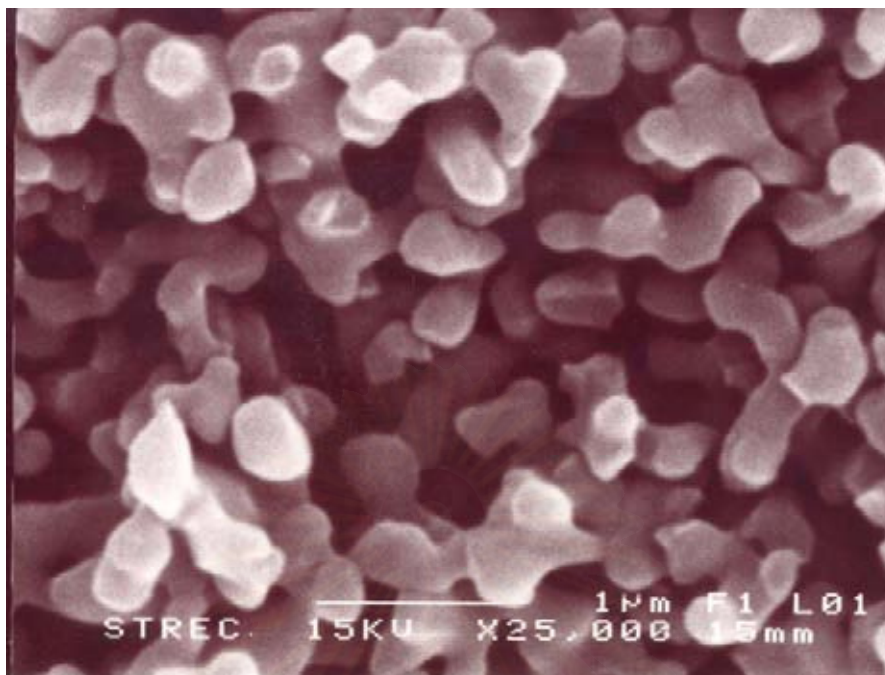
(E) TiO₂-R100

Figure 5.2 SEM micrographs of various TiO₂ consisting of various % rutile phase.

5.1.1.4 Electron spin resonance spectroscopy (ESR)

The number of Ti³⁺ defective sites of titania particles were determined using electron spin resonance spectroscopy technique. The ESR results are shown in Figure 5.3. Such Ti³⁺ species are produced by trapping of electrons at defective sites of TiO₂ and the amount of accumulated electrons may therefore reflect the number of defective sites (Ikeda, S. et al., 2003). The signal of g value less than 2 was assigned to Ti³⁺ (3d¹) (Salama, T.M. et al., 1993 and Howe, R.F. et al., 1985). TiO₂ samples show Ti³⁺ ESR signal at g = 1.93-1.999. No Ti³⁺ ESR signal was observed for TiO₂ consisting of %rutile phase ≥ 85%. It is suggested that Ti⁴⁺ in the TiO₂ with higher %rutile is more difficult to be reduced to Ti³⁺. As rutile titania is more thermodynamically and structurally stable than anatase titania so that the Ti³⁺ ions fixed in the surface lattice of anatase TiO₂ is easier to diffuse to the surface than one in the surface lattice of rutile TiO₂ (Li, Y. *et al.*,2004). The results in this study

suggest a threshold limit of maximum %rutile in the TiO_2 sample so that the presence of Ti^{3+} can be detected by ESR technique.

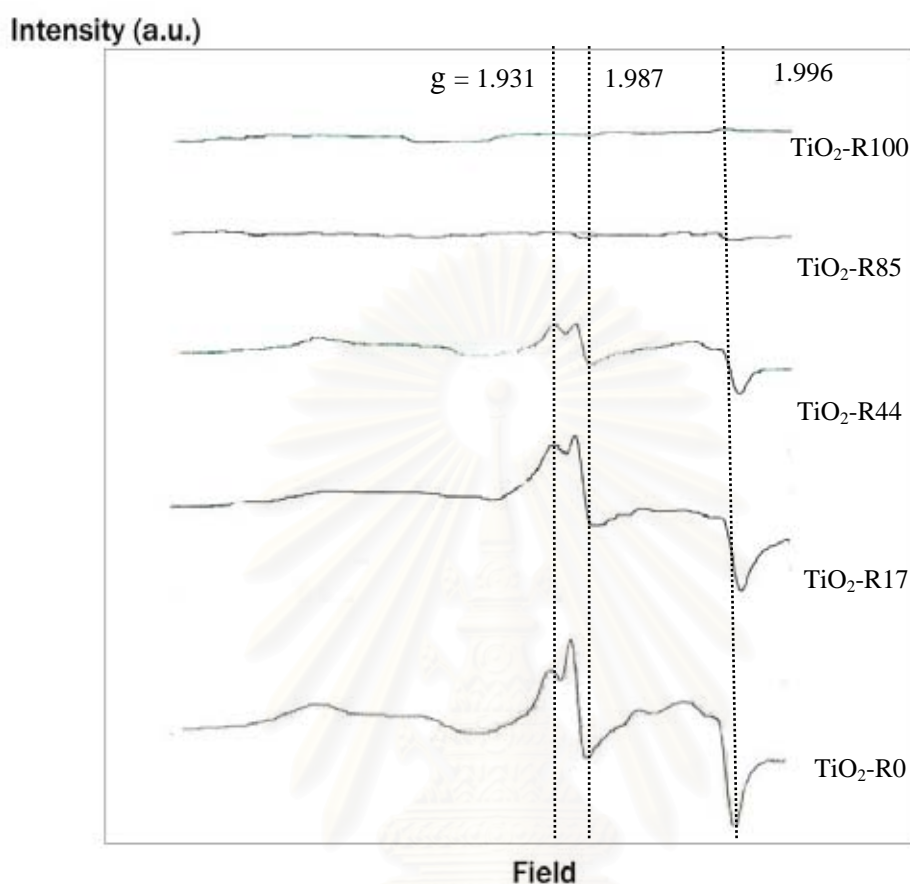


Figure 5.3 ESR spectra of TiO_2 consisting various % rutile phase.

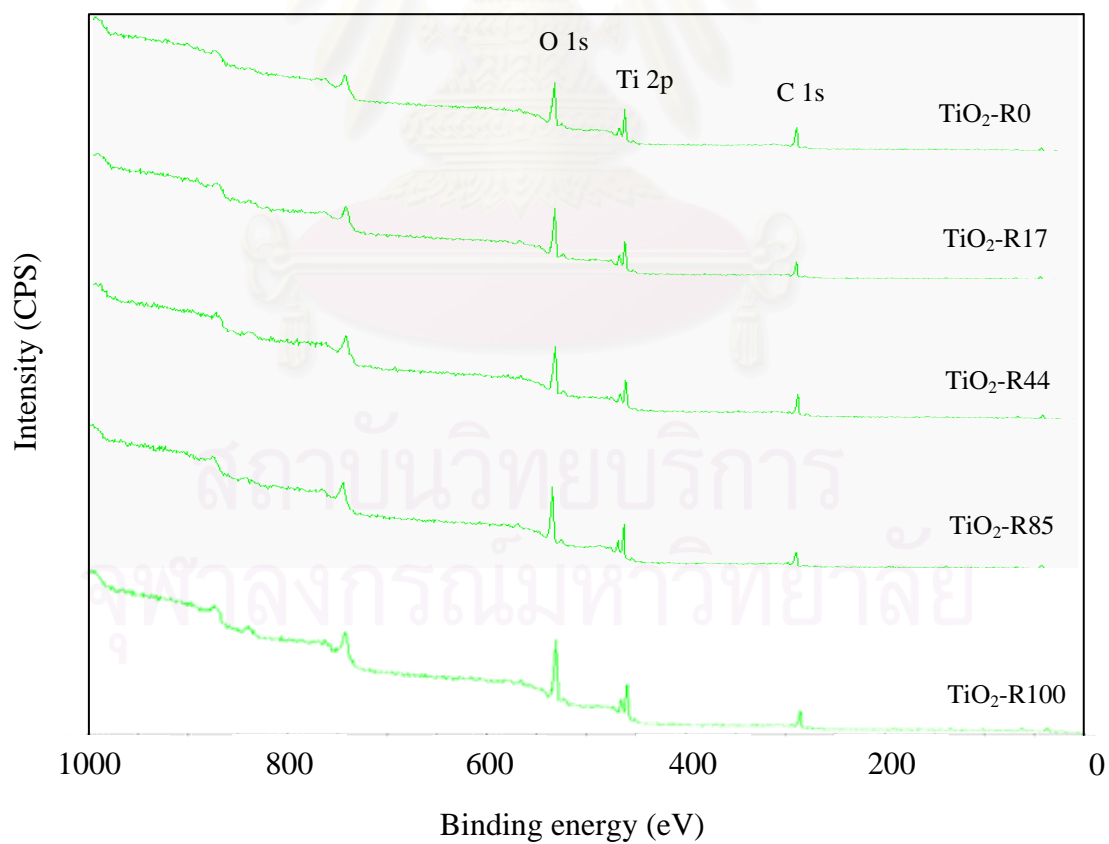
5.1.1.5 X-ray photoelectron spectroscopy, XPS

The survey XPS spectra for pure rutile and anatase TiO_2 samples were recorded with a photon energy of 1256 eV ($\text{Mg K}\alpha$), the kinetic energies of the emitted electrons being in the range of 0-1000 eV. The XPS results estimated the relative concentration of Ti and O on TiO_2 surface summarized in Table 5.2. The Ti/O ratios for TiO_2 were found to be range from 0.24-0.28 which decreased slightly when the amount of %rutile phase was raised, suggesting that The XPS survey spectra and the core level XPS spectra of Ti 2p, O 1s, and C 1s recorded from various TiO_2

samples are given in Figure 5.4, 5.5, 5.6, and 5.7, respectively. Sharp and intense peaks at binding energies 464.2 and 458.5 eV indicate only the presence of Ti^{4+} in the TiO_2 samples (Liqiang.J. et al., 2003 and Price. N. J. et al., 1999). O 1s and C 1s peak were identified at binding energy 530 and 285 eV, (Guillot, J. et al., 2001), respectively. No Ti^{3+} XPS spectra were seen for all the TiO_2 samples under these conditions. It is likely that there was an oxygen-rich layer near the surface of the TiO_2 particles, which is formed by oxygen adsorption and easy oxidation of titanium surface (Zhang, F. et al., 1997). In order to observe the reduced Ti species (i.e., Ti^{3+} , Ti^{2+}) that might exist in the bulk of the TiO_2 samples, TiO_2 surface were subjected to an argon-ion bombardment for 2 min. Ti 2p XPS spectra of the Ar^+ etched- TiO_2 samples and etched TiO_2 -R100 after various time are illustrated in Figure 5.8. The presence of new Ti $2p^{1/2}$ and $2p^{3/2}$ peaks at lower binding energies of 461.2 and 456.5 eV indicated Ti^{3+} species in the TiO_2 (Liqiang, J. et al., 2003; Price, N. J. et al., 1999; Kumar, P. et al., 2000 and Charles, E. et al., 2002). It was found that the intensities of Ti^{3+} for both Ti $2p^{1/2}$ and $2p^{3/2}$ peaks increased with decreasing amount of %rutile phase. In addition, increasing etching time on TiO_2 samples were found obviously intensity of Ti^{3+} for TiO_2 -R100 shown in figure 5.9 The results were found to be in accordance with our ESR results. Moreover, Ti 2p peaks indicative of Ti^{2+} species (Zhang, F. et al., 1997 and Charles, E. et al., 2002) were also observed at binding energies 451.8 and 454.3 eV for TiO_2 sample with low %rutile phase.

Table 5.2 %atomic concentration of Ti and O on TiO₂ surface from XPS results

Sample	Binding energy (eV)		Atomic conc.%		Atomic ratio
	Ti 2p	O 1s	Ti 2p	O 1s	Ti/O
TiO ₂ -R0	458.704	529.978	13.18	45.98	0.287
TiO ₂ -R17	457.953	530.000	14.82	53.58	0.277
TiO ₂ -R44	458.790	530.123	13.79	50.82	0.271
TiO ₂ -R85	458.900	530.300	12.34	49.26	0.251
TiO ₂ -R100	458.800	530.229	10.53	42.73	0.246

**Figure 5.4** XPS survey spectra of TiO₂ samples

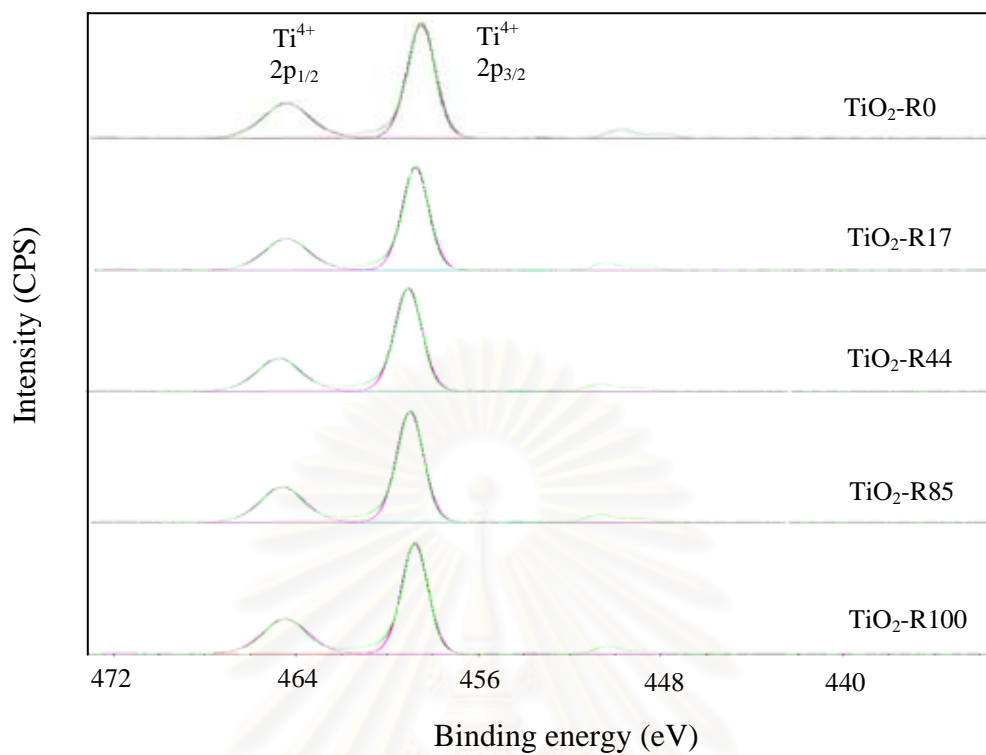


Figure 5.5 XPS Ti 2p spectra of TiO₂ samples

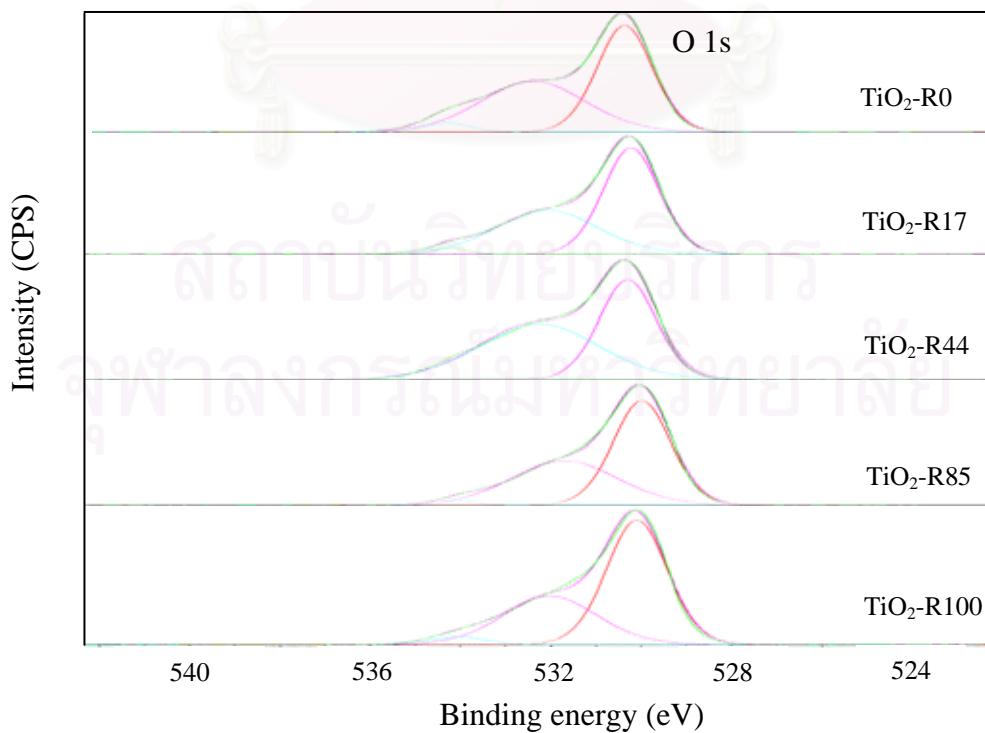


Figure 5.6 XPS O 1s spectra of TiO₂ samples

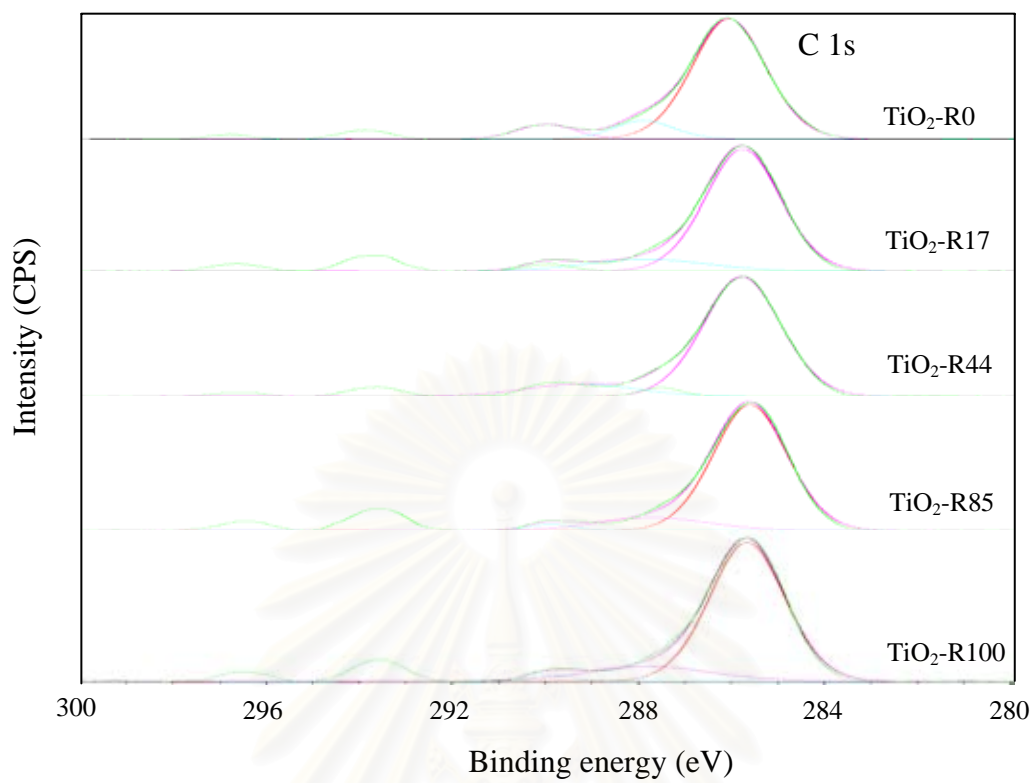


Figure 5.7 XPS C 1s spectra of TiO₂ samples

สถาบันวิทยบริการ
จุฬาลงกรณ์มหาวิทยาลัย

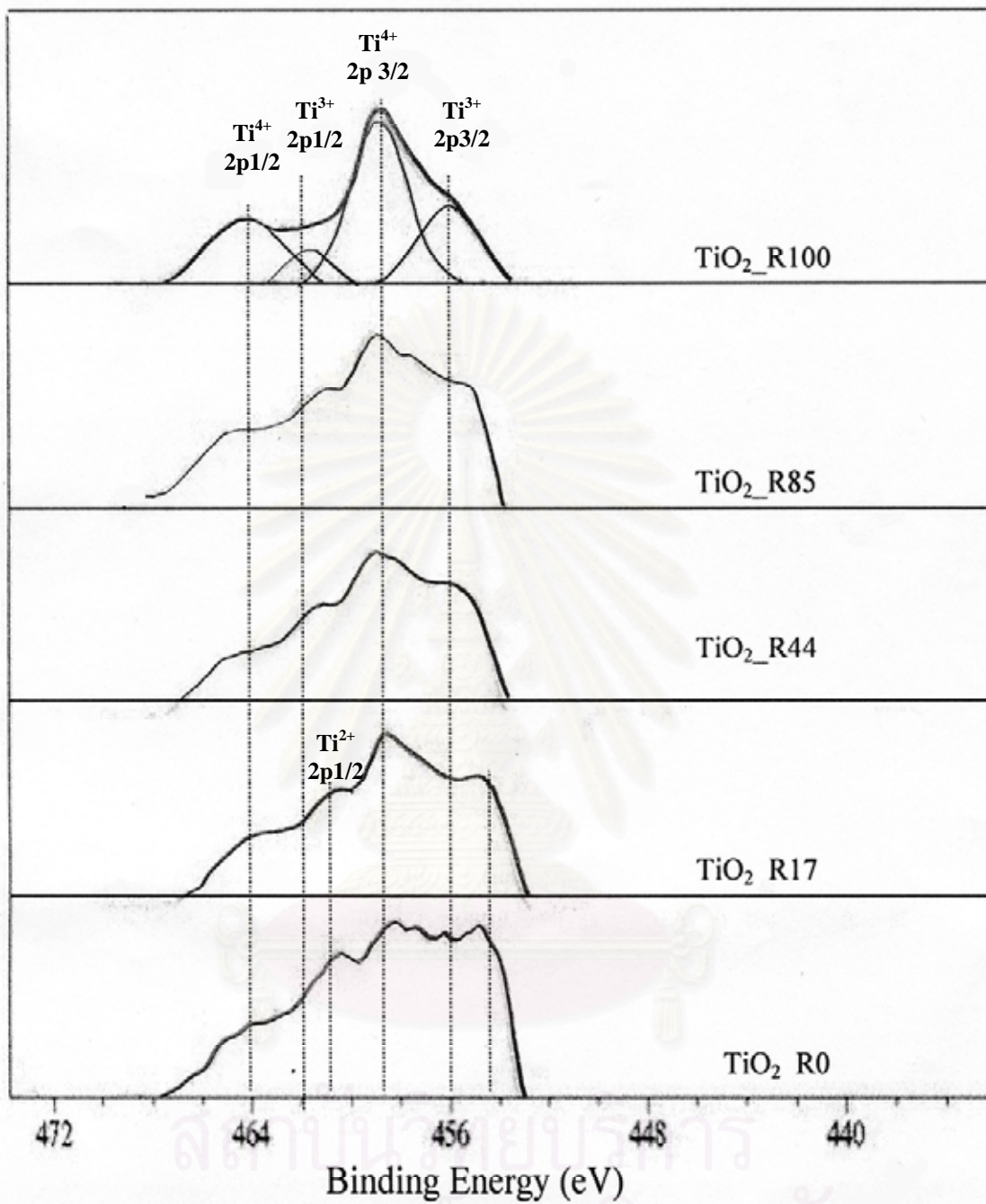


Figure 5.8 XPS Ti 2p spectra of TiO₂ samples after 2 min etching by Ar⁺.

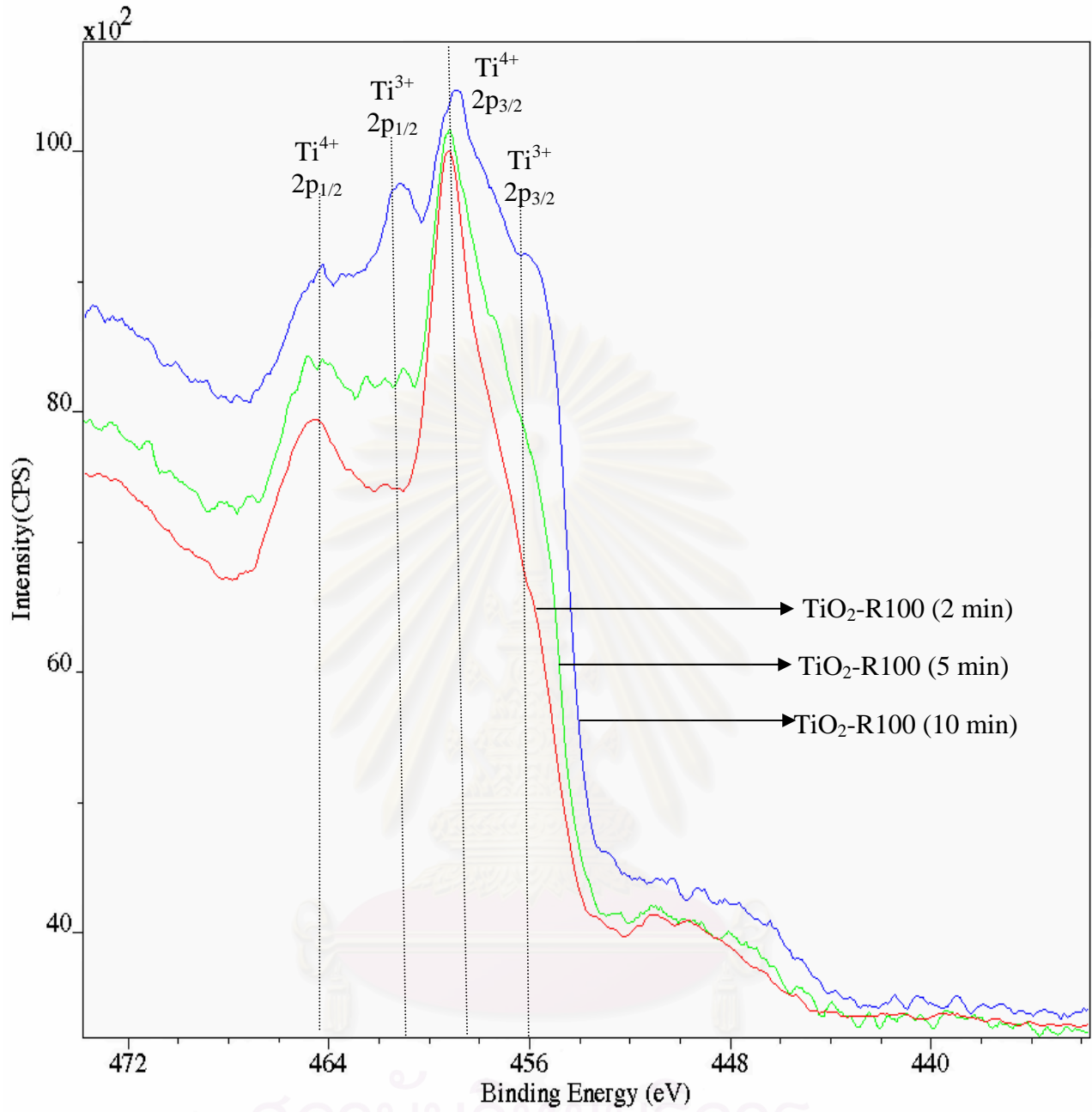


Figure 5.9 XPS Ti 2p spectra of $\text{TiO}_2\text{-R100}$ sample after 2, 5, and 10 mins etching by Ar^+ .

5.2. Catalyst Characterization of Pd catalysts

5.2.1 Properties of 1% Pd over TiO₂ catalysts

5.2.1.1 X-ray diffraction (XRD)

Phase structure of the prepared catalysts was characterized by X-ray diffraction technique. The XRD pattern of the titania supported palladium catalysts are shown in Figure 5.10. From the XRD results of 1%Pd/TiO₂, no diffraction peaks of PdO ($2\theta = 33.9^\circ$) or Pd⁰ ($2\theta = 40.2^\circ$ and 46.7°) were observed for the catalyst samples after calcinations at 500°C for 1 h suggesting that palladium was highly dispersed on the titania surface. The TiO₂ support peaks of various %rutile phase were still the same as those before Pd loading indicating that the phase compositions of the catalyst were not affected by impregnation of palladium.

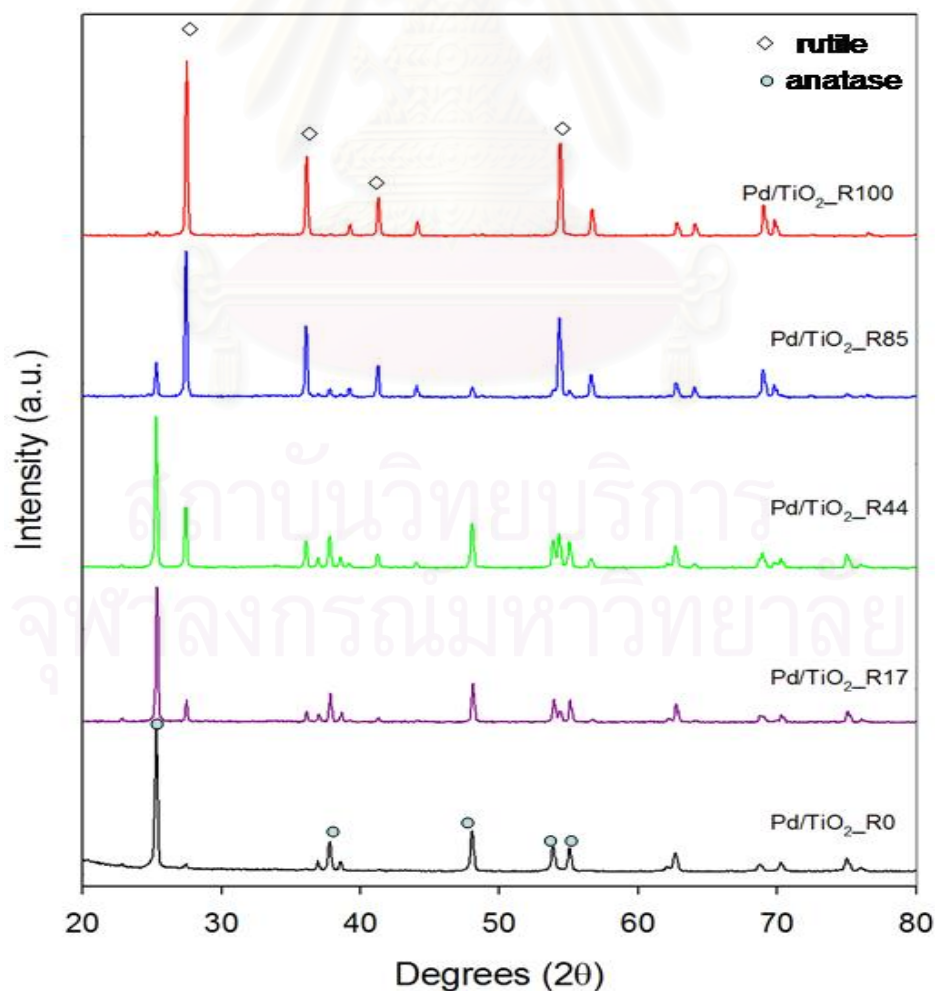


Figure 5.10 XRD pattern of 1%Pd/TiO₂ catalysts consisting various %rutile phase.

5.2.1.2 BET surface areas

BET surface area of the titania supported palladium catalysts determined by N₂ physisorption measurement are shown in Table 5.3. BET surface area of the TiO₂-supported Pd catalysts decreased from 44.5 for Pd/TiO₂-R0 to 17.2 m²/g for Pd/TiO₂-R100. When compared the BET surface area of the pure titania supports and the titania supported palladium catalysts, it was found that BET surface areas of the TiO₂-supported Pd catalysts were slightly less than that of the original TiO₂ supports suggesting that palladium was deposited in some of the pores of TiO₂.

Table 5.3 BET surface area Pd catalysts

Sample	BET S.A. (m ² /g)
Pd/TiO ₂ -R0	44.5
Pd/TiO ₂ -R17	27.1
Pd/TiO ₂ -R44	20.1
Pd/TiO ₂ -R85	19.8
Pd/TiO ₂ -R100	17.2

5.2.1.3 Metal active sites

The metal active sites measurement is based on CO chemisorption technique on the assumption that only CO molecule adsorbs on one palladium site (Anderson *et al.*,1985). The amounts of CO chemisorption on the catalysts reduced at high temperature, 500°C and the percentages of palladium dispersion are given in Table 5.4. It was found that as %rutile phase increased from 0-100%, the amounts of CO chemisorption decreased from 2.23 x10¹⁸ for Pd/TiO₂-R0 to 1.55 x10¹⁸ molecules CO for Pd/TiO₂-R100 while the calculated average particle size of Pd⁰ metal increased from 28.5 to 41.0 nm. Thus, the presence of rutile phase significantly decreased dispersion of palladium on the titania supports.

In addition to the amounts of CO chemisorption on the catalysts reduced at room temperature, and the percentages of palladium dispersion are given in Table 5.5. It was found that the amounts of CO chemisorption were much higher than those of reduced at 500°C for all catalysts. Since the CO adsorption ability of the catalysts can be recovered so that the decline in the amount of CO adsorbed at high temperature reduction was caused by an SMSI effect between Pd metal and TiO₂ support.

Table 5.4 Results from CO chemisorption of 1%Pd supported on TiO₂ consisting of various %rutile (reduced at 500 °C)

Sample	CO chemisorption x10 ¹⁸ (molecule CO/g cat.)	Pd dispersion (%)	d _p Pd ⁰ (nm)
Pd/TiO ₂ -R0	2.23	3.93	28.5
Pd/TiO ₂ -R17	2.20	3.87	28.9
Pd/TiO ₂ -R44	1.66	2.92	38.3
Pd/TiO ₂ -R85	1.77	3.12	35.9
Pd/TiO ₂ -R100	1.55	2.73	41.0

Table 5.5 Results from CO chemisorption of 1%Pd supported on TiO₂ consisting of various %rutile (reduced at room temperature)

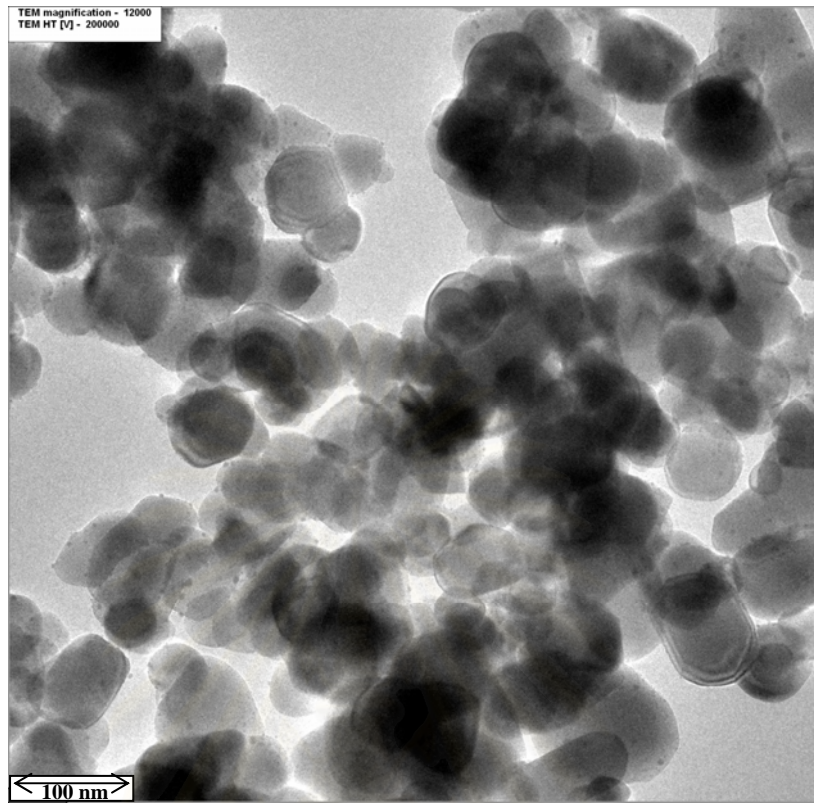
Sample	CO chemisorption x10 ¹⁸ (molecule CO/g cat.)	Pd dispersion (%)	d _p Pd ⁰ (nm)
Pd/TiO ₂ -R0	6.49	11.46	9.77
Pd/TiO ₂ -R17	6.44	11.38	9.84
Pd/TiO ₂ -R44	N/A	N/A	N/A
Pd/TiO ₂ -R85	3.97	7.01	15.98
Pd/TiO ₂ -R100	3.56	6.29	17.81

5.2.1.4 Transmission electron microscopy (TEM)

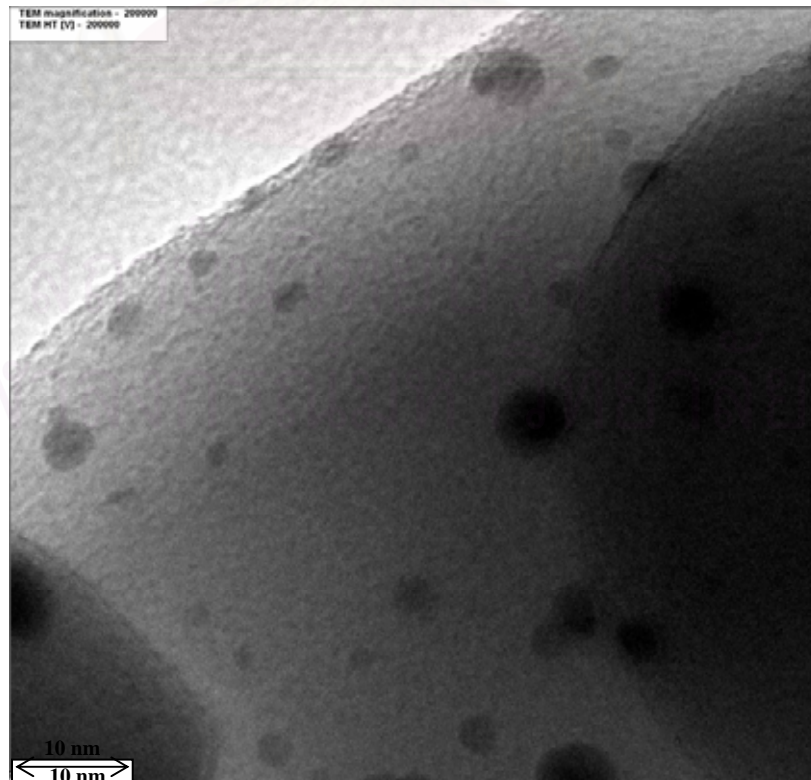
TEM is a useful tool for determining crystallite size and size distribution of supported metals. It allows determination of the micro-texture and microstructure of electron transparent samples by transmission of a focused parallel electron beam to a fluorescent screen with a resolution presently better than 0.2 nm.

TEM micrographs of Pd/TiO₂-R0 (pure anatase) reduce at 500°C and those of the one reduced at room temperature are shown in Figure 5.10. TEM micrographs were taken in order to physically measure the size of the palladium oxide particle and/or palladium clusters. Since the metal loading is low and the surface area of the sample is very high, in principle it is quite difficult to observe metal dispersion by TEM. However, a large number of pictures were collected from different portion of the samples in order to obtain further evidence about the dispersion of the palladium. Since no sintering of the Pd metal particles was observed, it is confirmed that the reduction of the amount of CO chemisorption after subjected to high temperature reduction was due to the SMSI effect between Pd metal and the TiO₂ support.

(A)



(B)



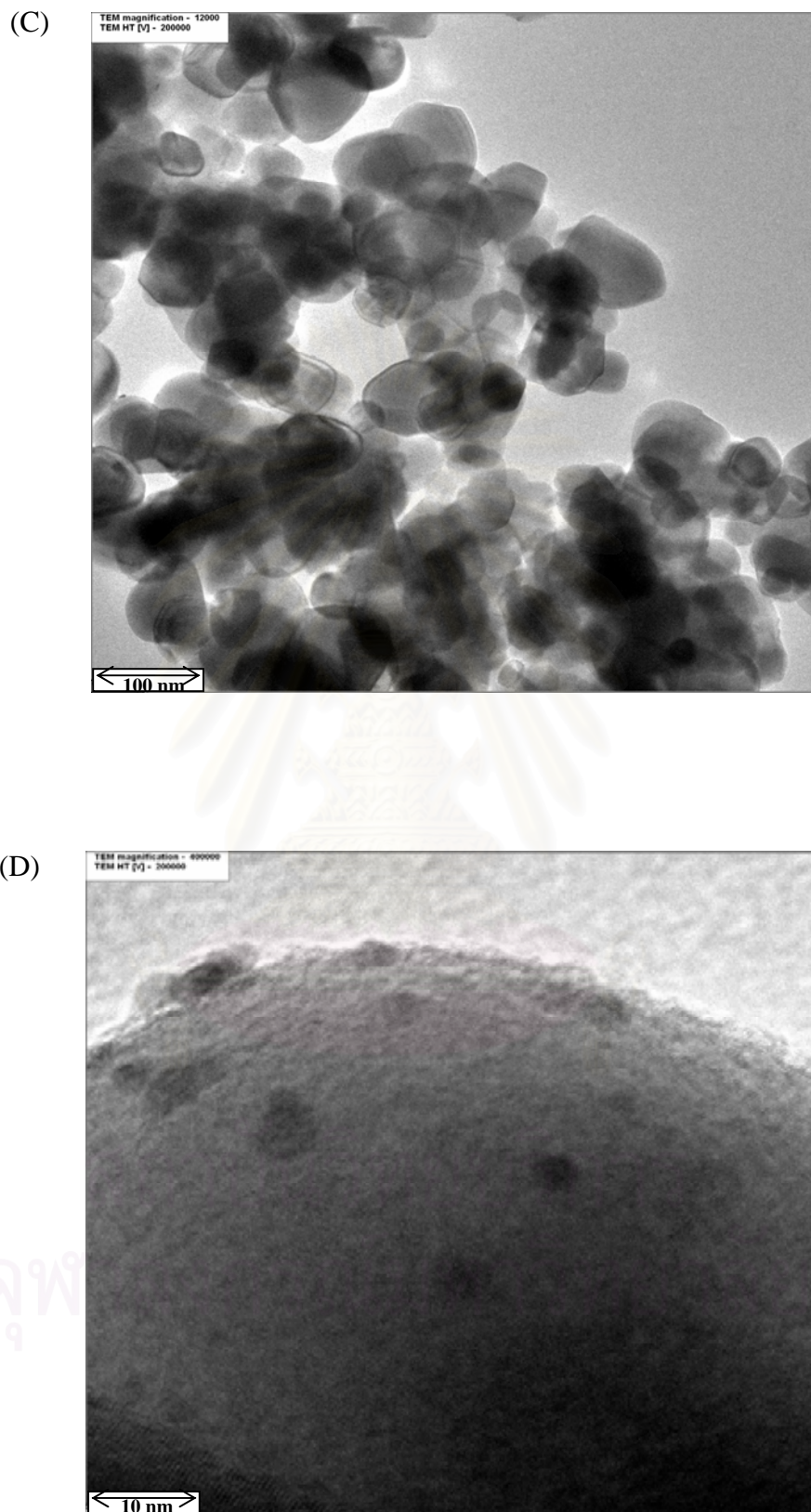


Figure 5.10 TEM micrographs of Pd/ TiO₂-R0 reduced at 500°C (A), (B) and reduced at room temperature (C) and (D).

5.2.1.4 Surface composition

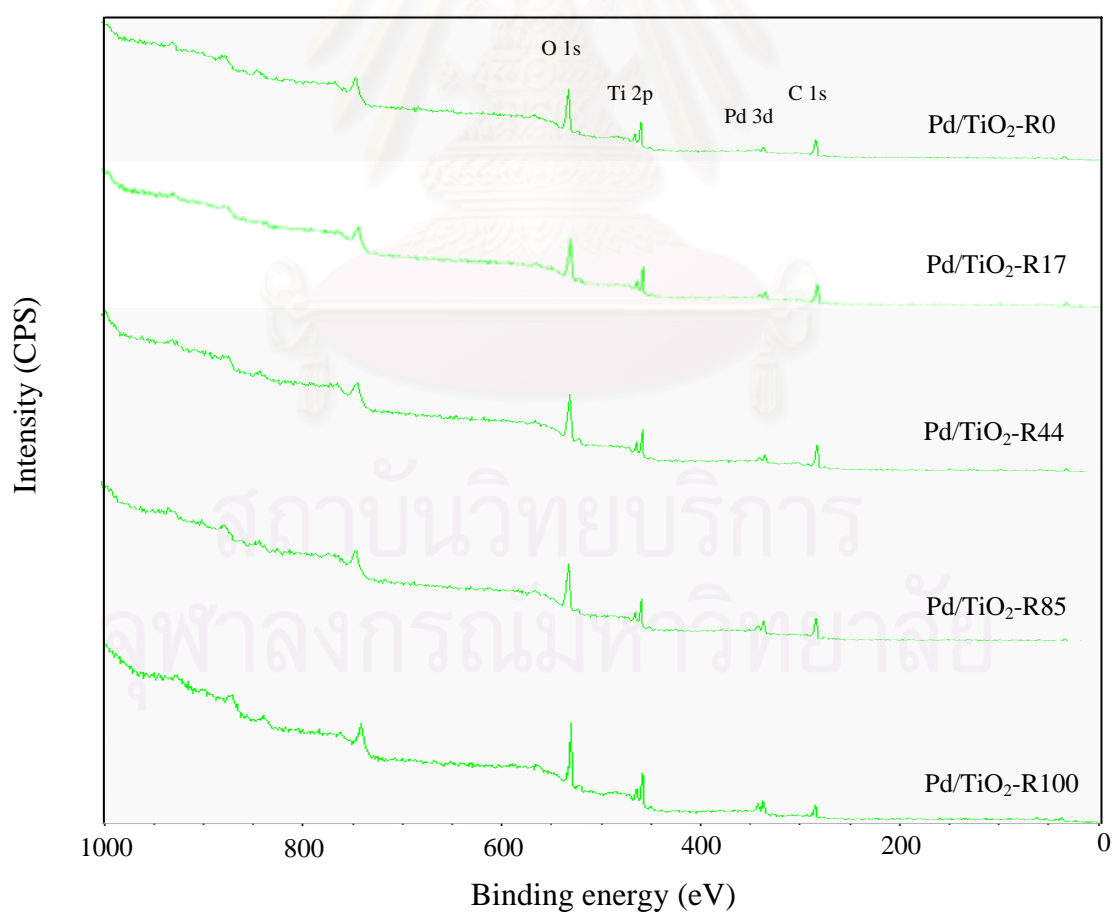
The surface compositions and electronic state of the metal catalysts were determined by X-ray photoelectron spectroscopy (XPS). The XPS spectra survey and Pd/Ti atomic ratio of Pd/TiO₂ catalysts are shown in figure 5.11 and table 5.6 respectively. The binding energies of Pd 3d_{5/2} and Ti 2p of Pd catalysts are found to be 336.6- 336.8 (Robert, N. et al., 2004) and 458.7-458.9 eV (Liqiang, J. et al., 2003 and Price, N. J. et al., 1999) respectively. The full width of half maximum (FWHM) values of Pd 3d_{5/2} and Ti 2p of Pd catalysts are found to be 1.4-1.6 (Robert, N. et al., 2004) and 1.3-1.5 eV (Liqiang, J et al., 2003 and Price, N. J et al., 1999). Moreover, It is seen from table 5.5 that an increasing Pd surface concentration with increasing amount of %rutile up to ca. 44%rutile. Further increase the amount of %rutile phase did not result in higher concentration of Pd on the TiO₂ surface and could lower the Pd surface concentration for pure rutile TiO₂.

Table 5.6 XPS binding energies and surface compositions of Pd catalysts

Sample	Bind energy (eV)			FWHM (eV)		
	Pd 3d	Ti 2p	O 1s	Pd 3d	Ti 2p	O 1s
Pd/ TiO ₂ -R0	336.675	458.798	530.252	1.646	1.418	2.121
Pd/ TiO ₂ -R17	336.603	458.800	530.177	1.549	1.386	1.719
Pd/ TiO ₂ -R44	336.876	458.900	530.379	1.579	1.456	2.051
Pd/ TiO ₂ -R85	336.802	458.900	530.278	1.547	1.503	2.099
Pd/ TiO ₂ -R100	336.874	458.948	530.248	1.475	1.412	1.800

Table 5.7 % atomic concentration of Ti and O on TiO₂ surface from XPS results

Sample	% Atomic concentration			Atomic Conc (%)
	Pd 3d	Ti 2p	O 1s	Pd/Ti
Pd/ TiO ₂ -R0	0.86	10.28	40.69	0.084
Pd/ TiO ₂ -R17	1.17	10.09	40.7	0.116
Pd/ TiO ₂ -R44	1.91	9.76	41.76	0.196
Pd/ TiO ₂ -R85	2.24	11.28	49.29	0.199
Pd/ TiO ₂ -R100	2.16	12.83	53.07	0.168

**Figure 5.11** XPS survey spectra of various Pd/TiO₂ catalysts

5.2.2 The catalytic activities of Pd/TiO₂ catalysts in selective acetylene hydrogenation

5.2.2.1 Reaction study in selective hydrogenation in excess ethylene

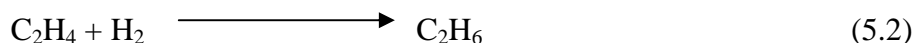
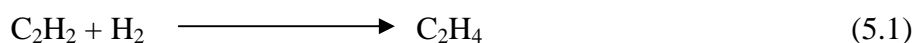
The performance of the catalysts in selective hydrogenation of acetylene was determined in terms of acetylene conversion and selectivity towards ethylene. Acetylene conversion is defined as moles of acetylene converted with respect to acetylene in the feed. Selectivity is the ratio of the amount of acetylene converted to ethylene and total amount of acetylene converted. Ideally, there should be one acetylene molecule converted to ethylene for every hydrogen molecule consumed, or 100% selectivity, since all of the acetylene is converted into ethylene. In actual practice, some hydrogen will always be consumed in the side reaction of ethylene conversion to ethane.

In this study, selective hydrogenation of acetylene was carried using a gas mixture containing 1.46% C₂H₂, 1.71% H₂, 15.47% C₂H₆ and balanced C₂H₄ (Rayong Olefin Co., Ltd) as reactant feed. The selectivity can be measured by observing the change in ethane and ethylene from the inlet and the outlet. The performance of the catalyst in this study was reported in terms of acetylene conversion and ethylene gain observed from acetylene and hydrogen concentrations as detailed below:

Conversion of acetylene is the ratio of acetylene converted and acetylene in the feed:

$$\text{C}_2\text{H}_2 \text{ conversion (\%)} = 100 \times \frac{\text{acetylene in feed} - \text{acetylene in product}}{\text{acetylene in feed}}$$

Ethylene gain is considered from the following reaction scheme:



Ethylene gain is defined as the ratio of those parts of acetylene that are hydrogenated to ethylene to the amount of totally hydrogenated acetylene:

$$\text{C}_2\text{H}_4 \text{ gain (\%)} = 100 \times \frac{\text{C}_2\text{H}_2 \text{ hydrogenated to C}_2\text{H}_4}{\text{totally hydrogenated C}_2\text{H}_2} \quad (\text{i})$$

Where total hydrogenated acetylene is the difference between moles of acetylene in the product with respect to those in the feed ($d\text{C}_2\text{H}_2$). In other words, acetylene hydrogenated to ethylene is the difference between the total hydrogenated acetylene ($d\text{C}_2\text{H}_2$) and the ethylene being lost by hydrogenation to ethane (equation 5.2). Regarding the difficulty in precise measurement of the ethylene change in the feed and product, the indirect calculation using the difference in the hydrogen amount (hydrogen consumed: $d\text{H}_2$) was used.

The ethylene being hydrogenated to ethane is the difference between all the hydrogen consumed and all the acetylene totally hydrogenated.

$$\text{C}_2\text{H}_4 \text{ gain (\%)} = 100 \times \frac{[d\text{C}_2\text{H}_2 - (d\text{H}_2 - d\text{C}_2\text{H}_2)]}{d\text{C}_2\text{H}_2} \quad (\text{ii})$$

As shown in equation (5.1) and (5.2), 2 moles of hydrogen were consumed for the acetylene lost to ethane, but only 1 mole of hydrogen for the acetylene gained as ethylene. The overall gain can also be written as:

$$\text{C}_2\text{H}_4 \text{ gain (\%)} = 100 \times \left[2 - \frac{d\text{H}_2}{d\text{C}_2\text{H}_2} \right] \quad (\text{iii})$$

Equation (ii) and (iii) are, of course the same, and ethylene gain discussed in this research is then calculated based on equation (iii). This value is the percentage of the theoretically possible ethylene gain which has been achieved in the operation. A positive value represents net production of ethylene. When the negative value refers to ethylene loss. However, it should be noted that these calculations can not provide a measure of acetylene polymerization reaction that forms green oil.

Typically, the normal operating temperature in an acetylene converter lies in the range 65-85°C (Derrien, M.L. et al., 1986 and Molnár, A. et al., 2001). During

start-up, the reaction can proceed at as low as 45°C. After a short period during which the catalyst has stabilized, the reactor temperature would reach the normal operating range and remain constant throughout its life-time. According to the literature, acetylene hydrogenation usually exhibits three distinct phases (Bond, G.C. et al., 1958; Al-Ammar, A.S. et al., 1978 and McGown, W.T. et al., 1978). In a brief initial period (0-2 min on stream), the reaction is rapid, forming both ethylene and ethane. In the second phase (2-60 min on stream), the rates of acetylene consumption, and ethylene and ethane production are all constant. During this period, hydrogenation of acetylene is the primary reaction. The selectivity is usually high, and is the characteristic of changes occurring in the catalyst. The third phase begins when acetylene hydrogenation is nearly complete and in this region approximates to the industrial situation.

In order to investigate the catalytic performance of Pd/TiO₂ catalysts consisting of various %rutile phase, selective hydrogenation of acetylene to ethylene was performed in a fixed bed flow reactor with a GHSV of 2,8818.88 h⁻¹. Removal of trace amount of acetylene in ethylene feed stream is vital for the commercial production of polyethylene since acetylene acts as a poison to the polymerization catalysts. Figure 5.12 shows acetylene conversions and ethylene selectivities obtained from various Pd/TiO₂ catalysts. Acetylene conversions were in the range of 40-59% and were found to be merely dependent on the Pd dispersion. However, a rapid change of catalytic properties in terms of ethylene selectivity was observed. When the TiO₂ supports with rutile contents of 44% or less were employed, ethylene selectivities were positive varied from 58-93% with a maximum for the Pd/TiO₂-R44. On the contrary, ethylene selectivities became negative when Pd catalysts supported on TiO₂ consisting ≥ 85% rutile phase were used resulting in ethylene losses. Over-hydrogenation of ethylene to ethane was likely to occur for such cases. Ethylene hydrogenation is usually believed to take place on the support by means of a hydrogen transfer mechanism (Aplund, S *et al.*, 1996). There may be some relationship between the presence of Ti³⁺ ions in the TiO₂ supports and high ethylene selectivity since only the Pd catalysts supported on TiO₂ with significant amount of Ti³⁺ yielded high ethylene gains. This could probably be explained in terms of strong metal-support interaction (SMSI) effect. Generally, SMSI occurs for Pd/TiO₂ catalysts after

reduction at high temperature lowering the adsorption strength of ethylene on catalyst surface thus high ethylene selectivity can be obtained (Kang. J. H *et al.*, 2002). Besides, the amounts of CO adsorbed on the catalysts reduced at 500°C were much smaller than those reduced at room temperature. Since the CO adsorption ability of the catalysts can be recovered so that the decline in the amount of CO adsorbed at high temperature reduction was caused by an SMSI effect. Recently, Fan *et al.* suggested that diffusion of Ti^{3+} from the lattice of anatase TiO_2 to surface Pd particle can lower the temperature to induce SMSI (Li. Y *et al.*, 2004)

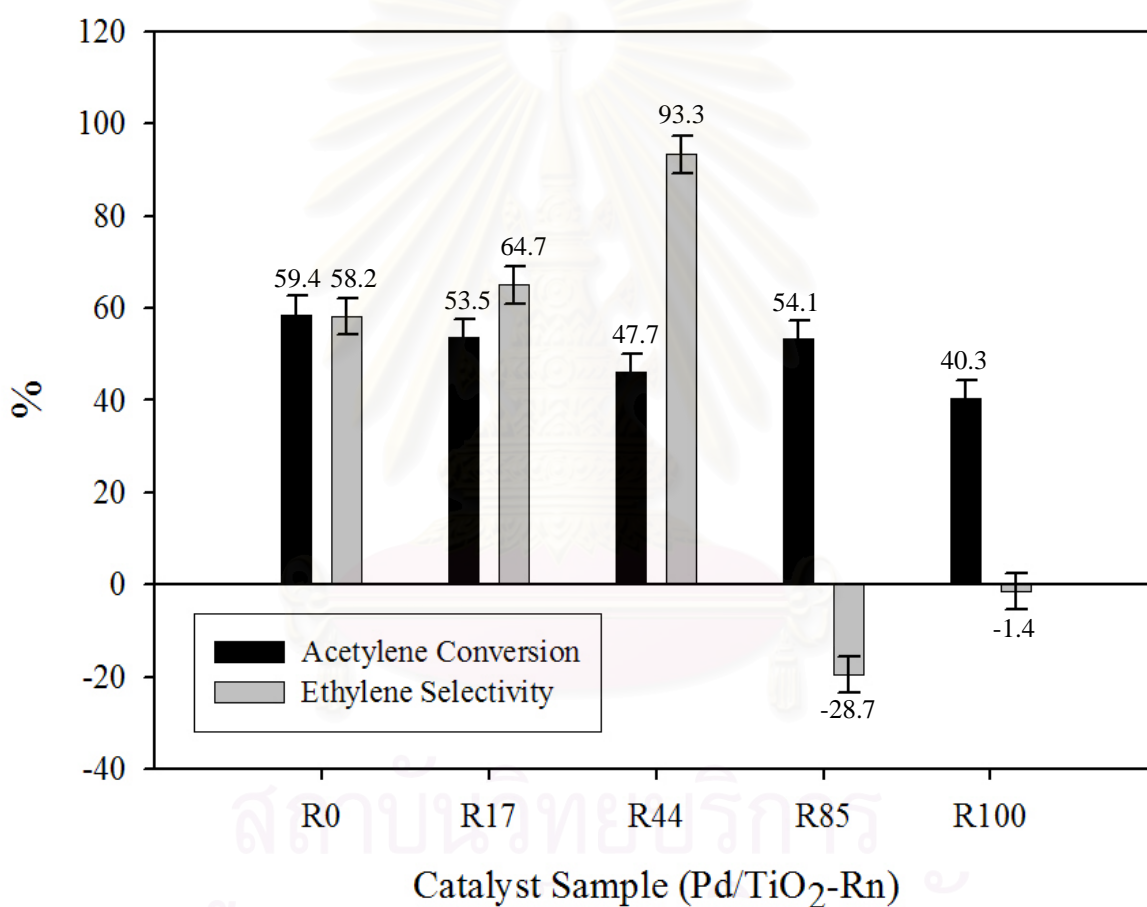
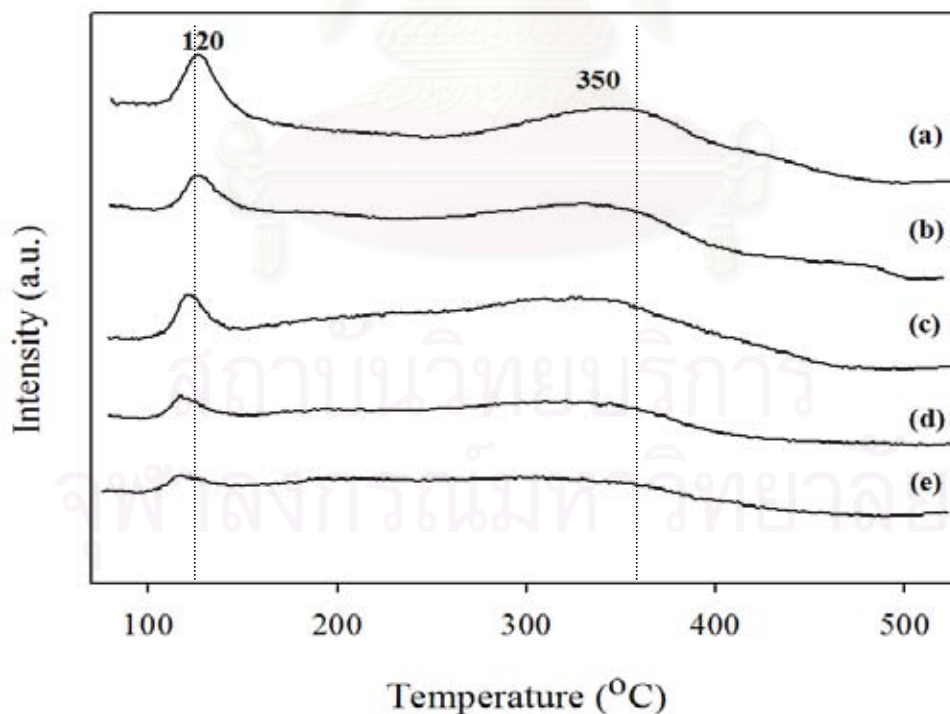


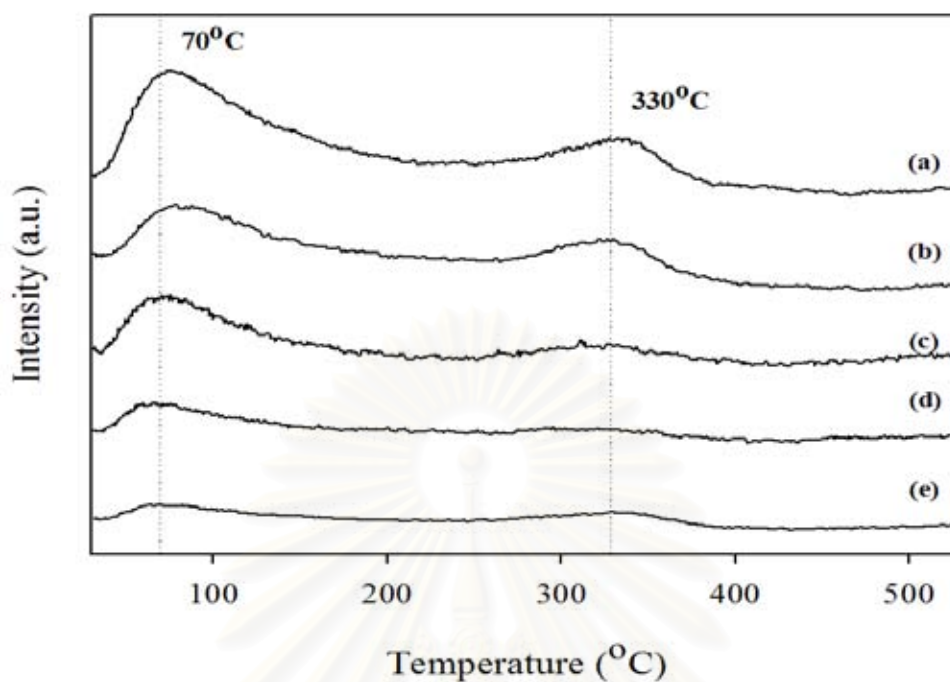
Figure 5.12 Catalytic performances of various Pd/TiO₂ catalysts in selective acetylene hydrogenation.

5.2.3 Temperature programmed desorption study

Temperature programmed desorption (TPD) of CO and C₂H₄ for Pd catalysts was performed in order to obtain an information about ethylene adsorption behavior on the catalyst samples. The samples were reduced in H₂ at 500°C for 1 h prior to adsorption of CO and C₂H₄ then the adsorbed Pd catalysts were purged with He at the same adsorption temperature to remove physisorption. The results are shown in Figures 5.13A and 13B, respectively. Similar profiles were found for both CO and ethylene temperature programmed desorption in which two main desorption peaks were observed. Such results suggest that there were two different active sites on the catalysts, probably Pd and Ti³⁺ sites. Since the high temperature peaks were diminished with increasing amount of %rutile in the TiO₂ supports, these peaks could be attributed to the adsorption on Ti³⁺ sites. The low temperature peaks, therefore, were attributed to adsorption on Pd sites. Adsorption of CO on Ti³⁺ sites has also been observed by an IR study by Benvenuti et al.,1999.



(A)



(B)

Figure 5.13 Temperature programmed desorption of (A) CO and (B) C₂H₄ for the various Pd/TiO₂ catalysts: (a) Pd/TiO₂_R0 (b) Pd/TiO₂_R17 (c) Pd/TiO₂_R44 (d) Pd/TiO₂_R85 (e) Pd/TiO₂_R100.

5.3 1% Pd-Ag/TiO₂ catalysts consisting of various TiO₂ phase compositions

5.3.1 Catalyst Characterization of Pd-Ag catalysts

5.3.1.2 X-ray diffraction (XRD)

X-ray diffraction analysis was used to determine the bulk crystalline phase in the catalysts. The XRD patterns of 1%Pd-3%Ag/TiO₂ catalysts are depicted in Figure 5.14. From the XRD results of Pd-Ag/TiO₂ catalysts, no XRD peaks for PdO and AgO were observed. This suggests that the PdO, Ag or AgO may be highly dispersed. No structural changes of the titania supports were found during the palladium-silver impregnations and calcination since the XRD analysis still exhibited structure of both anatase and rutile phase of TiO₂.

5.3.1.1 BET surface area

The results of BET surface area of 1%Pd-3%Ag/TiO₂ catalysts determined by N₂ adsorption are summarized in Table 5.8. The data in Table 5.1 and 5.6 indicated that impregnation of palladium and silver onto the titania supports decreased the surface area of titania support. However, BET surface areas of the Pd/TiO₂ catalysts after re-impregnated with Ag were not significantly different from single metal Pd/TiO₂ catalysts, suggesting that most Ag were covered on Pd surface and not blocked the pores of titania supports.

Table 5.8 BET surface area of Pd-Ag catalysts

Sample	BET Surface area (m ² /g)
Pd- Ag/ TiO ₂ -R0	65.2
Pd- Ag/ TiO ₂ -R17	38.4
Pd- Ag/ TiO ₂ -R44	30.0
Pd- Ag/ TiO ₂ -R85	27.1
Pd- Ag/ TiO ₂ -R100	24.6

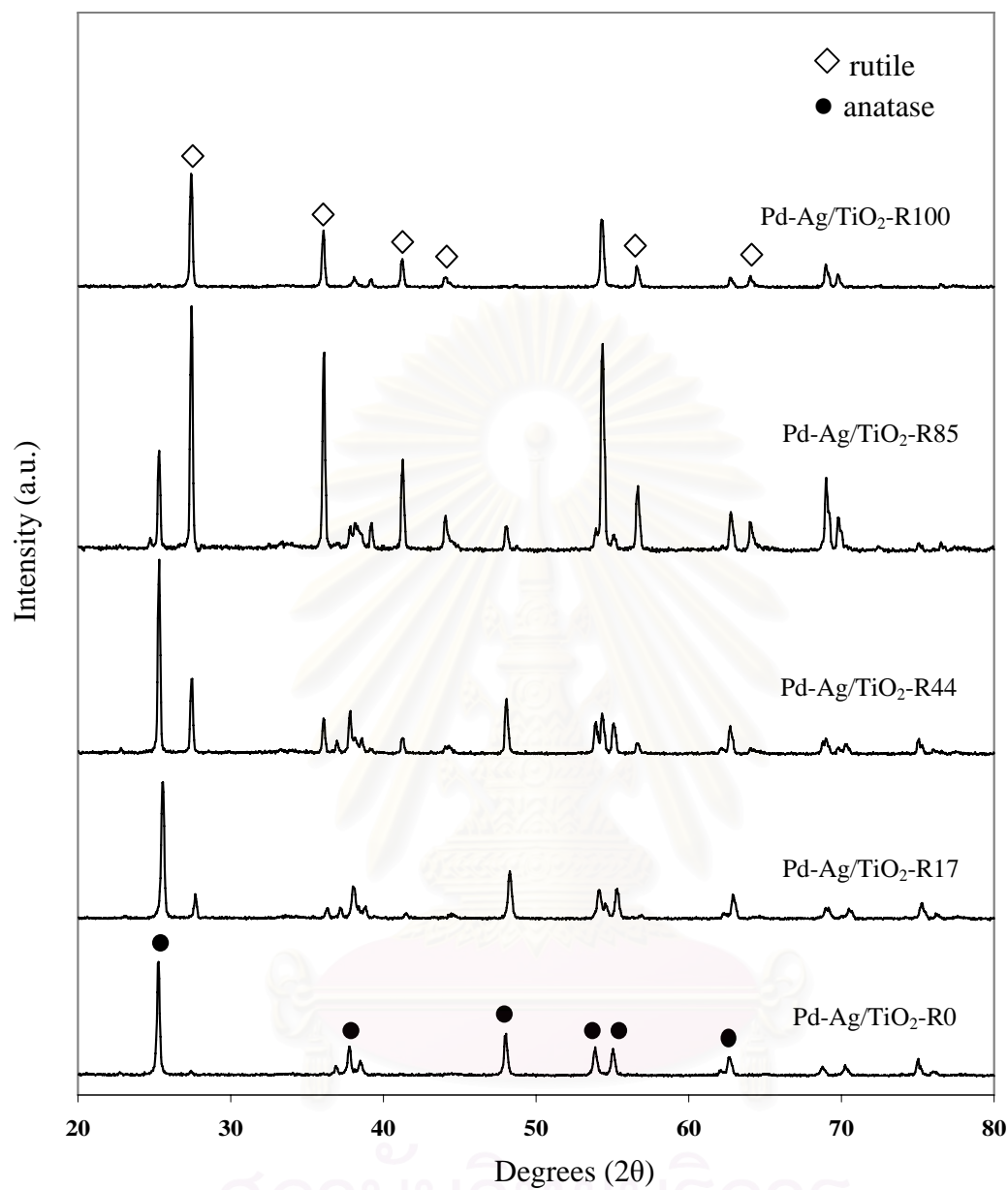


Figure 5.14 XRD pattern of Pd-Ag/TiO₂ catalysts consisting various %rutile phase.

5.3.1.3 Metal active sites

CO chemisorption technique provides the information on the number of palladium active sites and percentages of metal dispersion. The total CO uptakes and the percentages of palladium metal dispersion are reported in Table 5.9.

It is obvious that addition of Ag to Pd/TiO₂ catalysts resulted in lower amount of active surface Pd than Pd/TiO₂ catalysts since CO did not adsorb on Ag metal. However, the bimetallic Pd-Ag catalyst has been reported to show many beneficial effects in selective hydrogenation of acetylene to ethylene, for examples, suppression of oligomers formation and improvement of ethylene selectivity (Huang, D.C. et al., 1998). These beneficial effects are due to the altered surface arrangement of Ag atoms on the Pd surface. Roder, H. *et al.* (1993) suggested that Ag atoms are likely to stay at the surface in segregated form with Pd rather than forming an alloy.

Table 5.9 Results from pulse CO chemisorption Pd-Ag catalysts

Sample	CO chemisorption $\times 10^{18}$ (molecule CO/g cat.)	Pd dispersion (%)	d_p Pd ⁰ (nm)
Pd-Ag/ TiO ₂ -R0	0.96	1.90	59.9
Pd-Ag/ TiO ₂ -R17	0.89	1.45	77.2
Pd-Ag/ TiO ₂ -R44	1.43	2.40	46.7
Pd-Ag/ TiO ₂ -R85	0.59	1.30	86.2
Pd-Ag/ TiO ₂ -R100	0.83	1.41	79.4

5.3.1.4 Surface composition

This section is aimed to study the surface composition as well as the electronic state of the metal catalysts using X-ray photoelectronic spectroscopy, XPS. Results of XPS are presented in Table 5.10. The Ag 3d binding energies full width of half maximum (FWHM) and of Pd-Ag catalysts were found to be 368- 374 and 1.9-2.1 eV. Respectively, indicating that oxide form of Ag (Robert, N. et al., 2004) . The Pd 3d binding energies of Pd-Ag catalysts are found to be 336-337 eV, indicating that

of PdO on surface (Robert, N. et al., 2004). Considering of Pd:Ag atomic ratios of Pd-Ag catalysts in Table 5.9, the ratios were increased as % rutile phase of TiO₂ increased from 0.32 for Pd-Ag/TiO₂-R0 to 1.29 for Pd-Ag/TiO₂-R100. The Pd:Ag atomic ratio of Pd-Ag catalysts showed the same trend for Pd:Ti of Pd catalysts.

Table 5.10 XPS binding energies and surface compositions of Pd-Ag catalysts

Sample	Bind energy (eV)				FWHM (eV)			
	Pd 3d	Ag 3d	Ti 2p	O 1s	Pd 3d	Ag 3d	Ti 2p	O 1s
Pd-Ag/ TiO ₂ -R0	337.024	368.397	459.073	530.500	1.644	1.916	1.804	2.523
Pd-Ag/ TiO ₂ -R17	336.876	368.224	459.039	530.593	1.887	2.188	1.649	2.472
Pd-Ag/ TiO ₂ -R44	336.913	368.150	459.050	530.595	1.712	2.030	1.864	2.564
Pd-Ag/ TiO ₂ -R85	336.907	368.224	458.930	530.609	1.823	1.983	1.721	2.746
Pd-Ag/ TiO ₂ -R100	336.900	368.100	458.975	530.475	1.796	2.076	1.770	2.414

Table 5.11 % atomic concentration of Pd and Ag on Pd-Ag catalysts from XPS results

Sample	% Atomic concentration				Atomic ratio
	Pd 3d _{5/2}	Ag 3d _{5/2}	Ti 2p	O 1s	Pd/Ag
Pd-Ag/ TiO ₂ -R0	0.53	1.68	10.29	46.93	0.32
Pd-Ag/ TiO ₂ -R17	1.01	1.63	9.90	51.17	0.62
Pd-Ag/ TiO ₂ -R44	1.41	1.64	10.41	54.22	0.86
Pd-Ag/ TiO ₂ -R85	1.02	1.16	8.24	40.16	0.88
Pd-Ag/ TiO ₂ -R100	1.80	1.43	11.78	54.8	1.29

5.3.2 The catalytic activities of Pd-Ag/TiO₂ catalysts in selective acetylene hydrogenation

The performance of 1%Pd-3%Ag catalysts supported on TiO₂ catalysts consisting of different phase compositions in acetylene hydrogenation was evaluated at the temperature 40°C, a space velocity 2,8818.88 h⁻¹, and a gas mixture containing 1.46% C₂H₂, 1.71% H₂, 15.47% C₂H₆ and balanced C₂H₄ (Rayong Olefin Co., Ltd) as reactant feed which were the same conditions for Pd/TiO₂ catalysts.

Figure 5.15 illustrates acetylene conversion and ethylene selectivities obtained from various Pd-Ag/TiO₂ catalysts. The conversions of Pd-Ag/TiO₂ catalysts were in range of 5-15% and were found to be consecutive of the increased % rutile phase, 5.3 for R0 to 15 % conversion for R100. Additionally, ethylene selectivities were observed to be in a similar trend as the acetylene conversions.

When the conversions and selectivities were compared between the single metal Pd and the bimetallic catalysts Pd-Ag catalysts. It was found that all of the Ag-promoted catalysts exhibited less acetylene conversions than those of non-promoted ones. Ethylene selectivities for the Ag-promoted catalysts were less than the Pd catalysts with containing % rutile phase from 0- 44%. However the catalysts consisting ≥ 85% rutile phase now exhibited positive ethylene selectivities. The results suggest that the Pd catalyst surface on various phase composition of TiO₂ supports was modified by Ag atoms. For those of without Ti³⁺ (high rutile contents) the presence of Ag probably blocked the sites for ethylene hydrogenation to ethane of Pd catalysts thus a significant improvement in ethylene selectivity. However, for those containing Ti³⁺ addition of Ag showed a negative effect. This is probably due to suppression of both Ti³⁺ and SMSI effects on the Pd-Ag/TiO₂ catalysts.

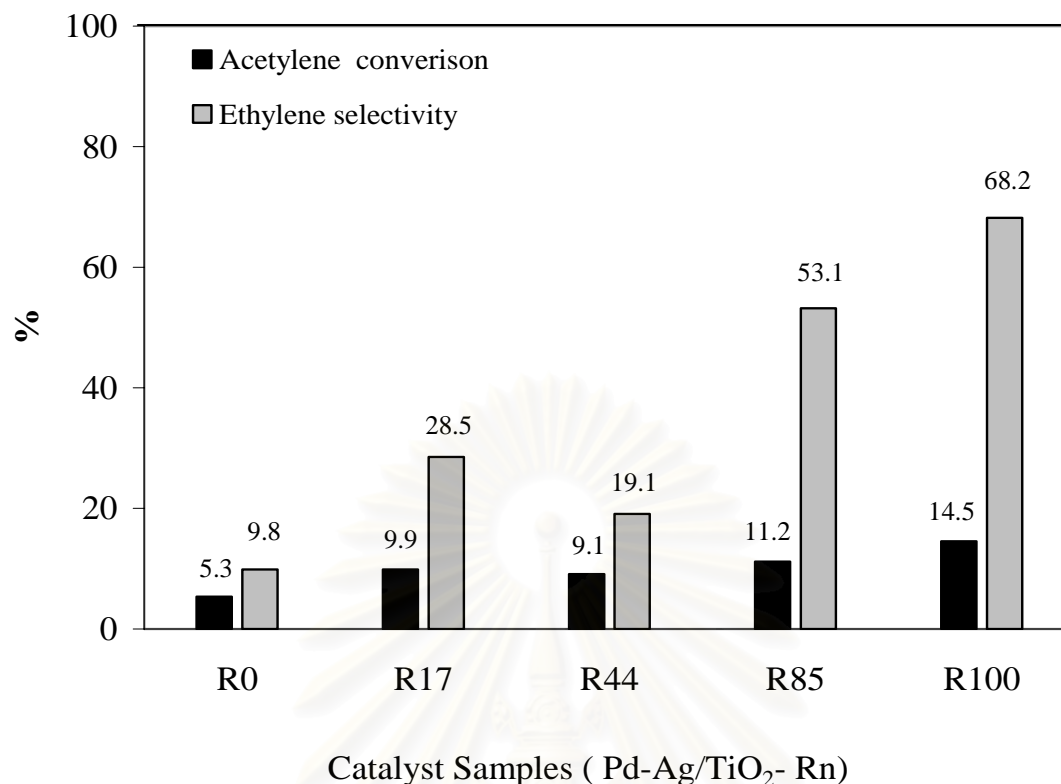


Figure 5.15 Catalytic performances of various Pd-Ag/TiO₂ catalysts in various phase composition acetylene hydrogenation.

5.4 Proposed mechanism for selective acetylene hydrogenation over Pd catalyst supported on TiO₂

The mechanism of selective hydrogenation of acetylene to ethylene on the various phase composition of TiO₂ supported Pd catalysts are illustrated in Figure 5.16. We propose that ethylene can adsorb on Ti³⁺ sites and hydrogenate to ethane. However, simultaneously Ti³⁺ species that were in contact with palladium surface promoted SMSI effect and ethylene desorption (Li. Y. *et al.*, 2004). Thus, without Ti³⁺ on the TiO₂ surface, low selectivity for ethylene was observed (as seen for the cases of Pd/TiO₂-R85 and Pd/TiO₂-R100) while with too many Ti³⁺ (that were not in contact with Pd), ethylene hydrogenation also occurred. Therefore, among the three catalysts with significant amounts of Ti³⁺ used in this study, Pd/TiO₂-R44 exhibited higher ethylene gains than Pd/TiO₂-R17 and Pd/TiO₂-R0, respectively.

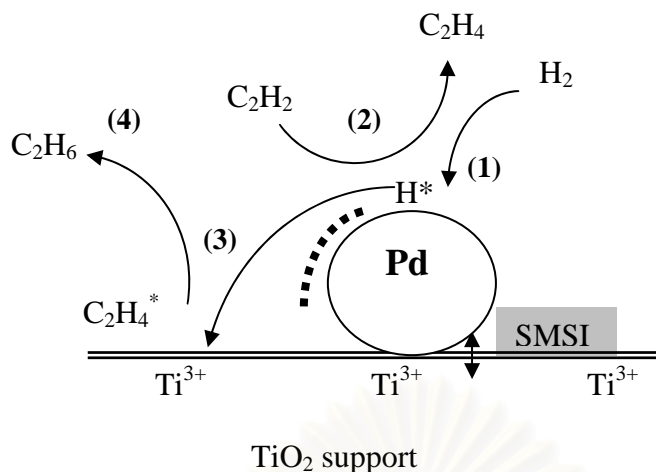


Figure 5.16 A conceptual model for selective acetylene hydrogenation mechanism on Pd/TiO₂ catalysts: (1) H₂ transfer from the metal to the support (2) acetylene hydrogenation to ethylene followed by ethylene desorption (3) adsorption of ethylene on Ti³⁺ sites (4) hydrogenation of ethylene to ethane.

The mechanism of the selective hydrogenation of acetylene to ethylene on the TiO₂ supported Pd-Ag catalysts are illustrated in Figure 5.17. The model demonstrated that four main types of surface sites are involved in the Ag-promoted Pd catalyst; three types of which located on the Pd metal surface, are responsible for selective conversion of acetylene to ethylene, direct ethane from acetylene, and oligomer formation from acetylene. Another site located on the support surface involves the hydrogenation of ethylene to ethane. (Al-Ammar, A.S. et al., 1978; Margitfalvi, J. et al., 1981; Moses, J.M. et al., 1984; and Weiss, A.H. et al., 1984). It was reported that additional of Ag to Pd catalyst decrease the quantity of absorption hydrogen, and reduces absorption hydrogen spill over from the bulk of the metals to react with acetylene, which increase the selectivity of acetylene hydrogenation to ethylene. Thus, the Ag-promoted catalysts exhibited less acetylene conversions than those of non-promoted ones. Ethylene selectivities for the Ag-promoted catalysts consisting $\geq 85\%$ rutile phase now were exhibited positive ethylene selectivities.

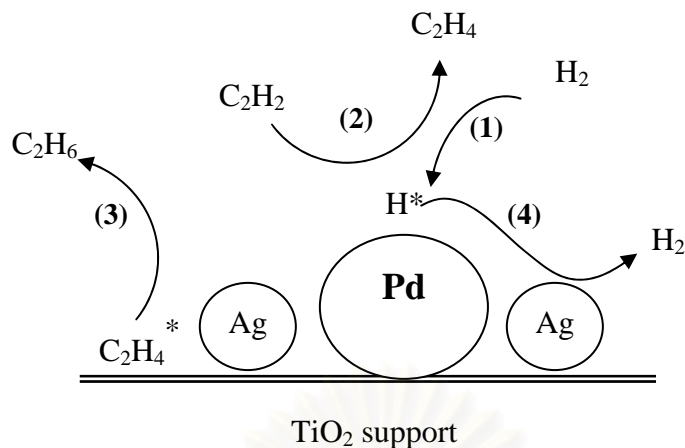


Figure 5.17 A conceptual model demonstrating for selective acetylene hydrogenation mechanism on Pd-Ag/TiO₂ catalysts and the role of Ag promoter as desorption site for transferred H₂.

5.5 Solvothermal and sol gel – derived TiO₂

5.5.1 Properties of solvothermal and sol gel – derived TiO₂ supports

Titania was prepared by solvothermal method using TNB as a precursor in 1,4-butanediol solvent for 6 h holding time and by sol-gel method using titanium ethoxide as a precursor in mixed water-ethanol solution. The properties of the TiO₂ supports synthesized by different routes were investigated by various analytical techniques.

5.5.1.1 X-ray diffraction (XRD)

The phase identification of titania is based on the results from X-ray diffraction. The XRD patterns of the titania prepared by solvothermal and sol-gel methods in the 2θ ranges from 20° to 80° are shown in Figure 5.18. XRD spectra of the titania show strong diffraction peaks at 25°, 37°, 48°, 55°, 56°, 62°, 71°, and 75° 2θ and all of those peaks can be attributed to titania anatase phase without any contamination of other phases.

5.5.1.2 BET surface areas and crystallite size

The BET surface of TiO₂ supports prepared by solvothermal and sol-gel method are shown in Table 5.12. The BET surface areas of the solvothermal TiO₂ (26.8 m²/g) was slightly less than that of sol-gel TiO₂ (39.3 m²/g). The average crystallite sizes of the titania supports synthesized by different methods were found to be ca. 10-17 nm. Thus, nanocrystalline pure anatase titania can be produced by both solvothermal and sol gel technique.

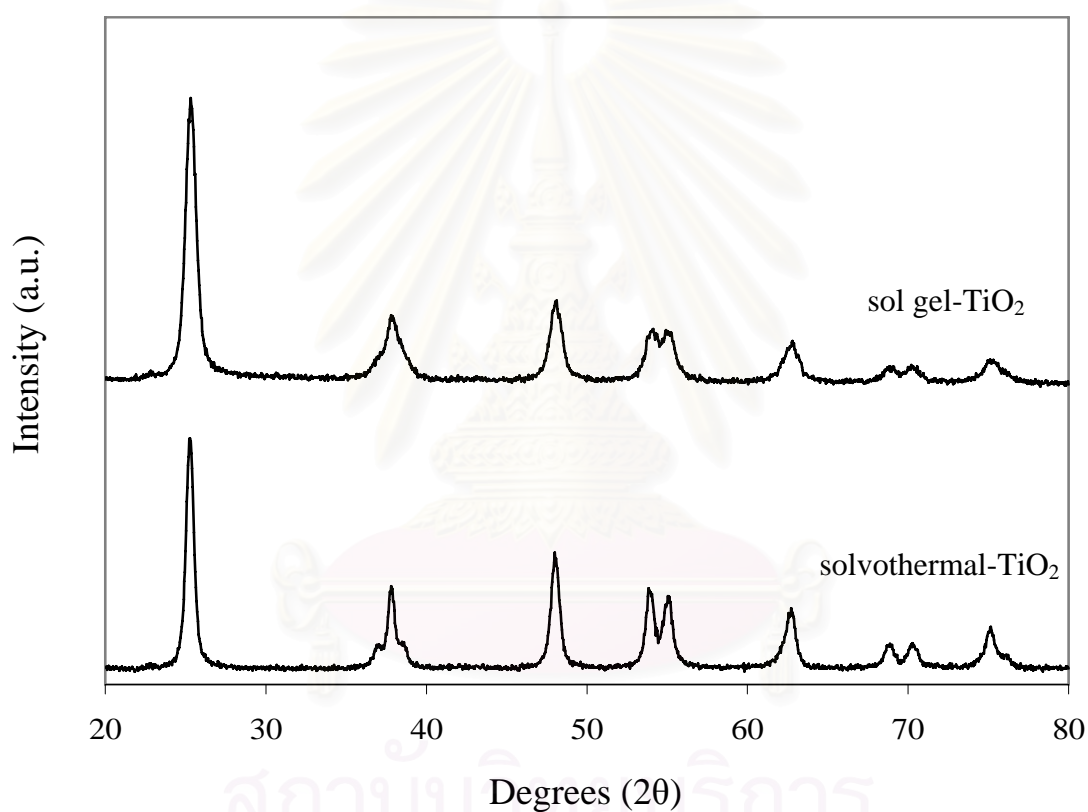


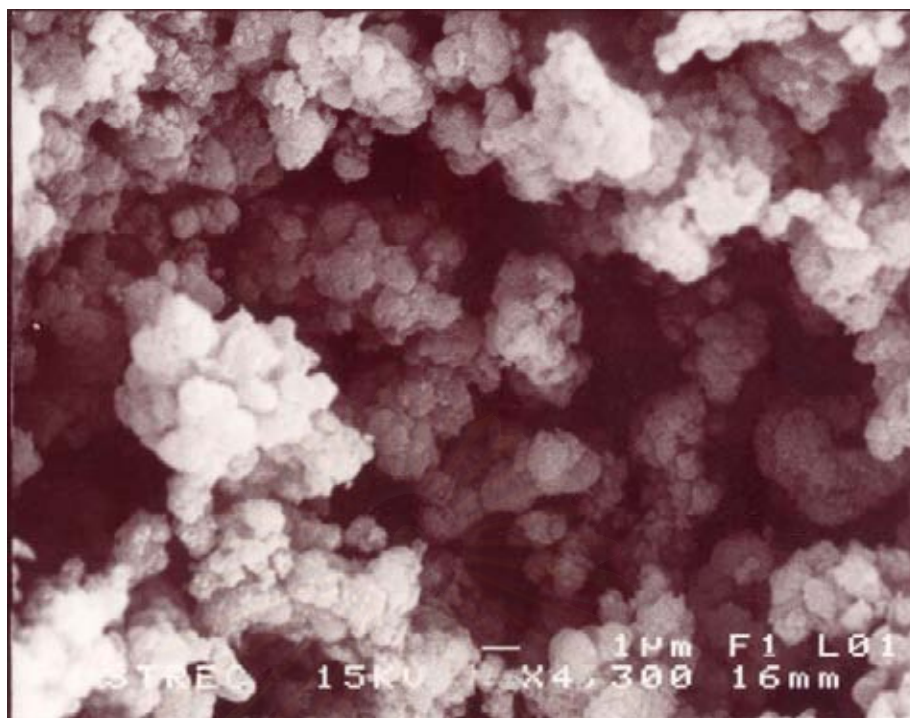
Figure 5.18 XRD patterns of the solvothermal and sol gel - titania supports.

Table 5.12 BET surface areas and average crystallite sizes of TiO₂ synthesized by solvothermal and sol- gel method

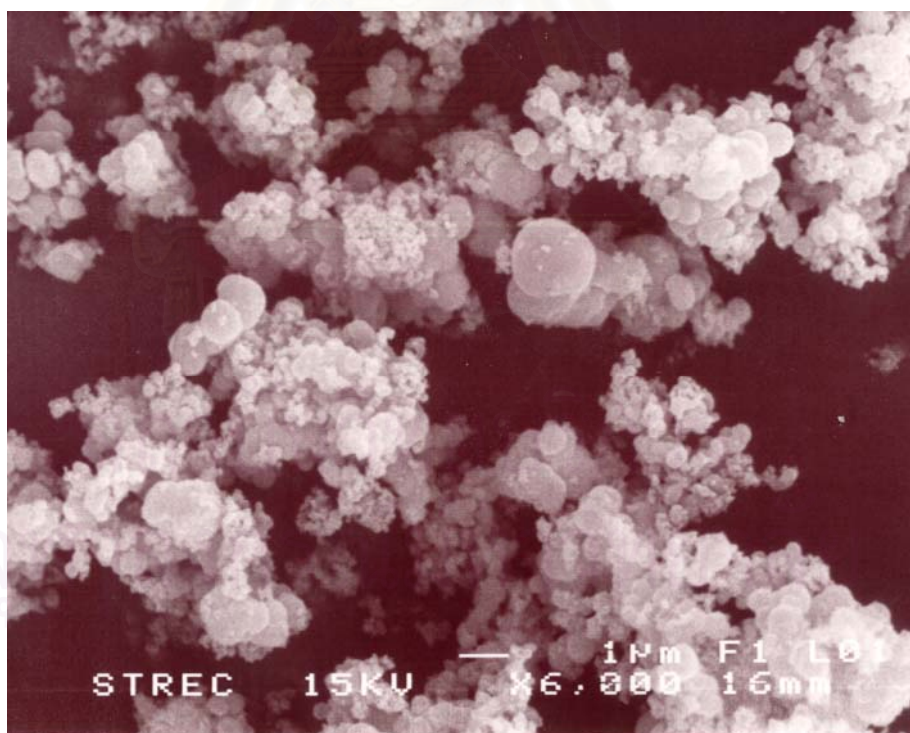
Sample	BET S.A. (m ² /g)	Average crystallite size Diameter (nm)
TiO ₂ (sol-gel)	39.3	10
TiO ₂ (solvothermal)	26.8	17

5.5.1.3 Scanning electron microscopy (SEM)

The SEM micrographs of the titania products synthesized by solvothermal and sol-gel method are shown in Figure 5.19 (A) and (B), respectively. The morphology of the titania particles was found to be irregular shape. The SEM micrographs of titania products synthesized in 1,4-butanediol for 6 h showed irregular fine particles. Park, A.K. et al. (1997) synthesized titania in thermal hydrolysis of TiCl₄. They found that the particle shape depended on the dielectric constant of solvent and the particle potential. The SEM micrographs of titania synthesized by sol-gel method showed spherical shape of some of the secondary particles.



(A)



(B)

Figure 5.19 SEM images of titania products synthesized by (A) solvothermal and (B) sol-gel methods.

5.5.1.4 Surface Composition

The XPS survey spectra and XPS results for binding energy and %atomic concentration of Ti and O on TiO₂ surface synthesized by different methods were showed in Figure 5.20 and Table 5.13, respectively. Ti 2p, O 1s binding energies and full width of half maximum (FWHM) TiO₂ were found to be 458, 530, 1.2- 1.3, and 1.5-1.7 eV, respectively. The sol gel- TiO₂ and solvothermal- TiO₂ had a similar Ti/O ratio.

Table 5.13 Binding energy and atomic concentration of TiO₂ samples from XPS

Sample	Binding energy (eV)		FWHM (eV)		Atomic conc.%		Atomic Conc (%)
	Ti 2p	O 1s	Ti 2p	O 1s	Ti 2p	O 1s	Ti/O
TiO ₂ (sol-gel)	458.80	530.00	1.27	1.57	12.59	57.15	0.22
TiO ₂ (solvothermal)	458.85	530.10	1.35	1.72	12.77	54.98	0.23

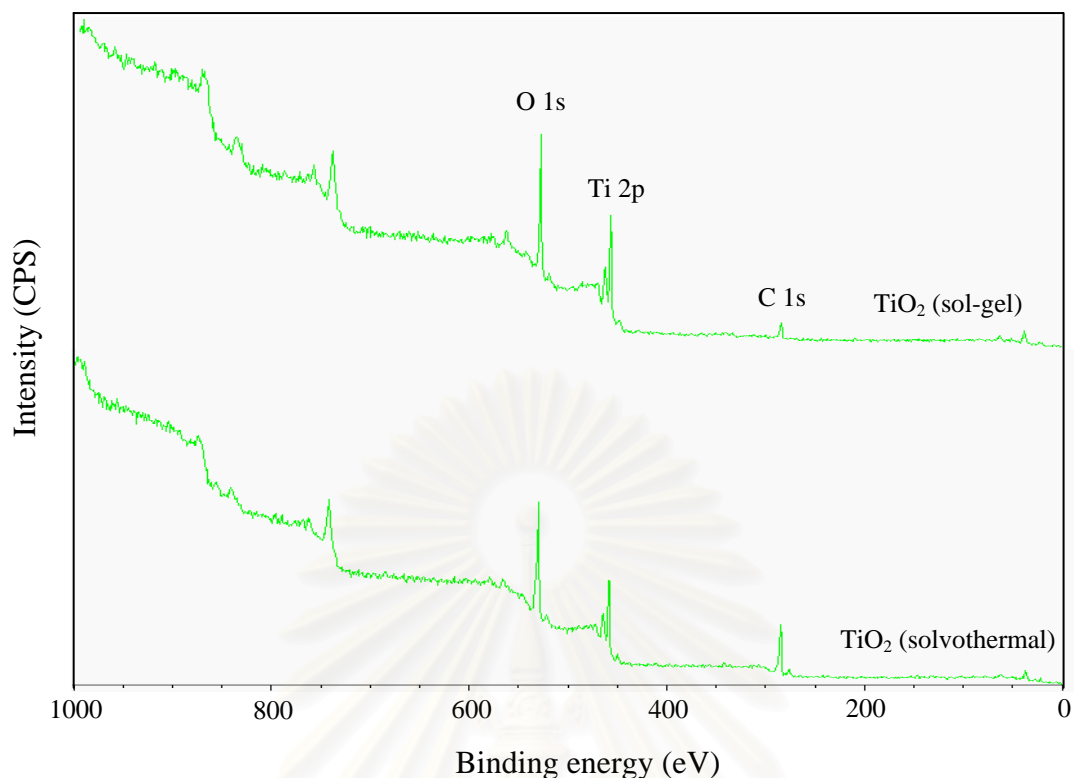


Figure 5.20 XPS survey spectra of TiO_2 synthesized by the solvothermal and sol gel methods.

5.5.1.4 Electron spin resonance spectroscopy (ESR)

The number of Ti^{3+} defective sites of titania particles were determined using electron spin resonance spectroscopy technique. The ESR results are shown in Figure 5.21. The signal of g value less than 2 was assigned to Ti^{3+} ($3d^1$) (Salama, T.M. et al., 1993; and Howe, R.F. et al., 1985). Both TiO_2 synthesized by solvothermal and sol-gel methods shown Ti^{3+} ESR signal at $g = 1.997$ with TiO_2 synthesized by solvothermal method exhibited much higher intensity than that of TiO_2 synthesized by sol-gel technique. It is indicated that the solvothermal- TiO_2 possessed more Ti^{3+} defective sites than the one synthesized by sol-gel method.

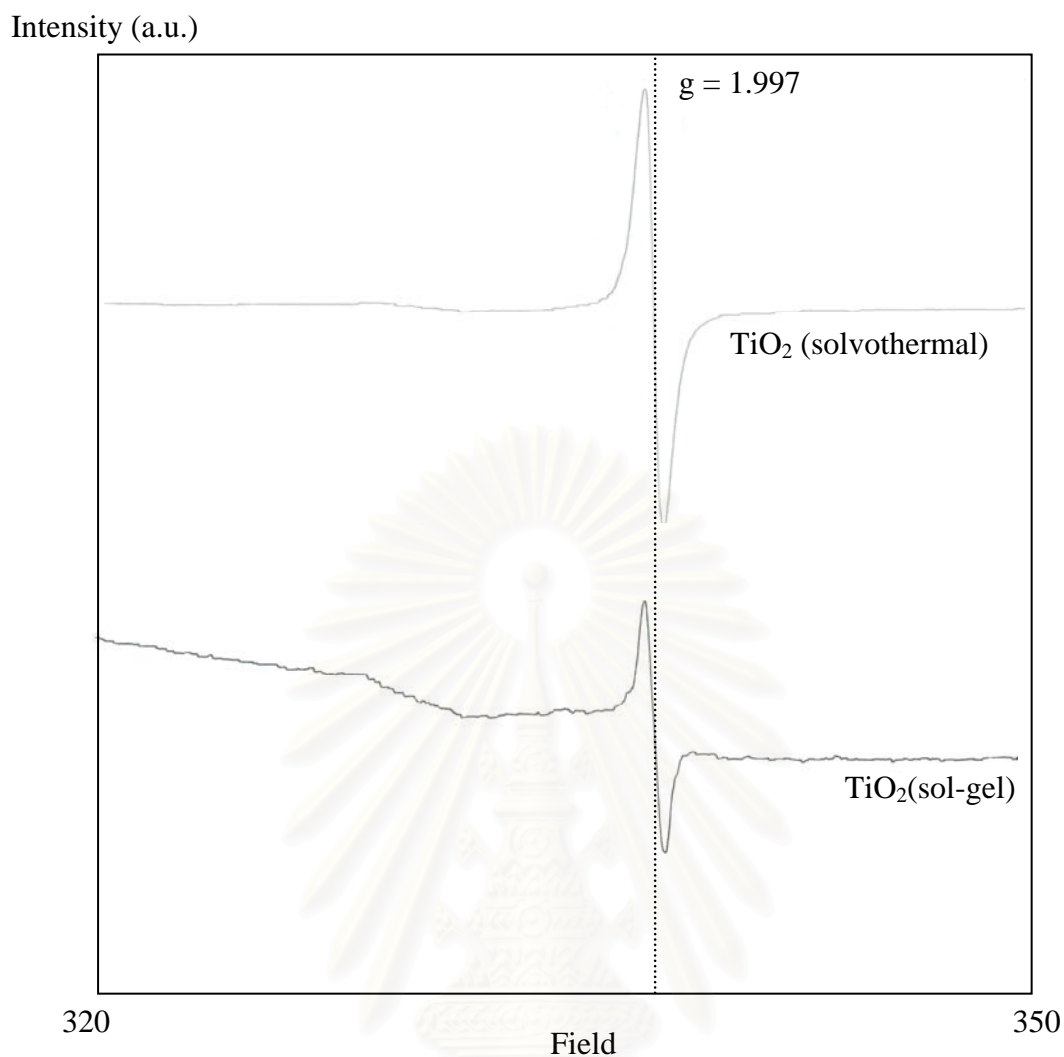


Figure 5.21 ESR results of the solvothermal and sol gel TiO_2 supports.

5.6 1% Pd catalysts on TiO_2 synthesized by the different methods

5.6.1 Properties of 1% Pd on supported TiO_2 catalysts

5.6.1.1 X-ray diffraction (XRD)

Phase structure of the prepared catalysts was characterized by X-ray diffraction technique. The XRD diffractograms of the titania supported palladium catalysts are shown in Figure 5.22. From the XRD results of 1%Pd/ TiO_2 , diffraction peak of palladium oxide (PdO) for the Pd/ TiO_2 using solvothermal method was detectable at $33.8^\circ 2\theta$. No XRD peak of PdO were observed for Pd/ TiO_2 prepared by sol-gel method suggesting that Pd was highly dispersed on the TiO_2 surface. It was

also found that titania support did not undergo structural changes during palladium impregnation and calcination because the XRD analysis only exhibited titania pure anatase phase for both catalysts.

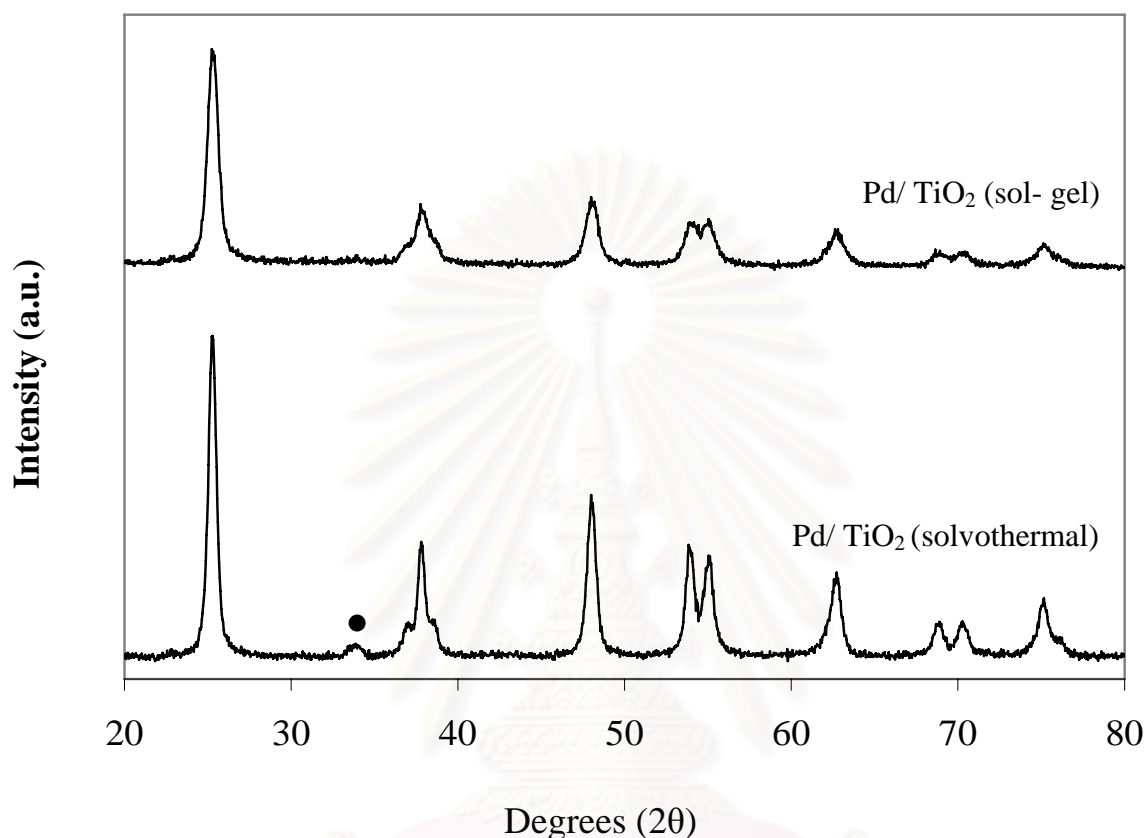


Figure 5.22 XRD patterns of Pd/TiO₂ synthesized by the solvothermal and sol gel methods.

5.6.1.2 BET surface areas

BET surface area of the titania supported palladium catalysts determined by N₂ physisorption measurement are shown in Table 5.14. It was found that BET surface area of the titania synthesized by solvothermal method was less than that of the one synthesized by sol-gel method. Compared the BET surface areas of the pure titania supports and the titania supported palladium catalysts, it was found that BET surface areas of the titania supports were slightly decreased after impregnation of Pd for Pd/TiO₂ synthesized by sol-gel method suggesting that the metals were deposited in some of the pores of titania. However, the BET surface area of pure TiO₂ supports

and TiO₂ supported Pd of the solvothermal- derived ones were similar suggesting that the metals were hardly desposited into the pores of TiO₂ supports.

Table 5.14 BET surface area Pd/TiO₂ synthesized by different methods

Sample	BET S.A. (m ² /g)
Pd/TiO ₂ (sol-gel)	33.8
Pd/TiO ₂ (solvothermal)	26.8

5.6.1.3 Metal active sites

The amounts of CO chemisorption on the catalysts, the percentages of palladium dispersion and the average particle size of Pd⁰ calculated from CO chemisorption are given in Table 5.15. It was found that Pd/TiO₂ synthesized by sol gel method exhibited higher amount of CO chemisorption than the one synthesized by solvothermal method . Since the sol gel- TiO₂ supports possessed higher BET surface areas than the solvothermal-TiO₂, the differences in the amount of active surface Pd were probably induced by the difference in BET surface areas. The calculated average particle size of Pd⁰ metal was 53.3 nm for Pd/TiO₂ synthesized by sol gel method and 130.2 nm for the other.

Table 5.15 Results from CO chemisorption of 1%Pd on TiO₂ synthesized by different methods

Sample	Active site *10 ¹⁸ (molecule CO/g cat.)	% Pd dispersion	d _p Pd ⁰ (nm)
Pd/ TiO ₂ (sol-gel)	1.19	2.10	53.3
Pd/ TiO ₂ (solvothermal)	0.49	0.86	130.2

5.6.1.4 Surface composition

The surface compositions and electronic state of the metal catalysts were determined by X-ray photoelectron spectroscopy (XPS). The binding energy, %atomic concentration, and the XPS spectra survey and of Pd/TiO₂ synthesized by sol gel and solvothermal method are shown in Table 5.16, 5.17, and Figure 5.23, respectively. The binding energies of Pd 3d_{5/2}, Ti 2p, O 1s, and C 1s of Pd catalysts are found to be 336.6- 336.8 (Robert, N. et al., 2004), 458.7-458.9 eV (Liqiang, J. et al., 2003 and Price, N.J. et al., 1999), 530, and 285 eV, (Guillot, J. et al., 2001) respectively. The Pd/Ti ratio for Pd catalysts synthesized by sol-gel method was slightly higher than the one synthesized by solvothermal method.

Table 5.16 Binding energy of Pd/TiO₂ samples from XPS results

Sample	Binding energy (eV)			FWHM (eV)		
	Pd 3d	Ti 2p	O 1s	Pd 3d	Ti 2p	O 1s
Pd/TiO ₂ (sol-gel)	336.493	458.873	530.126	1.391	1.441	1.655
Pd/TiO ₂ (solvothermal)	336.146	459.000	530.146	0.566	1.365	1.594

Table 5.17 %atomic concentration for Pd/TiO₂ catalysts from XPS results

Sample	Atomic conc. %			Atomic ratio
	Pd 3d	Ti 2p	O 1s	Pd/Ti
Pd/TiO ₂ (sol-gel)	0.2	17.57	62.33	0.011
Pd/TiO ₂ (solvothermal)	0.1	17.44	63.56	0.006

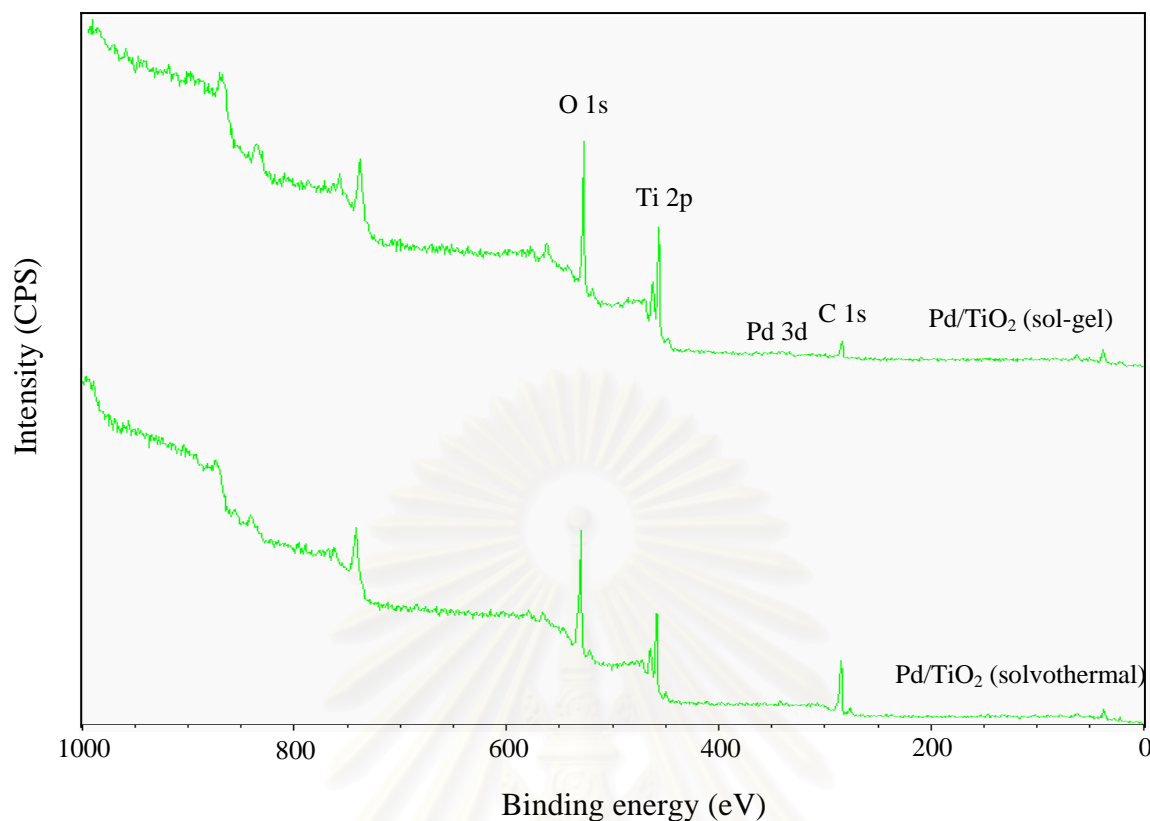


Figure 5.23 XPS survey spectra of Pd/TiO₂ synthesized by the solvothermal and sol gel methods.

5.6.2 The catalytic activities of Pd/TiO₂ catalysts in selective acetylene hydrogenation

5.6.2.1 Reaction study in selective hydrogenation in excess ethylene

The performance of 1% Pd catalysts supported on TiO₂ catalysts synthesized by the different methods in acetylene hydrogenation was evaluated at the temperature 40°C, a space velocity 2,8818.88 h⁻¹ and a gas mixture containing 1.46% C₂H₂, 1.71% H₂, 15.47% C₂H₆ and balanced C₂H₄ (Rayong Olefin Co., Ltd) as reactant feed

The conversion and selectivity of Pd catalysts supported on TiO₂ synthesized by solvothermal and sol-gel method in selective acetylene hydrogenation are shown in Figures 5.24. Acetylene conversions and ethylene selectivity were found to be in the range of 16- 19% and 64-76% respectively. The use of TiO₂ synthesized by sol-gel method as the support for Pd catalysts resulted in slight higher acetylene conversion and ethylene selectivity than the one supported on TiO₂ synthesized by solvothermal

method. It is revealed that the use of solvothermal-TiO₂ with higher concentration of Ti³⁺ than sol gel-TiO₂ as support for Pd catalyst resulted in lower conversion and selectivity after the reduction at 500°C. The results in this section consistent with the results in the section 5.2 for Pd on TiO₂ containing various rutile/anatase phase compositions (0-44 %rutile) that ethylene selectivity decreased with increasing amount of Ti³⁺.

In addition, the conversion and selectivities of the Pd catalysts supported by synthesized TiO₂ were compared to the one supported on commercial anatase TiO₂. The results are shown in Figure 5.15. It was found that acetylene conversion of the Pd catalysts supported on commercial TiO₂ was higher than those of the Pd catalyst supported on either sol gel or solvothermal TiO₂. This may due to that the Pd supported on commercial-TiO₂ possessed higher BET surface area than Pd supported on solvothermal and sol gel TiO₂. However, ethylene selectivity was highest when the sol-gel TiO₂ was used.

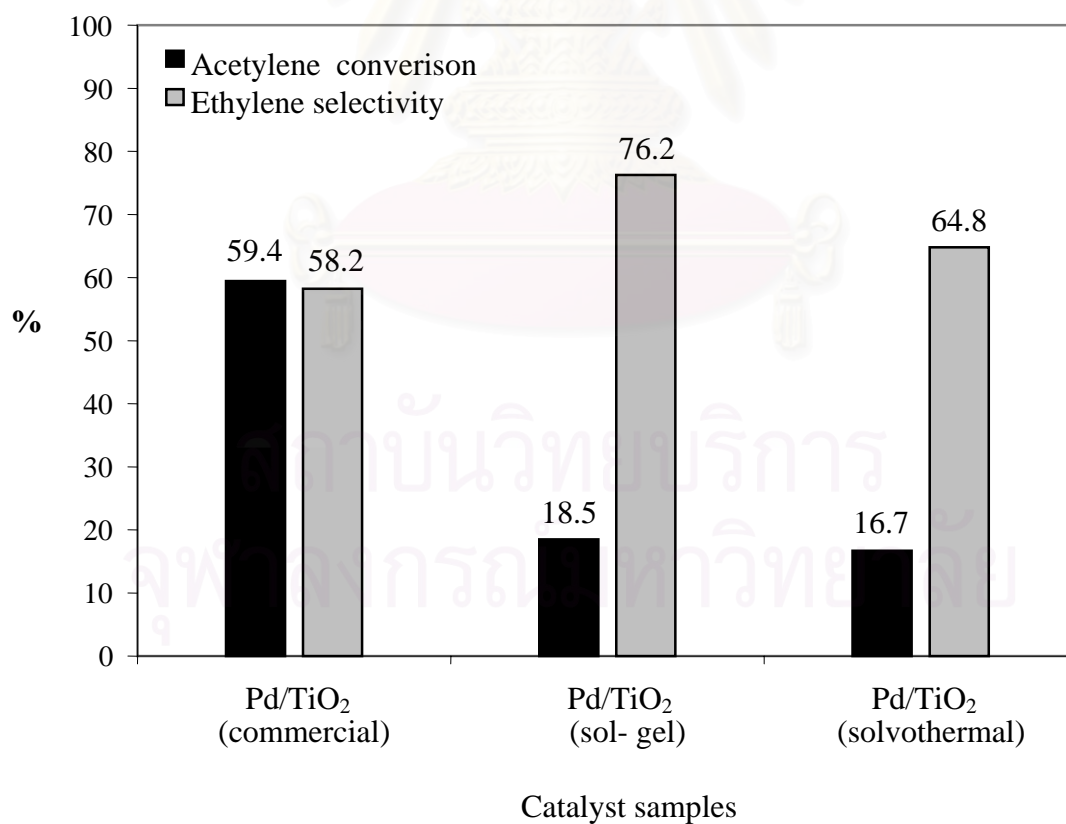


Figure 5.24 Catalytic performances of Pd catalysts in different synthesized methods in acetylene hydrogenation.

5.7 1%Pd- 3%Ag over TiO₂ catalysts synthesized TiO₂ using the different methods

5.7.1 Catalyst Characterization of Pd-Ag catalysts

5.7.1.1 X-ray diffraction (XRD)

X-ray diffraction analysis was used to determine the bulk crystalline phase in the catalysts. The XRD patterns of 1%Pd-3%Ag/TiO₂ catalysts are depicted in Figure 5.25.

From the XRD results of 1%Pd-3%Ag/TiO₂ catalysts, diffraction peaks for palladium oxide (PdO) were detectable at $33.8^\circ 2\theta$. However, no XRD peaks for AgO were observed. This suggests that the Ag or AgO may be highly dispersed. No structural changes of the titania supports were found during the palladium-silver impregnations and calcination since the XRD analysis only exhibited the pure anatase TiO₂ phase for both catalysts.

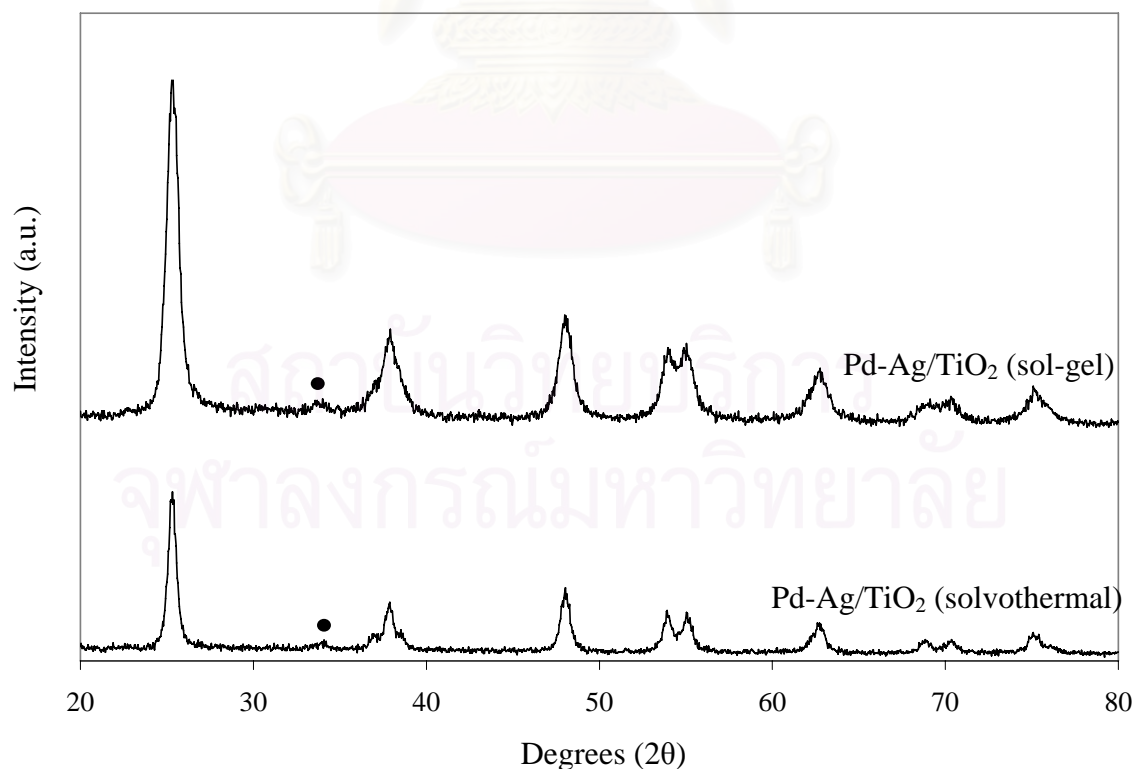


Figure 5.25 XRD patterns of Pd-Ag/TiO₂ synthesized by the solvothermal and sol gel methods.

5.7.1.2 BET surface areas

The results of BET surface area of 1%Pd-3%Ag/TiO₂ catalysts analyzed by N₂ adsorption are summarized in Table 5.18. It is shown that BET surface areas of the Pd-Ag catalyst prepared on TiO₂ synthesized by solvothermal method was slightly less than the one prepared by sol-gel-method. The data in Table 5.12 and 5.14 indicated that impregnation of palladium onto the titania supports decreased the surface area of titania support. Moreover, when the Pd/TiO₂ catalysts were re-impregnated with Ag, the surface area was further decreased, suggesting that some of the pores of titania support were blocked by the metal.

The BET surface areas of the titania supports, titania supported palladium catalysts and titania supported palladium-silver catalysts which synthesized by the different methods were found to be in the order of titania supports > titania supported Pd catalysts > titania supported Pd-Ag catalysts.

Table 5.18 BET surface area of Pd-Ag/TiO₂ synthesized by different methods

Sample	BET S.A. (m ² /g)
Pd-Ag/TiO ₂ (sol-gel)	30.7
Pd-Ag/TiO ₂ (solvothermal)	23.3

5.7.1.3 Metal active sites

CO chemisorption technique provides the information on the number of palladium active sites, percentages of metal dispersion and average particle size of Pd metal. The total CO uptakes and the percentages of palladium metal dispersion are reported in Table 5.19. The addition of Ag to Pd/TiO₂ catalysts were found to result in higher amount of active surface Pd catalysts. This is probably due to the absence of

SMSI effect for the Pd-Ag/TiO₂ catalysts prepared by solvothermal and sol-gel method. Hence higher amount of CO chemisorption was found.

Table 5.19 Results from CO chemisorption of Pd-Ag/TiO₂ synthesized by different methods

Sample	Active site *10 ¹⁸ (molecule CO/g cat.)	% Pd dispersion	d _p Pd ⁰ (nm)
Pd-Ag/ TiO ₂ (sol-gel)	4.98	51.8	2.2
Pd-Ag/ TiO ₂ (solvothermal)	1.22	12.7	8.8

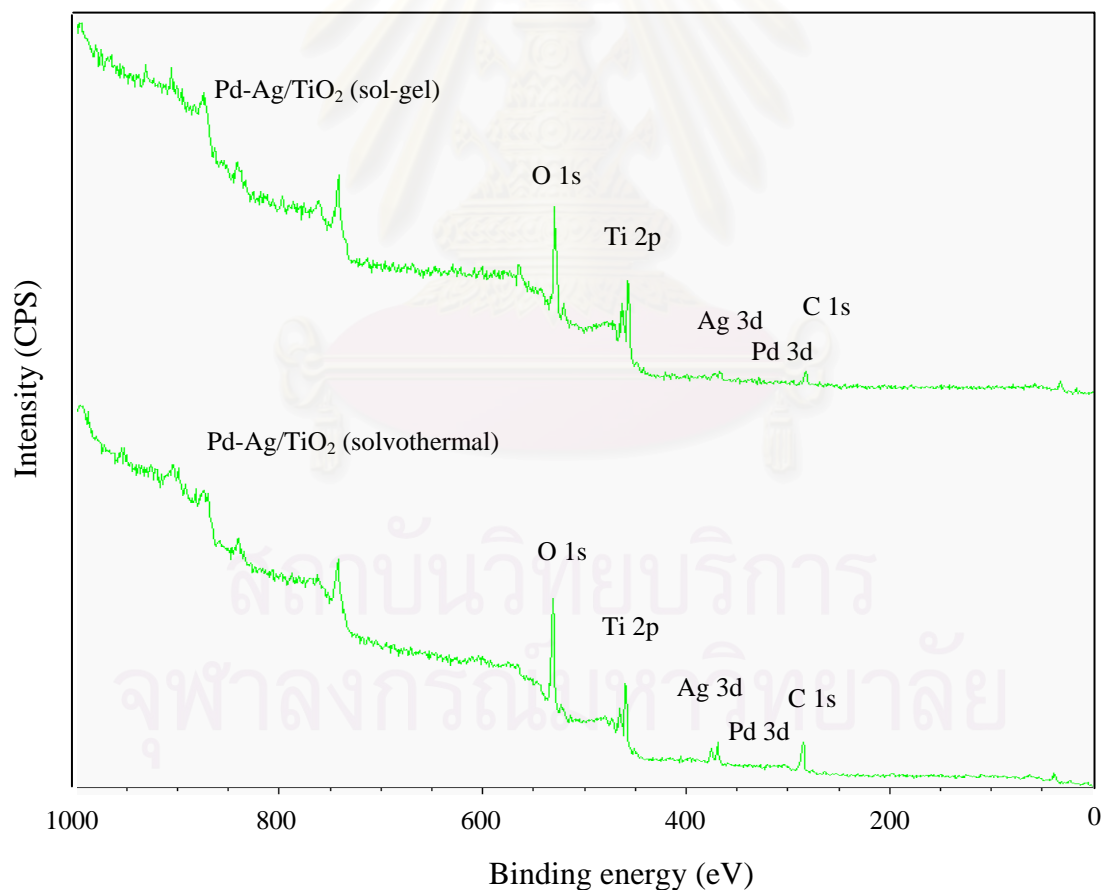
5.7.1.4 Surface composition

The surface compositions and electronic state of the metal catalysts were determined by X-ray photoelectron spectroscopy (XPS). The binding energy, %atomic concentration, and the XPS spectra survey and of Pd-Ag/TiO₂ synthesized by sol gel and solvothermal method are shown in Table 5.20, 5.21, and Figure 5.26, respectively. The binding energies of Pd 3d, Ag 3d, Ti 2p, O 1s, and C 1s of Pd catalysts are found to be 337.2- 346.5, 468.2-468.98 eV (Robert, N. et al., 2004), 458.9-459.7 (Liqiang, J. et al., 2003 and Price, N.J. et al., 1999), 530, and 285 eV, (Guillot, J. et al., 2001) respectively. The Pd/Ag ratio for Pd-Ag catalysts synthesized by sol-gel method was slightly higher than the one synthesized by solvothermal method.

Sample	Binding energy (eV)				FWHM (eV)			
	Pd 3d	Ag 3d	Ti 2p	O 1s	Pd 3d	Ag 3d	Ti 2p	O 1s
Pd-Ag/TiO ₂ (sol-gel)	337.220	368.287	458.967	530.367	0.566	1.846	2.158	2.436
Pd-Ag/TiO ₂ (solvothermal)	346.475	368.801	459.651	531.101	0.691	1.848	1.775	2.401

Table 5.20 Binding energy of Pd-Ag/TiO₂ samples from XPS results**Table 5.21** %atomic concentration for Pd-Ag/TiO₂ catalysts from XPS results

Sample	Atomic conc. %				Atomic ratio
	Pd 3d	Ag 3d	Ti 2p	O 1s	Pd/Ag
Pd-Ag/TiO ₂ (sol-gel)	0.06	0.52	14.22	62.47	0.115
Pd-Ag/TiO ₂ (solvothermal)	0.02	0.97	7.54	48.79	0.021

**Figure 5.26** XPS survey spectra of Pd-Ag/TiO₂ synthesized by the solvothermal and sol gel methods.

5.7.2 The catalytic activities of Pd-Ag/TiO₂ catalysts in selective acetylene hydrogenation

5.7.2.1 Reaction study in selective hydrogenation in excess ethylene

The performance of 1%Pd-3%Ag catalysts supported on TiO₂ catalysts consisting of the different phase compositions in acetylene hydrogenation was evaluated at the temperature 40°C, a space velocity 2,8818.88 h⁻¹ and a gas mixture containing 1.46% C₂H₂, 1.71% H₂, 15.47% C₂H₆ and balanced C₂H₄ (Rayong Olefin Co., Ltd) as reactant feed that is the same condition of Pd/TiO₂ catalysts.

Figure 5.27 illustrates the performances of 1%Pd-3%Ag/TiO₂ synthesized by the different methods. The titania supported Pd-Ag catalysts synthesized by sol gel-method showed slightly higher acetylene conversion than the one synthesized by solvothermal method. Ethylene selectivity Pd-Ag catalysts synthesized by solvothermal and sol gel-method were quite similar but were much higher than that of Pd-Ag supported on commercial TiO₂

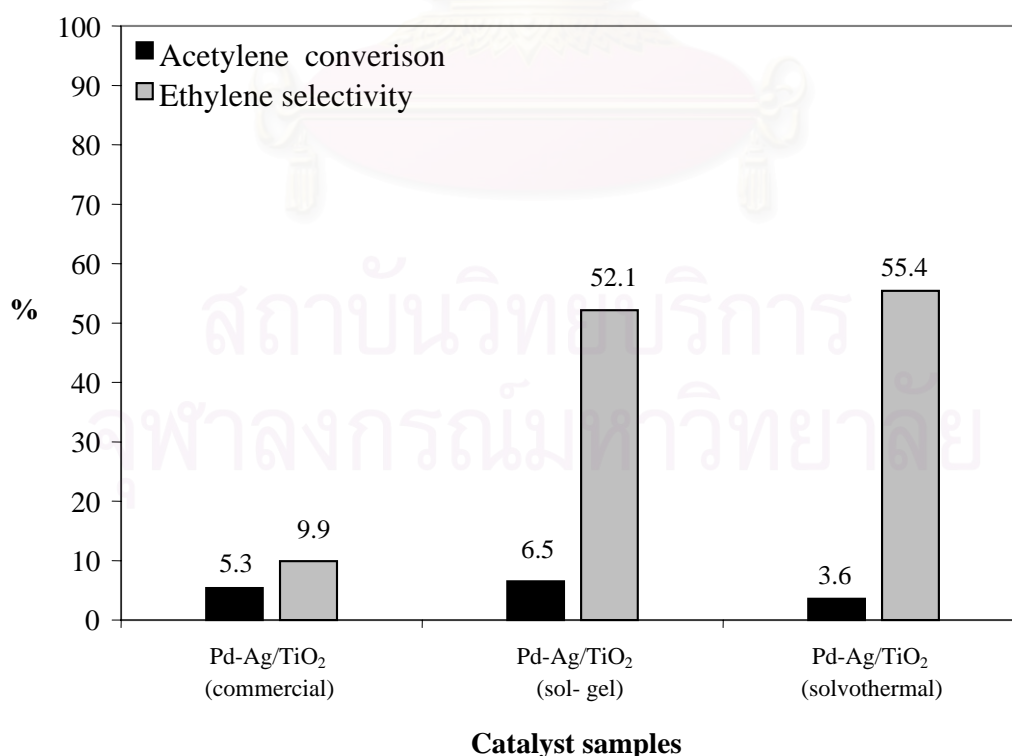


Figure 5.27 Catalytic performances of Pd-Ag catalysts in different synthesized methods in acetylene hydrogenation.

CHAPTER VI

CONCLUSIONS AND RECOMMENDATIONS

In this chapter, section 6.1 provides the conclusions obtained from the experimental results of the titania supports consisting of various phase compositions, synthesized by different methods, the titania supported palladium catalysts, and the silver promoted titania supported palladium catalysts. Additionally, recommendations for further study are given in section 6.2.

6.1 Conclusions

1. For the TiO_2 consisting of various anatase/rutile compositions, it is shown that higher amount of % rutile phase in the TiO_2 resulted in a decrease in BET surface areas and lower amount of Ti^{3+} defective sites. TiO_2 prepared by the sol-gel and solvothermal methods showed only anatase phase. BET surface area for the sol gel derived- TiO_2 is slightly higher than that of the solvothermal derived- TiO_2 . In addition, TiO_2 synthesized by solvothermal method possessed higher amount of Ti^{3+} defective sites than the one synthesized by sol-gel method.

2. The presence of Ti^{3+} in Pd/TiO_2 catalysts appeared to promote SMSI effect between Pd metal and TiO_2 support especially when Ti^{3+} sites were in contact with Pd resulted in high ethylene selectivities. Among the five crystalline phase compositions of titania used in this study, the one containing 44% rutile was found to be the best (optimum) composition to prepare TiO_2 -supported Pd catalysts with high ethylene selectivity. Pd/TiO_2 synthesized by sol-gel method exhibited higher activity and selectivity for selective acetylene hydrogenation than the one supported on titania synthesized by solvothermal method. The results suggest that the presence of too many Ti^{3+} that were not in contact with Pd can result in lower ethylene selectivity.

3. Acetylene conversion and ethylene selectivity of Pd-Ag catalyst were lower than those of single metal Pd catalysts supported on TiO_2 that contained significant

amount of Ti^{3+} . This was probably due to the absence of the SMSI effect between Pd metal and the TiO_2 support. However, the presence of Ag improved significantly ethylene selectivity of the catalysts without Ti^{3+} presented.

6.2 Recommendations

1. The effect of the TiO_2 defective sites should be studied for other catalytic reactions such as photocatalytic reaction.

2. Since it has been reported that Pd and Pd-Ag catalysts can be activated by pretreatment with N_2O and NO resulting in high acetylene conversion and ethylene gain, the effect of pretreatment with oxygen and oxygen-containing compounds on the characteristics and catalytic properties for selective hydrogenation of acetylene over Pd/ TiO_2 should be investigated.

3. The effect of crystalline phase composition of other supports such as alumina for selective hydrogenation of acetylene over Pd and Pd-Ag supported catalysts should be investigated.

4. Decreasing agglomeration of particle titania to increase of BET surface area for nanocrystalline titania can prepare by flame spray pyrolysis method.

REFERENCES

- Ali, S.H. and Goodwin, J.G. Jr. SSITKA Investigation of Palladium Precursor and Support Effects on CO Hydrogenation over Supported Pd Catalysts. J. of Catal. **176** (1998): 3–13.
- Al-Ammar, A.S. and Webb, G. Hydrogenation of acetylene over supported metal catalysts Part 2.-Adsorption of [¹⁴C] tracer study of deactivation phenomena. J. Chem. Soc. Faraday. **175** (1978): 657-664.
- Anderson, A.B. and Onwood, D.P. Why carbon monoxide is stable lying down on a negatively charged Ru(001) surface but not on Pt(111). Surface Science Letters **154** (1985): L261-L267.
- Asplund, S. Coke Formation and Its Effect on Internal Mass Transfer and Selectivity in Pd-Catalysed Acetylene Hydrogenation. J. of Catal. **158** (1996): 267-278.
- Boitiaux, J.-P.; Cosyns, J.; Derrien, M. and Leger, G. Newest hydrogenation catalysts. Hydrocarbon Processing (1985): 51-59.
- Bond, G.C.; Dowden, D.A. and Mackenzie, N. The selective hydrogenation of acetylene. Trans. Faraday Soc. **54** (1958): 1597-1546.
- Chou, P. and Vannice, M.A. Calorimetric heat of adsorption measurements on palladium : I. Influence of crystallite size and support on hydrogen adsorption. J. Catal. **104** (1987): 1-16.
- Chu, W.; Chen, M.; Qin, W. and Dai, X. Support effect of palladium catalysts for acetylene hydrogenation to ethylene. Proceeding of the 13th International Congress on Catalysis, Paris, July (2004)
- Cosyns, J. and Boitiaux, J.-P. Process for selective hydrogenating acetylene in a mixture of acetylene and ethylene. US Patent 4,571,442 (Institut Francais du Petrole), 1984
- Dean, J.A. Lange's Handbook of Chemistry. 5 th ed. United State of America: McGraw-Hill, 1999.
- Derrien, M.L. Selective hydrogenation applied to the refining of petrochemical raw materials produced by steam cracking. Stud. Surf. Sci. Catal. **27** (1986): 613-666.

- Ding, X. and Liu, X. Grain growth enhanced by anatase to rutile transformation in sol-gel- derived nanocrystalline titania powders. J. of Alloys and Compounds. 248 (1997): 143-145.
- Fujishima, A.; Hashimoto, K. and Watanabe, T., TiO₂ photocatalysis: fundamental and applications. 1st ed. Tokyo: BKC, 1999.
- Guillot, J.; Fabreguete, F.; Imhoff, L.; Heintz, O.; Marco de Lucas, M.C.; Sacilotti, M.; Domenichini, B. And Bourgeois, S. Amorphous TiO₂ in LP-OMCVD TiN_xO_y thin films revealed by XPS. Applied Surface Science. 177 (2001): 268-272.
- Guimon, C.; Auroux, A.; Romero, E. and Monzon A. Acetylene hydrogenation over Ni-Si-Al mixed oxides prepared by sol-gel technique. Appl. Catal. A. 251 (2003): 199-214.
- Herrmann, J.M.; Gravelle-Rumeau-Maillot, M. and Gravelle, P.C. A microcalorimetric study of metal-support interaction in the Pt/TiO₂ system. J. Catal. 104 (1987): 136-146.
- Hodnett, B.K. and Delmon, B. Catalytic Hydrogenation (Cerveny, L. ed.), Studies in surface science and catalysis, Elsevier, Amsterdam, 27 (1986):53.
- Howe, R.F. and Gratzel, M. EPR Observation of Trapped Electrons in Colloidal TiO₂. J. Phys. Chem. 89 (1985): 4495-4499.
- Huang, D.C.; Chang, W.F.; Pong W.F.; Tsang, P.K.; Hung, K.J. and Huang, W.F. Effect of Ag-promotion on Pd catalysts by XANES. Catal. Lett. 53 (1998): 155-159.
- Ikeda, S.; Sugiyama, N.; Murakami, S.; Kominami, H.; Kera, Y.; Noguchi, H.; Uosaki, K.; Torimoto, T. and Ohtani, B. Quantity analysis of defective sites in titanium (IV) oxide photocatalyst powders. Phys. Chem. Chem. Phys. 5 (2003): 778-783.
- Inoue, M.; Kominami, H. and Inui, T. Novel synthetic method for the catalytic use of thermally stable zirconia: thermal decomposition of zirconium alkoxides in organic media. Appl. Catal. A 97 (1993): L25-L30.
- Inoue, M.; Kondo, Y. and Inui, T. An Ethylene Glycol Derivative of Boehmite. Inorg. Chem. 27 (1988): 215-221.
- Iwamoto, S.; Saito, K.; Inoue, M. and Kagawa, K. Preparation of the Xerogels of Nanocrystalline Titanias by the Removal of the Glycol at the

- Glycothermal Method and Their Enhanced Photocatalytic Activities. Nano. Lett. 1, 8 (2001): 417 – 421.
- Jung, K. and Park, S. Anatase- phase titania: preparation by embedding silica and photocatalytic activity for the decomposition of trichloroethylene. J. of Photochemistry and Photobiology A: Chemistry. 127 (1999): 117-122.
- Kang, J.H.; Shin, E.W.; Kim, W.J.; Park, J.D. and Moon, S.H., Selective hydrogenation of acetylene on Pd/SiO₂ catalysts promoted with Ti, Nb and Ce oxides. Catal. Today 63 (2000): 183-188.
- Kang, J.H.; Shin, E.W.; Kim, W.J.; Park, J.D. and Moon S.H. Selective Hydrogenation of Acetylene on TiO₂-Added Pd Catalysts. J. Catal. 208 (2002) 310-320.
- Kim, C.S.; Moon, B.K.; Park, J.H.; Chung, S.T. and Son, S.M. Synthesis of nanocrystalline TiO₂ in toluene by a solvothermal route. J. Crystal Growth 254 (2003): 405–410.
- Kim, W.J.; Kang, J.H.; Ahn, I.Y. and Moon, S.H.; Deactivation behavior of a TiO₂-added Pd catalyst in acetylene hydrogenation. J. Catal. 226 (2004): 226-229.
- Kim, W.J.; Kang, J.H.; Ahn, I.Y. and Moon, S.H. Effect of potassium addition on the properties of a TiO₂-modified Pd catalyst for the selective hydrogenation of acetylene. Appl. Catal. A. 268 (2004): 77-82.
- Kim, W.J.; Shin, E.W.; Kang, J.H. and Moon, S.H. Performance of Si-modified Pd catalyst in acetylene hydrogenation: catalyst deactivation behavior. Appl. Catal. A. 251 (2003): 305-313.
- Kominami, H.; Kato, J.-I; Murakami, S.-Y; Kera, Y.; Inoue, M.; Inui, T. and Ohtani B. Synthesis of titanium (IV) oxide of ultra-high photocatalytic activity: high-temperature hydrolysis of titanium alkoxides with water liberated homogeneously from solvent alcohols. J. Mol. Catal.A: Chemical 144 (1999): 165–171.
- Kominami, H.; Kato, J.; Murakami, S.; Ishii, Y.; Kohno, M.; Yabutani, K.; Yamamoto, T.; Kera, Y.; Inoue, M.; Inui, T. and Ohtani, B. Solvothermal syntheses of semiconductor photocatalysts of ultra-high activities. Catal. Today 84 (2003): 181-189.

- Kominami, H.; Kato, J.; Takada, Y.; Doushi, Y. and Ohtani, B. Novel Synthesis of Microcrystalline Titanium (IV) Oxide having High Thermal Stability and Ultra-High Photocatalytic Activity: Thermal Decomposition of Titanium (IV) Alkoxide. Catal. Lett. **46** (1997): 235-240.
- Kominami, H.; Kohno, M.; Takada, Y.; Inoue, M.; Inui, T. and Kera, Y. Hydrothermal of Titanium Alkoxide in Organic Solvent at High Temperatures: A New Synthetic Method for Nanosized, Thermally Stable Titanium (IV) Oxide. Ind. Eng. Chem. Res. **38** (1999): 3925-3931.
- Kominami, H.; Murakami, S.Y.; Kohno, M.; Kera, Y.; Okada, K.; and Ohtani, B. Stoichiometric decomposition of water by titanium (IV) oxide photocatalyst synthesized in organic media: Effect of synthesis and irradiation conditions on photocatalytic activity. Phys. Chem. Chem. Phys. **3** (2001): 4102-4106.
- Kongwudthiti, S.; Prasertdam, P.; Silveston P. and Inoue M. Influence of synthesis conditions on the preparation of zirconia powder by the glycothermal method. Ceram. Int. **29** (2003): 807-814.
- Kumar, P.M.; Badrinarayanan, S. and Sastry, M. Nanocrystalline TiO₂ studied by optical, FTIR and X-ray photoelectron spectroscopy: correlation to presence of surface state. Thin Solid Films. **358** (2000): 122
- Lamb, R.N.; Ngamsom, B.; Trimm, D.L.; Gong, B.; Silveston, P.L. and Prasertdam, P. Surface characterisation of Pd-Ag/Al₂O₃ catalysts for acetylene hydrogenation using an improved XPS procedure. Appl. Catal. A. **268** (2004): 43-50.
- Lee, D.C.; Kim, H.; Kim, W.J.; Kang, J.H. and Moon, S.H., Selective hydrogenation of 1,3-butadiene on TiO₂-modified Pd/SiO₂ catalysts. Appl. Catal. A. **244** (2003): 83-91.
- Li, Y.; Fan, Y.; Yang, H.; Xu, B.; Feng, L.; Yang, M. and Chen, Y. Strong metal-support interaction and catalytic properties of anatase and rutile supported palladium catalyst Pd/TiO₂. Chem. Phys. Lett. **372** (2003): 160-165.
- Li, Y.; Xu, B.; Fan, Y.; Feng, N.; Qiu, A.; He, J. M. J.; Yang H. and Chen Y. The effect of titania polymorph on the strong metal-support interaction of Pd/TiO₂ catalysts and their application in the liquid phase selective

- hydrogenation of long chain alkadienes. J. Mol. Catal.A: Chemical 216 (2004): 107–114.
- Liqiang, J.; Xiaojun, S.; Weimin, C.; Zili, X.; Yaoguo, D. and Honggang, F. J. Phys. Chem. Solids. 64 (2003): 615.
- Mahata, N. and Vishwanathan, V. Influence of Palladium Precursors on Structural Properties and Phenol Hydrogenation Characteristics of Supported Palladium Catalysts. J. of Catal. 196 (2000): 262–270.
- Manzini, I.; Antonioli, G.; Bersani, D.; Lottici, P.P.; Gnappi, G. and Montenero, A. X-ray absorption spectroscopy study of crystallization processes in sol-gel- derived TiO₂. J. of Non-Crystalline Solids. 192 (1995): 519:523
- Margitfalvi, J.; Guzzi, L. and Weiss, A. Reaction routes for hydrogenation of acetylene- ethylene mixtures using a double labeling method. React. Kinet. Catal. Lett. 15 (1980): 475-479.
- McGown, W.T.; Kemball, C. and Whan, D.A. Hydrogenation of acetylene in excess ethylene on an alumina supported palladium catalyst at atmospheric pressure in a spinning basket reactor. J. Catal. 51 (1978): 173-184.
- Mekasuwandumrong, O.; Silveston, P.L. ; Praserthdam, P. ; Inoue, M. ; Pavarajarn, V. and Tanakulrungsank, W. Synthesis of thermally stable micro spherical γ -alumina by thermal decomposition of aluminum isopropoxide in mineral oil. Inorg. Chem. Commun. 6 (2003): 930-934.
- Molnár, Á.; Sárkány, A.; and Varga, M. Hydrogenation of carbon-carbon multiple bonds: chemo-, region- and stereo-selectivity. J. Mol. Catal. 173 (2001): 185-221.
- Moses. J.M.; Weiss, A.H.; Matusek, K. and Guzzi, L. The effect of catalyst treatment on the selective hydrogenation of acetylene over palladium/alumina. J. Catal. 86 (1984): 417-426.
- Ngamsom, B.; Bogdanchikova, N.; Borja, M.A. and Praserthdam, P. Characterisations of Pd–Ag/Al₂O₃ catalysts for selective acetylene hydrogenation: effect of pretreatment with NO and N₂O. Catal. Commun. 5 (2004): 243-248.
- Othmer, K. Encyclopedia of chemical technology. Vol. 6. 4 th ed. New York: A Wiley-Interscience Publication, John Wiley&Son, 1991.
- Panpranot, J.; Nakkararuang, L.; Ngamsom, B. and Praserthdam, P. Synthesis, characterization, and catalytic properties of Pd and Pd-Ag catalysts

- supported on nanocrystalline TiO₂ prepared by solvothermal method. Catal. Lett. **103** (2005): 53-58.
- Park, H.K.; Kim, D.K. and Kim, C.H. Effect of Solvent on Titania Particle Formation and Morphology in Thermal Hydrolysis of TiCl₄. J. Am. Ceram. Soc. **80**, 3 (1997): 743 – 749.
- Payakgul, W.; Mekasuwandumrong, O.; Pavarajarn, V. and Prasertthdam, P. Effects of reaction medium on the synthesis of TiO₂ nanocrystals by thermal decomposition of titanium (IV) n-butoxide. Ceram. Int. **31** (2005): 391–397.
- Prasertthdam, P.; Ngamsom B.; Bogdanchikova N.; Phatanasri S. and Pramotthana M., Effect of the pretreatment with oxygen and/or oxygen-containing compounds on the catalytic performance of Pd-Ag/Al₂O₃ for acetylene hydrogenation. Appl. Catal. A. **230** (2002): 41-51.
- Prasertthdam, P.; Phatanasri, S. and Meksikarin, J. Activation of acetylene selective hydrogenation catalysts using oxygen containing compounds. Catal. Today **63** (2000): 209-213.
- Price, N.J.; Reitz, J.B.; Madix R.J. and Solomon, E.I. A synchrotron XPS study of the vanadia- titania system as a model for monolayer oxide catalysts. J. Electron Spectroscopy and Related Phenomena. **257** (1999): 98-99.
- Rao, C. N. R.; Yuganarasimhan, S. R. and Faeth, P. A. Trans. Faraday Soc. **57** (1961): 504
- Raupp, G.B. and Dumesic J.A. Effect of varying titania surface coverage on the chemisorptive behavior of nickel. J. Catal. **95** (1985): 587-601.
- Reidy, D.J.; Holmes, J.D. and Morris, M.A. The critical size mechanism of anatase to rutile transformation for TiO₂ and dopped- TiO₂. J. of the European Ceramic Society. (2005).
- Robert, N.; Ngasom, B.; Trimm, D.L.; Gong, B.; Silveston, P.L. and Prasertthdam, P. Surface characterization of Pd-Ag/Al₂O₃ catalysts for acetylene hydrogenation using an improved XPS procedure. Applied Catalysis A: General. (2004).

- Roder, H.; Schuster, R.; Brune, H. and Kern, K. Monolayer-confined mixing at the Ag-Pt (111) interface. Phys. Rev. Lett. **71** (1993): 2086-2089.
- Salama, T.M.; Hattori, H.; Kita, H.; Ebitani, K. and Tanaka, T.J. Chem. Soc. Faraday Trans. **89** (12) (1993): 2067.
- Santos, J.; Phillips, J. and Dumesic, J.A. Metal-support interactions between iron and titania for catalysts prepared by thermal decomposition of iron pentacarbonyl and by impregnation. J. Catal. **81** (1983): 147-167.
- Sárkány, A.; Beck, A.; Horvath, A.; Revay, Zs. and Guzzi L. Acetylene hydrogenation on sol-derived Pd/SiO₂. Appl. Catal. A. **253** (2003): 283-292.
- Sárkány, A.; GuzziAlvin, L. and Weiss, H. On the aging phenomenon in palladium catalysed acetylene hydrogenation. App. Catal. **10** (1984): 369-388.
- Sárkány, A.; Horvath, A. and Beck, A. Hydrogenation of acetylene over low loaded Pd and Pd-Au/SiO₂ catalysts. Appl. Catal. A. **229** (2002): 117-125.
- Shin, E.W.; Choi, C.H.; Chang, K. S.; Na, Y.H. and Moon, S.H. Properties of Si-modified Pd catalyst for selective hydrogenation of acetylene. Catal. Today **44** (1998): 137-143.
- Shin, E.W.; Kang, J.H.; Kim, W.J.; Park, J.D. and Moon, S.H. Performance of Si-modified Pd catalyst in acetylene hydrogenation: the origin of the ethylene selectivity improvement. Appl. Catal. A. **223** (2002): 161-172.
- Sornnarong Theinkeaw. Synthesis of Large-Surface Area Silica Modified Titanium (IV) Oxide Ultra Fine Particles. Master's thesis, Department of Chemical Engineering, Graduated School, Chulalongkorn University, 2000.
- Suriye, K.; Prasertdam, P. and Jongsomjit, B. Impact of Ti³⁺ present in Titania on characteristics and catalytic properties of the Co/TiO₂ catalyst. Ind. Eng. Chem. **44** (2005): 6599-6604.
- Taylor, G.F.; Thomson, S.J. and Webb, G. The adsorption and retention of hydrocarbons by alumina-supported palladium catalyst. J.Catal.**12**(1968): 150-156.
- Vannice, M. A.; Wang, S-Y. and Moon, S.H. The effect of SMSI (strong metal-support interaction) behavior on CO adsorption and hydrogenation on Pd

catalysts: I. IR spectra of adsorbed CO prior to and during reaction conditions. J. of Catal 71 (1981): 152-166.

Weiss, A.; Leviness, S. and Naiv, V. The effect of Pd dispersion in acetylene selective hydrogenation. Proceeding of 8th International Congression Catalysis Vol.5. Berlin, 1984 Verlag Chemie, Weinheim, Dechema, Frankfurt am Nain. (1984): 59-600.

Yang, J.; Mei, S.; Ferreira, M.F. Hydrothermal Synthesis of Nanosized Titania Powders: Influence of Tetraalkyl Ammonium Hydroxides on particle Characteristics. J. Am. Ceram. Soc. 84, 8 (2001): 1696 – 1702.

Zhang, F.; Zheng, Z.; Liu, D.; Mao, Y.; Chen, Y.; Zhou, Z.; Yang, S. and Liu, X. Nuclear Instruments and Methods in Phys. Res. B. 132 (1997): 620.

Zhang, Q.; Li, J.; Liu, X. and Zhu, Q. Synergetic effect of Pd and Ag dispersed on Al₂O₃ in the selective hydrogenation of acetylene. Appl. Catal. A. 197 (2000): 221-228.



สถาบันวิทยบริการ
จุฬาลงกรณ์มหาวิทยาลัย



APPENDICES

สถาบันวิทยบริการ
จุฬาลงกรณ์มหาวิทยาลัย

APPENDIX A

CALCULATION FOR CATALYST PREPARATION

Preparation of 1%Pd/TiO₂ with and with promoted Ag catalysts by the incipient wetness impregnation method are shown as follows:

- Reagent:
- Palladium (II) nitrate hexahydrate (Pd (NO₃)₂ · 6H₂O)
Molecular weight = 230.41
 - Silver (III) nitrate (Ag (NO₃))
Molecular weight = 169.87
 - Support: - Titania [TiO₂]

Calculation for the preparation of unpromoted catalyst (1%Pd/TiO₂)

Based on 100 g of catalyst used, the composition of the catalyst will be as follows:

$$\begin{aligned} \text{Palladium} &= 1 \text{ g} \\ \text{Titania} &= 100-1 = 99 \text{ g} \end{aligned}$$

For 2 g of titania

$$\text{Palladium required} = 2 \times (1/99) = 0.02 \text{ g}$$

Palladium 0.02 g was prepared from Pd (NO₃)₂ · 6H₂O and molecular weight of Pd is 106.42

$$\begin{aligned} \text{Pd (NO}_3)_2 \cdot 6\text{H}_2\text{O required} &= \frac{\text{MW of Pd(NO}_3)_2 \cdot 6\text{H}_2\text{O} \times \text{palladium required}}{\text{MW of Pd}} \\ &= (230.41/106.42) \times 0.02 = 0.0437 \text{ g} \end{aligned}$$

Since the pore volume of the titania support is 0.2 ml/g. Thus, the total volume of impregnation solution which must be used is 0.4 ml for titania by the requirement of incipient wetness impregnation method, the de-ionized water is added until equal pore volume for dissolve Palladium (II) nitrate hexahydrate.

Calculation for the preparation of Ag-promoted catalyst (1%Pd-3%Ag/TiO₂)

Based on 100 g of catalyst used, the composition of the catalyst will be as follows:

$$\begin{aligned} \text{Palladium} &= 1 \text{ g} \\ \text{Silver} &= 3 \text{ g} \\ \text{Titania} &= 100-(1+3) = 96 \text{ g} \end{aligned}$$

For 2 g of titania

$$\begin{aligned} \text{Palladium required} &= 2 \times (1/96) = 0.021 \text{ g} \\ \text{Silver required} &= 2 \times (3/96) = 0.063 \text{ g} \end{aligned}$$

Palladium 0.021 g was prepared from Pd (NO₃)₂ · 6H₂O and molecular weight of Pd is 106.42.

$$\begin{aligned} \text{Pd (NO}_3)_2 \cdot 6\text{H}_2\text{O required} &= \frac{\text{MW of Pd (NO}_3)_2 \cdot 6\text{H}_2\text{O} \times \text{palladium required}}{\text{MW of Pd}} \\ &= (230.41/106.42) \times 0.021 = 0.045 \text{ g} \end{aligned}$$

Silver 0.063 g was prepared from (Ag (NO₃)₂) and molecular weight of Ag is 169.87.

$$\begin{aligned} \text{Ag (NO}_3)_3 \text{ required} &= \frac{\text{MW of (Ag (NO}_3)_3) \times \text{silver required}}{\text{MW of Ag}} \\ &= (169.87/107.868) \times 0.063 = 0.098 \text{ g} \end{aligned}$$

Dissolve of palladium (II) nitrate hexahydrate, silver nitrate and volume of de-ionized water like preparation of unpromoted catalyst.

สถาบันวิทยบริการ
จุฬาลงกรณ์มหาวิทยาลัย

APPENDIX B

CALCULATION OF THE CRYSTALLITE SIZE

Calculation of the crystallite size by Debye-Scherrer equation

The crystallite size was calculated from the half-height width of the diffraction peak of XRD pattern using the Debye-Scherrer equation.

From Scherrer equation:

$$D = \frac{K\lambda}{\beta \cos \theta} \quad (\text{B.1})$$

- where
- D = Crystallite size, Å
 - K = Crystallite-shape factor = 0.9
 - λ = X-ray wavelength, 1.5418 Å for CuK α
 - θ = Observed peak angle, degree
 - β = X-ray diffraction broadening, radian

The X-ray diffraction broadening (β) is the pure width of a powder diffraction free of all broadening due to the experimental equipment. Standard α -alumina is used to observe the instrumental broadening since its crystallite size is larger than 2000 Å. The X-ray diffraction broadening (β) can be obtained by using Warren's formula.

From Warren's formula:

$$\beta^2 = B_M^2 - B_S^2 \quad (\text{B.2})$$
$$\beta = \sqrt{B_M^2 - B_S^2}$$

- Where
- B_M = The measured peak width in radians at half peak height.
 - B_S = The corresponding width of a standard material.

Example: Calculation of the crystallite size of titania

$$\begin{aligned} \text{The half-height width of 101 diffraction peak} &= 0.93125^\circ \\ &= 0.01625 \text{ radian} \end{aligned}$$

$$\text{The corresponding half-height width of peak of } \alpha\text{-alumina} = 0.004 \text{ radian}$$

$$\begin{aligned} \text{The pure width} &= \sqrt{B_M^2 - B_S^2} \\ &= \sqrt{0.01625^2 - 0.004^2} \\ &= 0.01577 \text{ radian} \end{aligned}$$

$$B = 0.01577 \text{ radian}$$

$$2\theta = 25.56^\circ$$

$$\theta = 12.78^\circ$$

$$\lambda = 1.5418 \text{ \AA}$$

$$\begin{aligned} \text{The crystallite size} &= \frac{0.9 \times 1.5418}{0.0157 \cos 12.78} = 90.15 \text{ \AA} \\ &= 9 \text{ nm} \end{aligned}$$

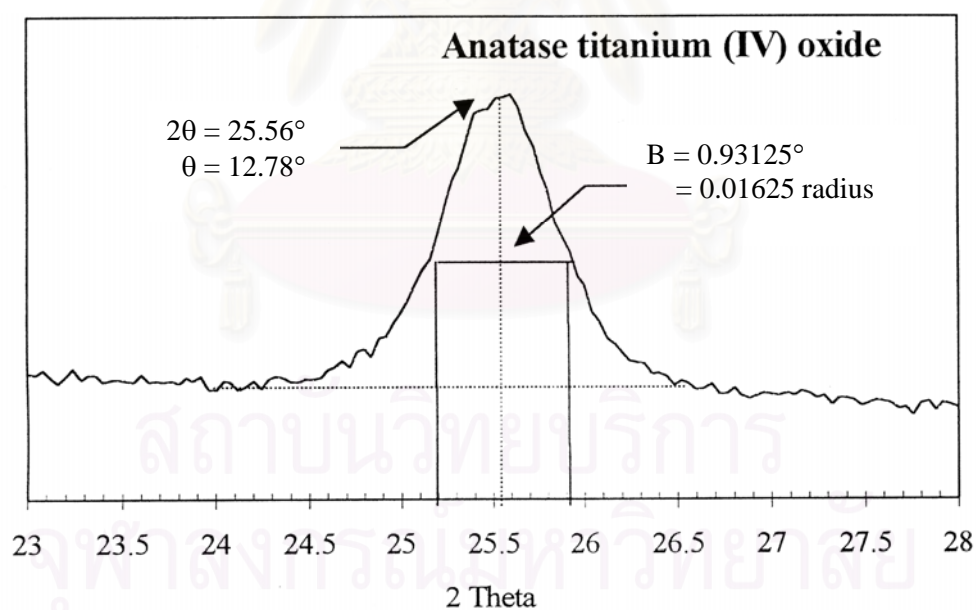


Figure B.1 The 101 diffraction peak of titania for calculation of the crystallite size

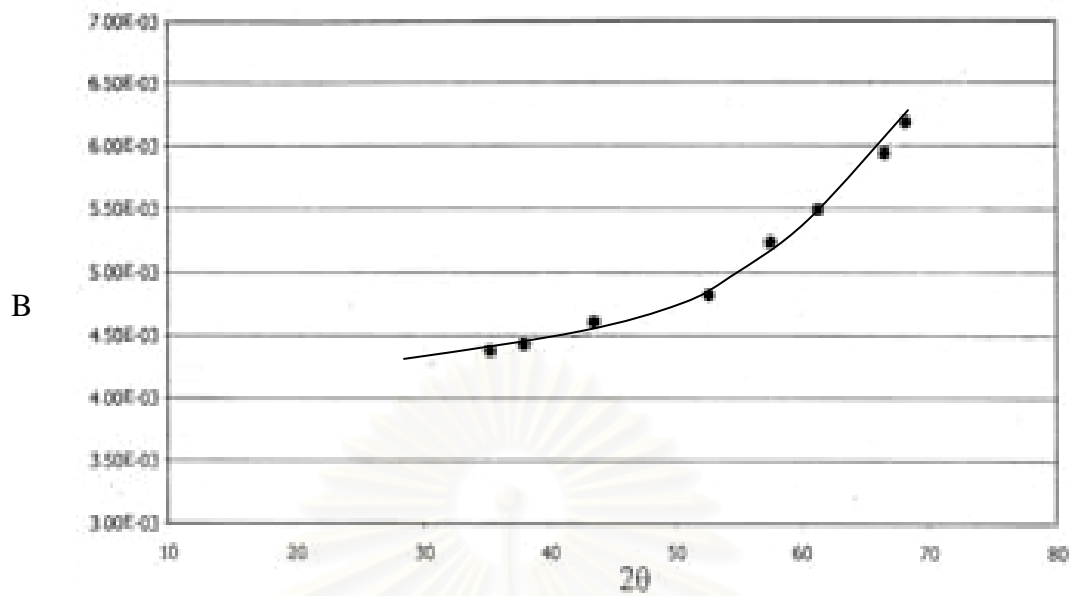


Figure B.2 The plot indicating the value of line broadening due to the equipment. The data were obtained by using α -alumina as standard

สถาบันวิทยบริการ
จุฬาลงกรณ์มหาวิทยาลัย

APPENDIX C

CALCULATION FOR METAL ACTIVE SITES AND DISPERSION

Calculation of the metal active sites and metal dispersion of the catalyst measured by CO adsorption is as follows:

Let the weight of catalyst used	= W	g
Integral area of CO peak after adsorption	= A	unit
Integral area of 50 μ l of standard CO peak	= B	unit
Amounts of CO adsorbed on catalyst	= B-A	unit
Volume of CO adsorbed on catalyst	= $50 \times [(B-A)/B]$	μ l
Volume of 1 mole of CO at 30°C	= 24.86×10^6	μ l
Mole of CO adsorbed on catalyst	= $[(B-A)/B] \times [50/24.86 \times 10^6]$	mole
Molecule of CO adsorbed on catalyst	= $[1.61 \times 10^{-6}] \times [6.02 \times 10^{23}] \times [(B-A)/B]$	molecules
Metal active sites	= $9.68 \times 10^{17} \times [(B-A)/B] \times [1/W]$	molecules of CO/g of catalyst
Molecules of Pd loaded	= $[\% \text{ wt of Pd}] \times [6.02 \times 10^{23}] / [\text{MW of Pd}]$	molecules/g of catalyst
Metal dispersion (%)	= $100 \times [\text{molecules of Pd from CO adsorption} / \text{molecules of Pd loaded}]$	

สถาบันวิทยบริการ
จุฬาลงกรณ์มหาวิทยาลัย

APPENDIX D

CALIBRATION CURVES

This appendix showed the calibration curves for calculation of composition of reactant and products in selective acetylene hydrogenation reaction. The reactant is 1.46% C₂H₂, 1.71% H₂, 15.47% C₂H₆ and balanced C₂H₄ (Rayong Olefin Co., Ltd) and the desired product is ethylene. The other product is ethane.

The thermal conductivity detector, gas chromatography Shimadzu model 8A was used to analyze the concentration of H₂ by using Molecular sieve 5A column.

The carbosieve S-II column is used with a gas chromatography equipped with a flame ionization detector, Shimadzu model 9A, to analyze the concentration of products including of methane, ethane, acetylene and ethylene.

Mole of reagent in y-axis and area reported by gas chromatography in x-axis are exhibited in the curves. The calibration curves of acetylene and hydrogen are illustrated in the following figures.

สถาบันวิทยบริการ
จุฬาลงกรณ์มหาวิทยาลัย

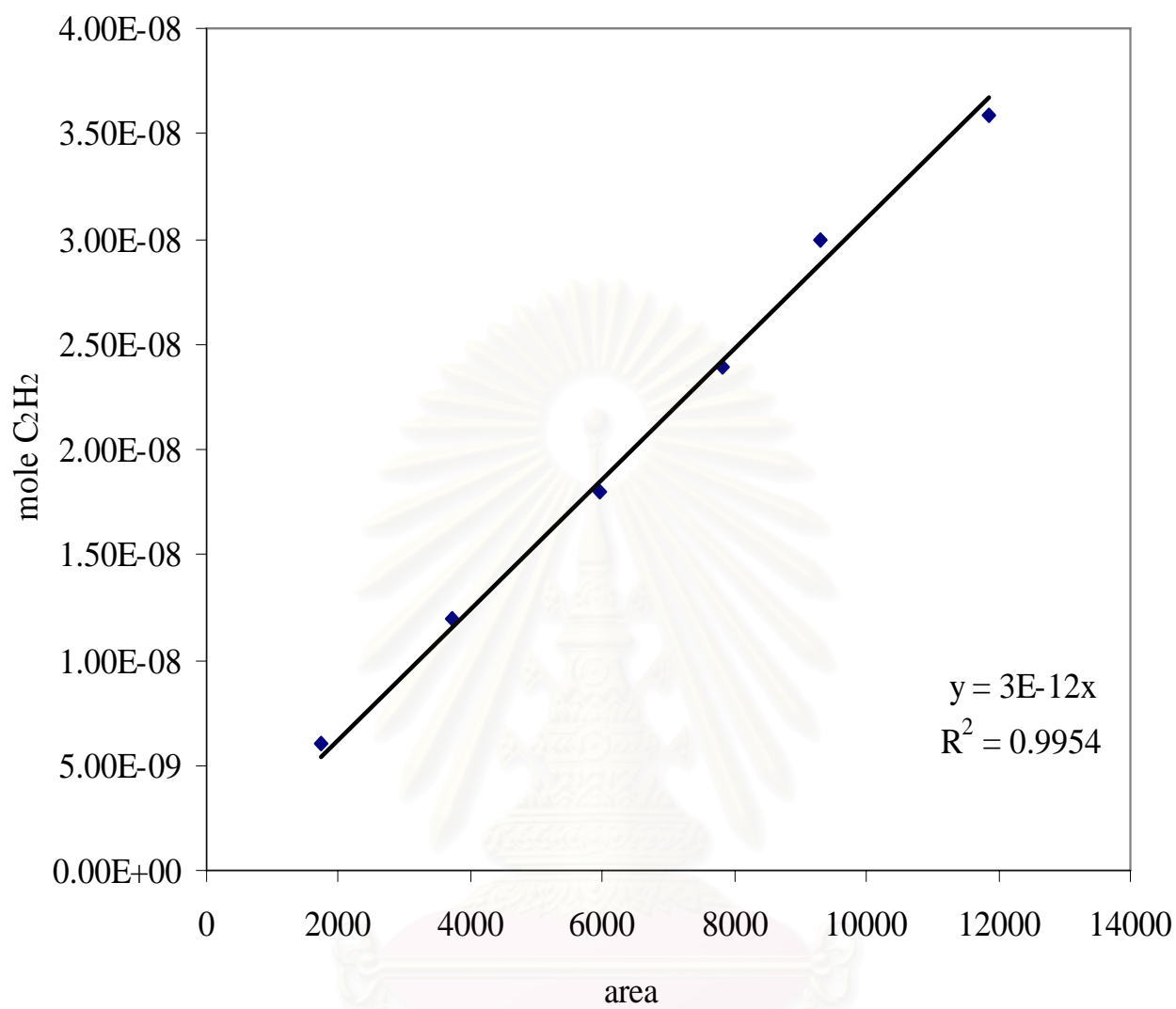


Figure D.1 The calibration curve of acetylene.

สถาบันวิทยบริการ
จุฬาลงกรณ์มหาวิทยาลัย

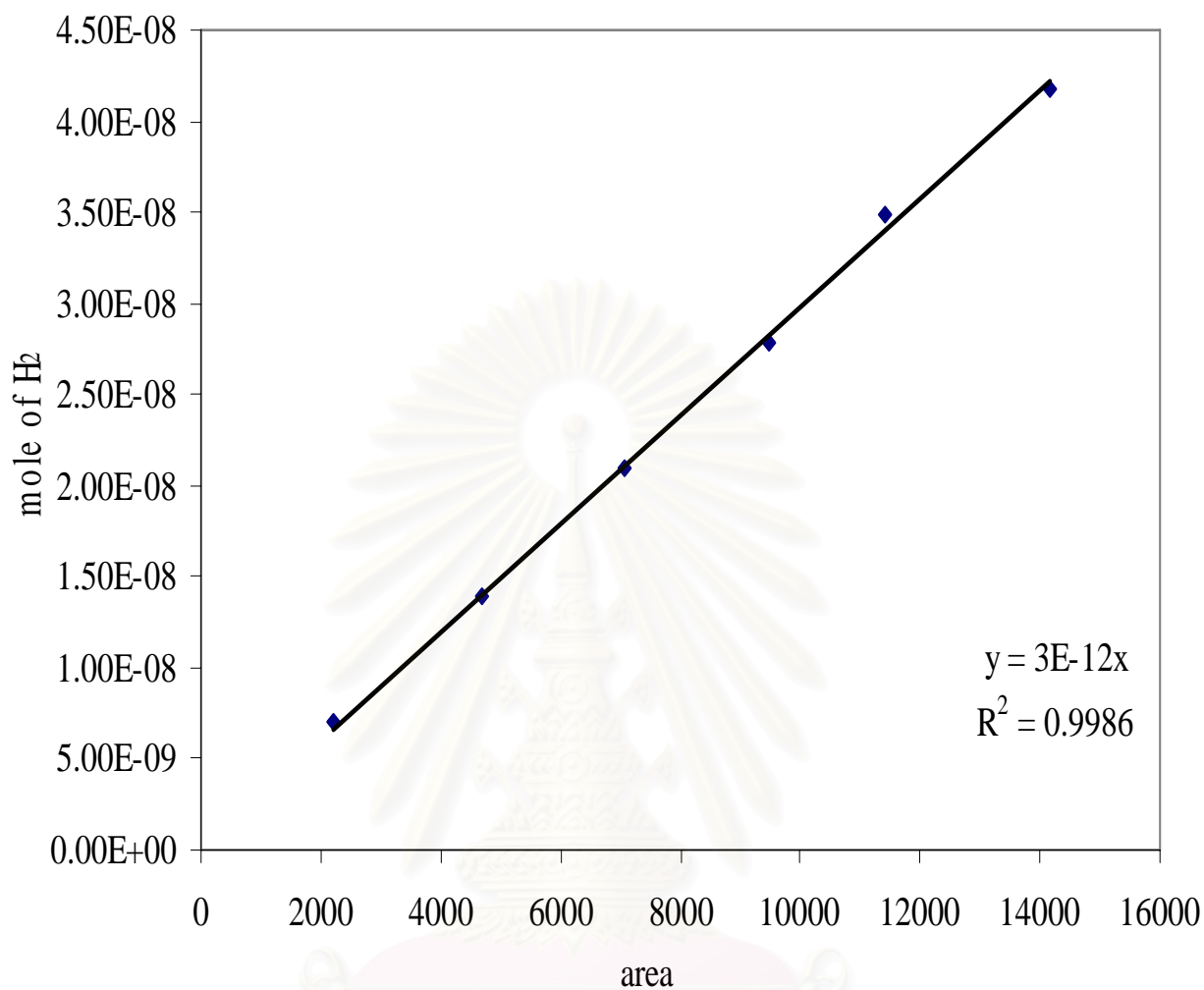


Figure D.2 The calibration curve of hydrogen.

สถาบันวิทยบริการ
จุฬาลงกรณ์มหาวิทยาลัย

APPENDIX E

CALCULATION OF CONVERSION AND SELECTIVITY

The catalyst performance for the selective hydrogenation of acetylene was evaluated in terms of activity for acetylene conversion and selectivity base on the following equation.

Activity of the catalyst performed in term of acetylene conversion is defined as moles of acetylene converted with respect to acetylene in feed:

$$\text{C}_2\text{H}_2 \text{ conversion (\%)} = \frac{100 \times [\text{mole of C}_2\text{H}_2 \text{ in feed} - \text{mole of C}_2\text{H}_2 \text{ in product}]}{\text{mole of C}_2\text{H}_2 \text{ in feed}} \quad (\text{i})$$

where mole of C_2H_2 can be measured employing the calibration curve of C_2H_2 in Figure D.1, Appendix D., i.e.,

$$\text{mole of C}_2\text{H}_2 = (\text{area of C}_2\text{H}_2 \text{ peak from integrator plot on GC-9A}) \times 2.3 \times 10^{-13} \quad (\text{ii})$$

Selectivity of ethylene is defined as moles of ethylene in product with respect to acetylene converted:

$$\text{Selectivity of C}_2\text{H}_4 \text{ (\%)} = 100 \times \frac{\text{mole of C}_2\text{H}_4 \text{ in product}}{\text{mole of C}_2\text{H}_2 \text{ converted}} \quad (\text{iii})$$

where mole of C_2H_4 can be measured employing the calibration curve of C_2H_4 in Figure D.2, Appendix D., i.e.,

$$\text{mole of C}_2\text{H}_4 = (\text{area of C}_2\text{H}_4 \text{ peak from integrator plot on GC-9A}) \times 3.37 \times 10^{-13} \quad (\text{iv})$$

APPENDIX F

LIST OF PUBLICATIONS

1. Kontapakdee, K; Panpranot, J. and Praserthdam, P. Effect of Titania Polymorph on the Characteristics and Catalytic properties of Pd/TiO₂ in Selective Hydrogenation of Acetylene Proceeding of the Regional Symposium on Chemical Engineering , 30 Nov.- 2 Dec. (2005), Hanoi, Vietnam.
2. Panpranot, J.; Kontapakdee, K. and Praserthdam, P. Effect of TiO₂ Crystalline Phase Composition on the Physicochemical and Catalytic Properties of Pd/TiO₂ in Selective Acetylene Hydrogenation. Journal of Physical Chemistry B (2006), in press.



สถาบันวิทยบริการ
จุฬาลงกรณ์มหาวิทยาลัย

VITAE

Miss Kanyaluck Kontapakdee was born on 1st January 1981, in Bangkok, Thailand. She received her Bachelor degree of Engineering with Chemical Engineering from Kasetsart university, Thailand in March 2003. She continued her Master study in the same major at Chulalongkorn university, Thailand in June 2004.



สถาบันวิทยบริการ
จุฬาลงกรณ์มหาวิทยาลัย